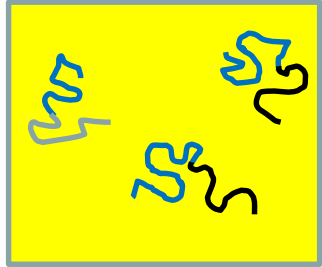# Short Course on Polymer Physics of Self-Assembly
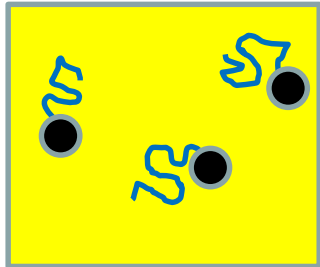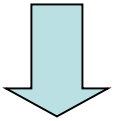
Lecture 2
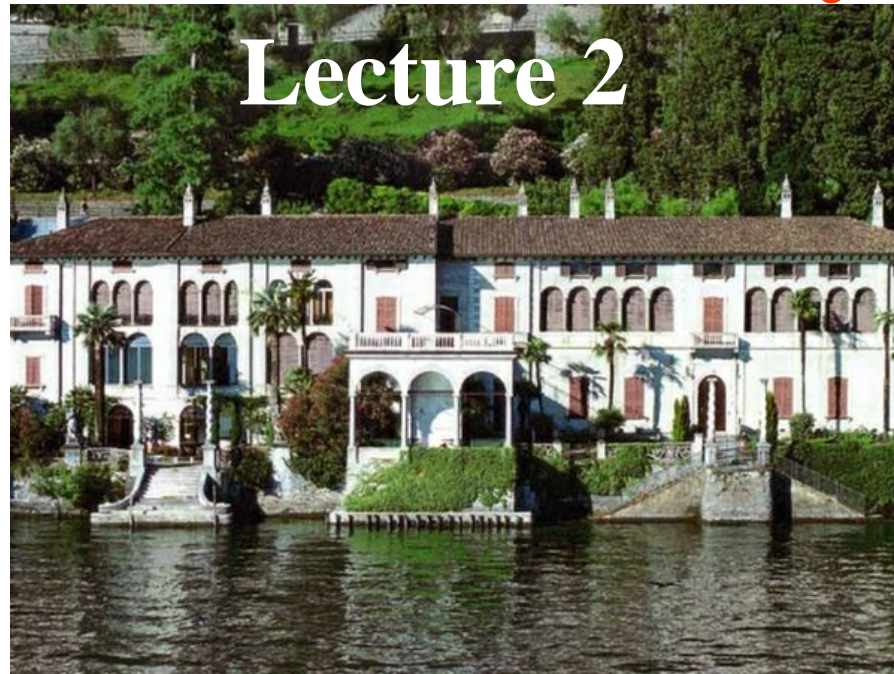
Audience Participation is Required

Self-Assembly of Diblock Copolymers in Selective Solvents

Non-selective solvent (good or theta for both blocks): solution of diblock coils
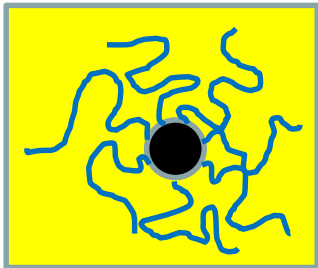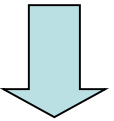
Reduce solvent quality for one block (T, p, pH, etc.)

Hydrophobic block collapses into a globule converting diblock coils into tadpoles.
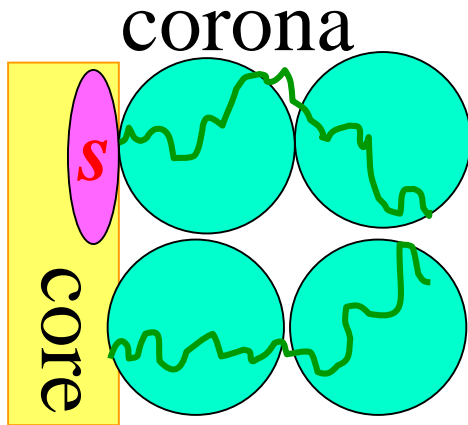
Above critical micelle concentration CMC (temperature CMT) tadpoles self-assemble into micelles in order to lower interfacial energy.

Stabilization mechanism – steric repulsion between hydrophilic corona blocks

Interface – Corona Balance

Self-assembly is driven by the "desire" or core blocks to reduce interfacial energy (and thus area *s* per chain).

This results in increasing overlap, steric repulsion, and elongation of corona blocks that limits the decrease of *s*.
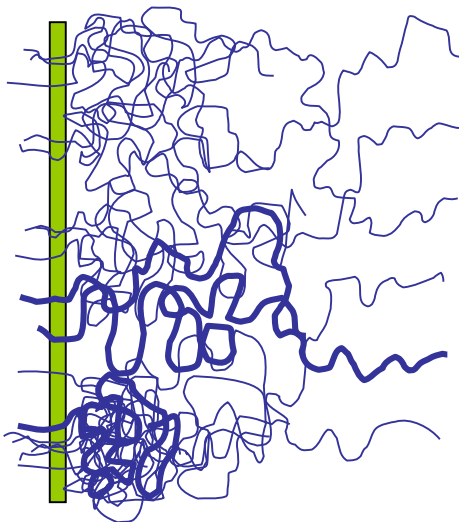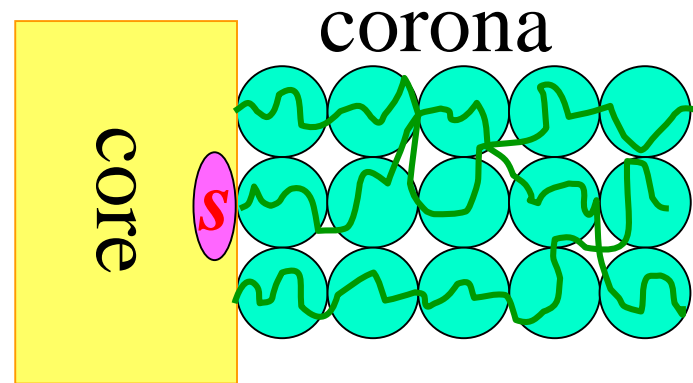
Equilibrium properties of micelles are determined by the balance of corona and interfacial free energies.

$$F_{corona} \sim F_{interface} >> kT$$

Shapes of Micelles

spherical   **cylindrical (worm-like)**   **planar (bilayer)**

Terminology of micellar hair-styles
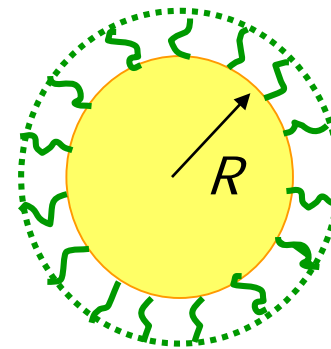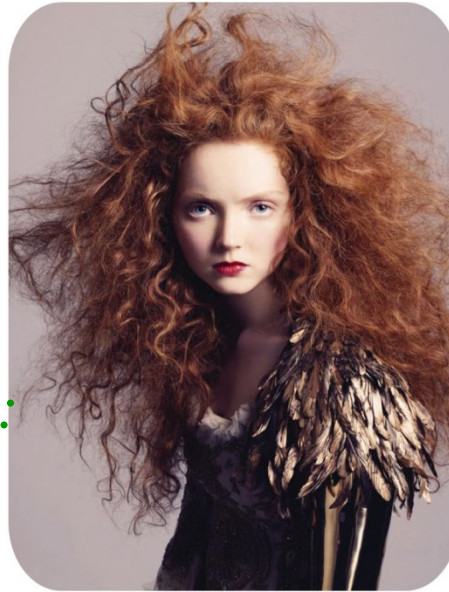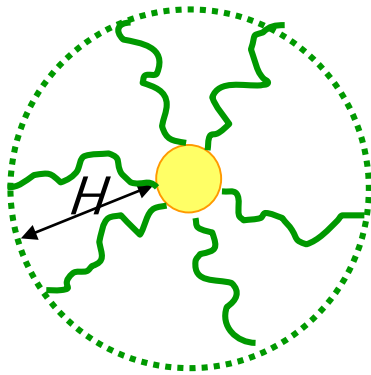
Hairy (star-like) micelle:
corona thickness
H > core radius R

Crew-cut micelle: corona
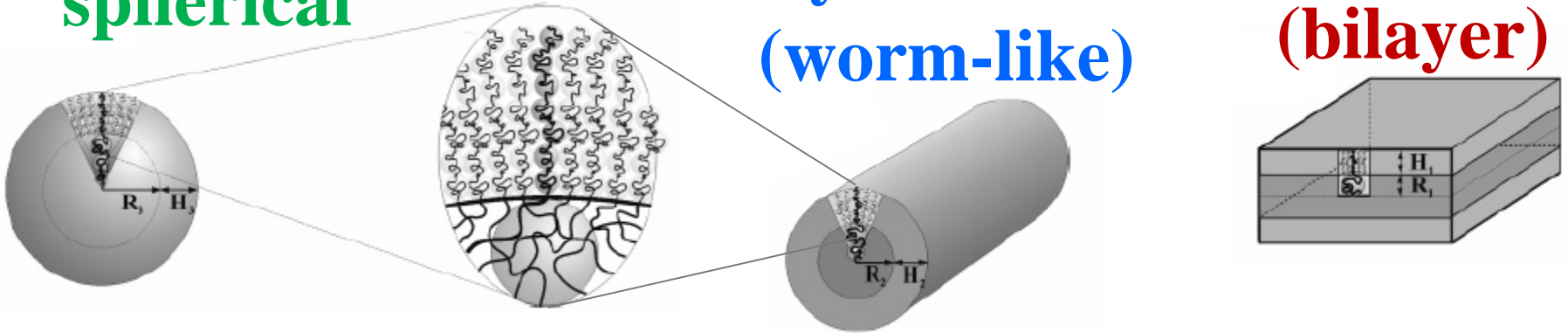thickness H < core radius R

Balancing Free Energies Within Micelle

$$F_{Total} = F_{corona} + F_{interface} + F_{core}$$

Free energy of the **corona** depends on the **solvent quality** determined by measuring **second virial coefficient** (A_2) of hydrophilic chain.

R_{core}

Core

Corona

$$F_{interface} = 4\pi R_{core}^2 \gamma$$

Surface free energy at the **interface** arises from the interaction of **hydrophobic core blocks** with water in corona.

Coronas Desire More Space

Area per chain s in coronas of micelles of morphology j varies with distance r from core center

$$s(r) = s(R)(r/R)^{j-1}$$

planar $j = 1$ $s(r) = const$

cylindrical $j = 2$

spherical $j = 3$

Steric repulsion between corona chains is weakest in spherical and strongest in planar geometries.
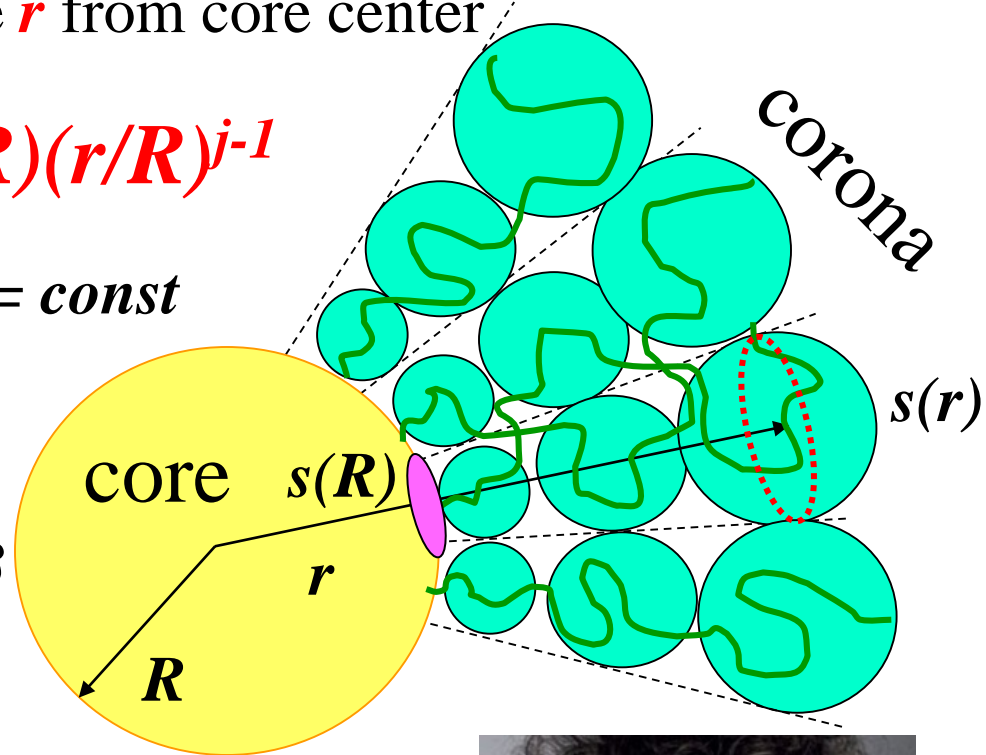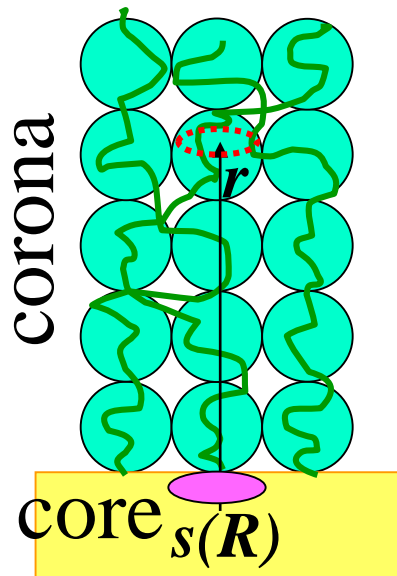
Star-like spherical micelles are favorable for very long hydrophilic blocks.

Equilibrium - lowest total free energy $\boldsymbol{F} = \boldsymbol{F_{core}} + \boldsymbol{F_{corona}} + \boldsymbol{F_{interface}}$

Core Free Energy $\boldsymbol{F_{core}}$

Hydrophobic interaction between core blocks B determines core volume fraction ϕ'' and does not depend on micelle morphology j.

Core volume fraction $\phi`` = j\dfrac{b^3 N_b}{sR_j}$

s – interface area per chain

sR_j/j – core volume per chain

Elastic stretching of core blocks $\boldsymbol{F_{core}}$ depends on micelle morphology j

$$\frac{F_{core}}{kT} = k_j \frac{R_j^2}{b^2 N_B} = k_j j^2 \frac{b^4 N_B}{s^2 \phi``^2} \qquad k_1 = \frac{\pi^2}{8} \quad k_2 = \frac{\pi^2}{16} \quad k_3 = \frac{3\pi^2}{80}$$

$$R_j = j\frac{b^3 N_b}{s\phi``}$$

Elastic free energy of core $\boldsymbol{F_{core}}$ is the smallest term of total $\boldsymbol{F}$.

$$\boldsymbol{F_{core}} < \boldsymbol{F_{corona}} \sim \boldsymbol{F_{interface}}$$
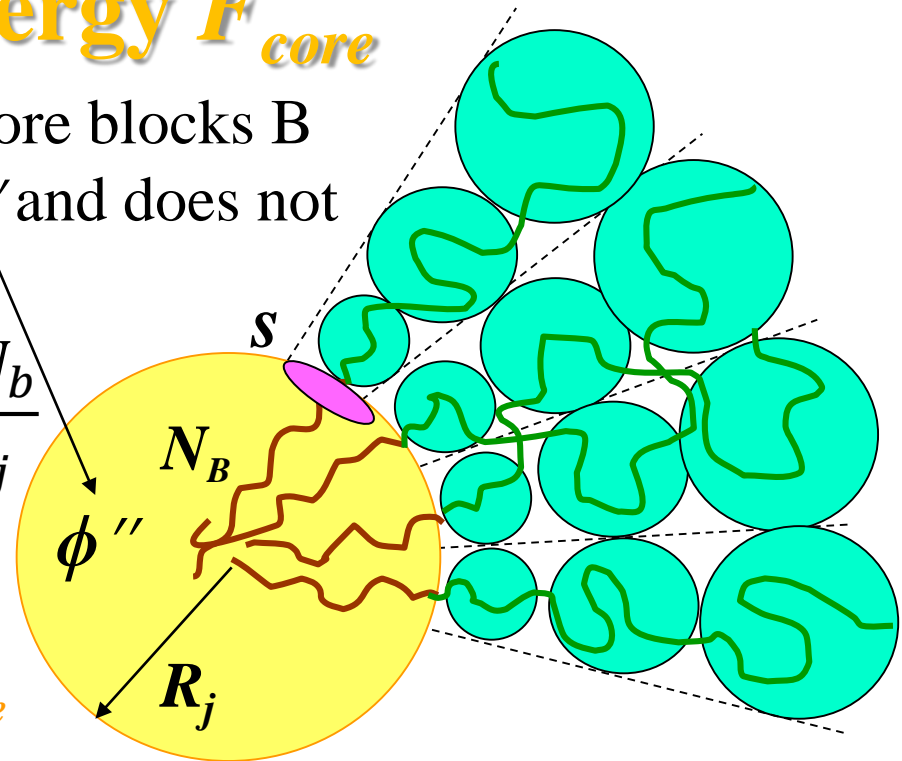
Equilibrium - lowest total free energy $F = F_{core} + F_{corona} + F_{interface}$

Interfacial Free Energy $F_{interface}$

Interfacial free energy per chain

$$\frac{F_{interface}}{kT} = \gamma \frac{s}{b^2} = \gamma j \frac{N_B b}{\phi`` R_j}$$

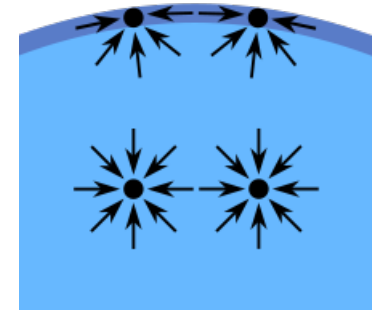γ – interfacial (surface) energy per monomer b^2

s - interface area per chain $\quad s = j \frac{b^3 N_b}{\phi`` R_j}$

Isolated Spherical Globule

Radius of the globule
– single collapsed block B $\quad R_{B0} = b \left(\frac{3 N_B}{4 \pi \phi``} \right)^{1/3}$
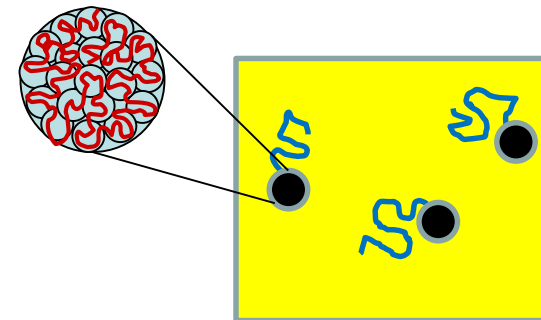
Surface free energy
of a unimer $\quad \frac{F_{s0}}{kT} = 4 \pi \gamma \left(\frac{R_{B0}}{b} \right)^2 = (36\pi)^{1/3} \gamma \left(\frac{N_B}{\phi``} \right)^{2/3}$
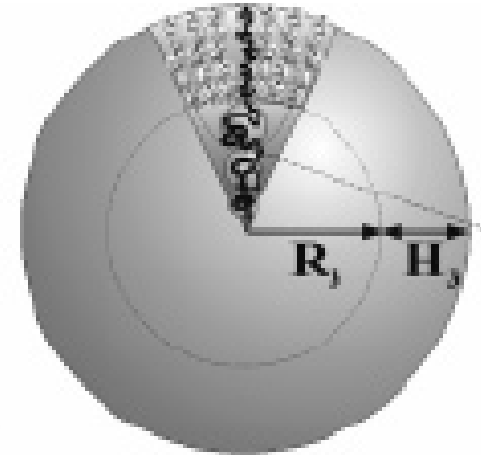
Spherical Micelle

$$F_3 = F_{core} + F_{interface} + F_{corona}$$

$$\frac{F_3}{kT} = \frac{3\pi^2 R_3^2}{80 N_B b^2} + \gamma \frac{3 N_B b}{\phi`` R_3} + C_F \frac{\phi``^{1/2} R_3^{3/2}}{N_B^{1/2} b^{3/2}} \ln\left[1 + C_H N_A \left(\frac{\phi`` b}{R_3 N_B}\right)^{1/2}\right]$$

Minimize total free energy $\partial F_3 / \partial R_3$ to calculate core radius R_3

Corona thickness

$$H_3 = R_3 \left\{ \left[1 + C_H N_A \left(\frac{\phi`` b}{R_3 N_B}\right)^{1/2}\right]^{1/2} - 1 \right\}$$

Total size of a spherical micelle $\quad R_3^{tot} = R_3 + H_3$

Aggregation number – total number of chains per micelle

$$Q = \frac{4\pi R_3^3 \phi``}{3 N_b b^3}$$

Zhulina, E.B.; Adam, M.; LaRue, I.; Sheiko, S.S. Rubinstein, M. *Macromolecules* 2005, *38*, 5330.

Strong Micellization: Spherical Micelles

Equilibrium properties of spherical micelles are determined by the balance of corona and interfacial free energies

$$F_{corona} \sim F_{interface} \gg kT$$

Aggregation number Q decreases with increasing DP N_A of solvophilic block (PI in n-heptane) and increases with DP N_B of core block (PS).
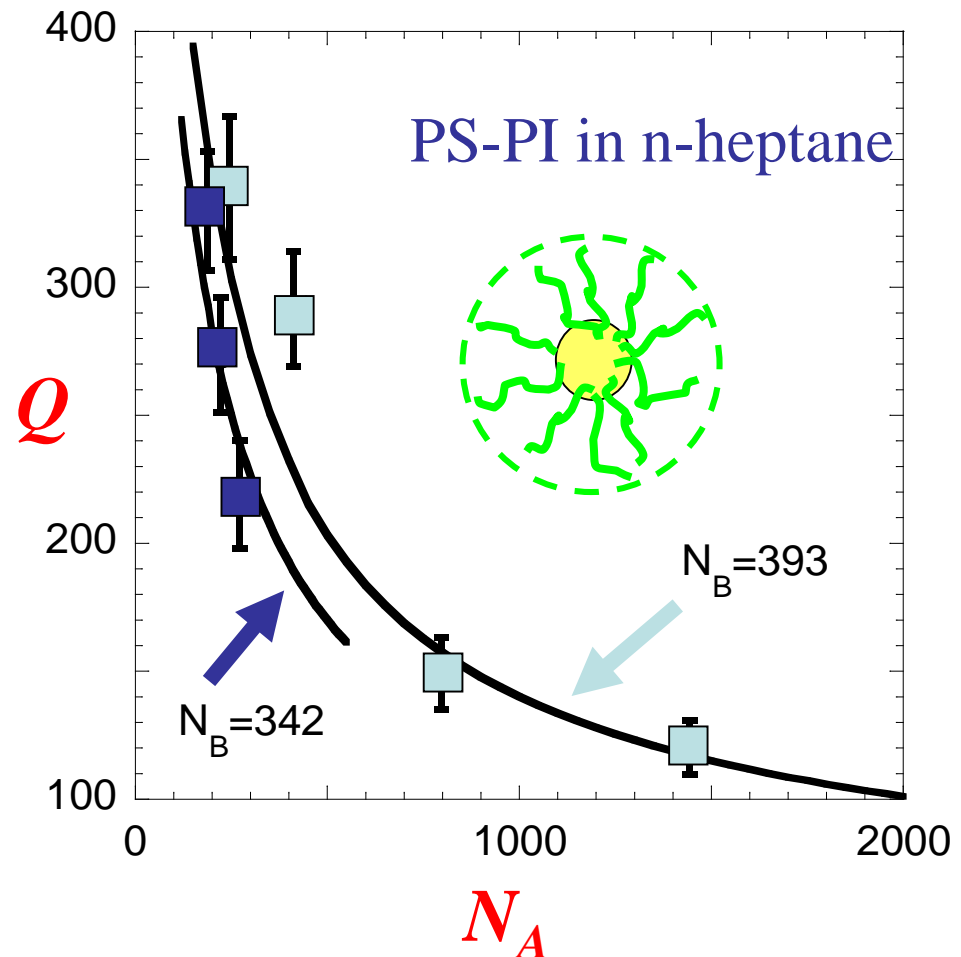
$$Q \sim N_B^2 N_A^{-0.47}$$

Solid lines – scaling theory
Points – data from light scattering
Zhulina, E.B.; Adam, M.; LaRue, I.; Sheiko, S.S. Rubinstein, M. *Macromolecules* 2005, *38*, 5330.

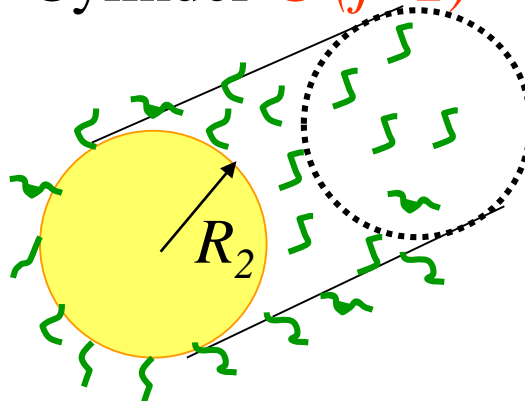
PS-PI in n-heptane

N_B=393

N_B=342

Q

N_A

Morphological Transitions of Strong Micelles

Morphological transitions occur for crew-cut micelles.
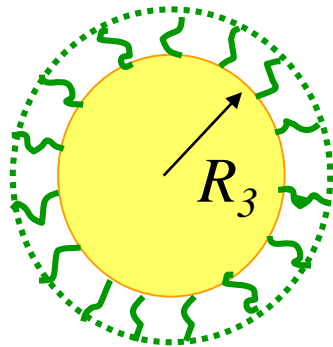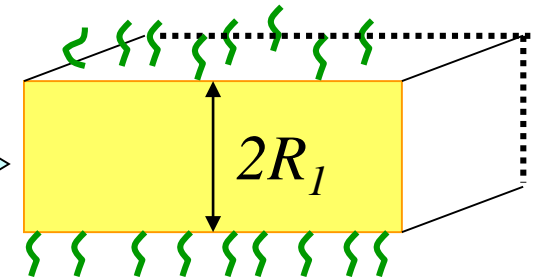
Sphere S *(j=3)*   Cylinder C *(j=2)*   Lamella L *(j=1)*

Free energy per chain **F/kT**
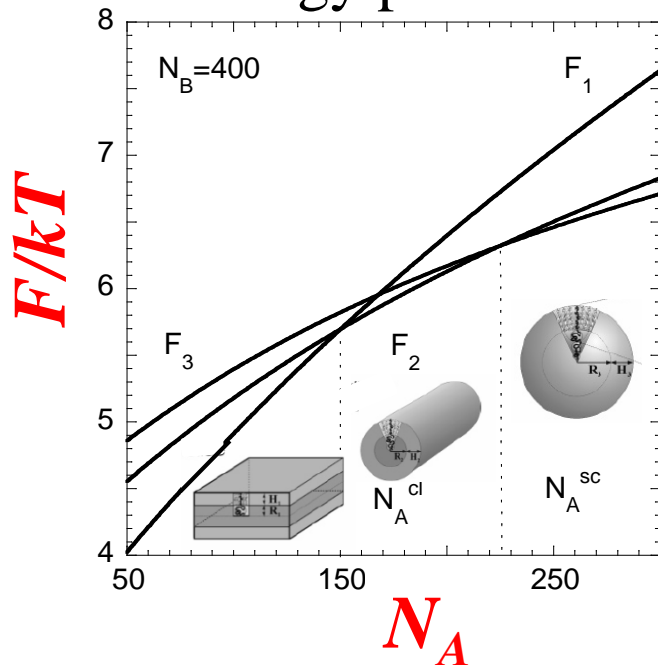
corona-to-core size ratio H_j/R_j

Balance of core block elongation F_{core} and shape corrections to F_{corona}
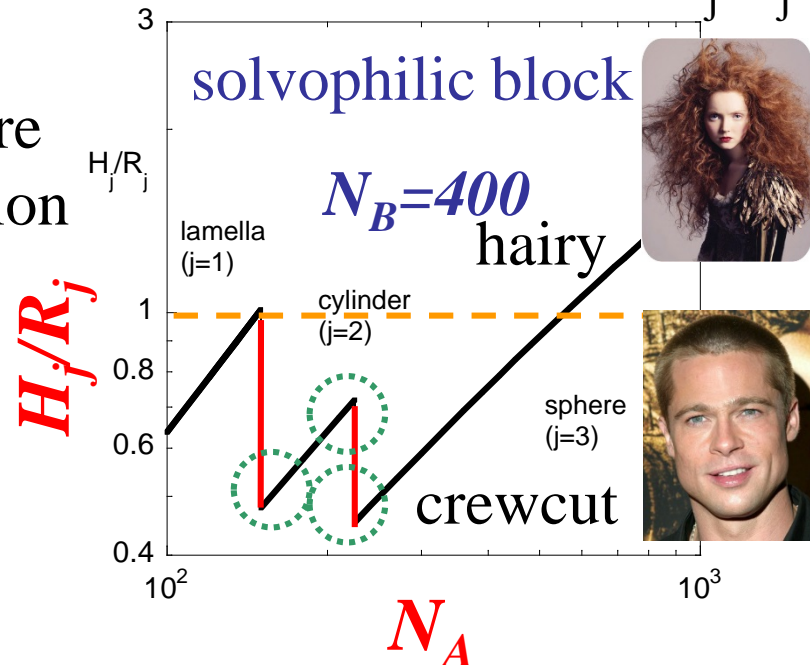
Diagram of States for Strong Block-Copolymer Micelles

PS-PI in n-heptane

◆ Spherical micelle
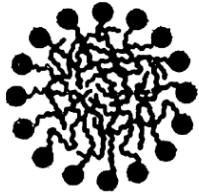
▲ Cylindrical micelle

■ Lamellar mesophase

S

Crew-cut micelles with elongated corona block

C

L

N_{PI}

N_{PS}

250   350   450

280

200

120

125nm

1μm

250nm

vesicles

Exact binodals ——
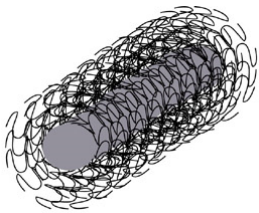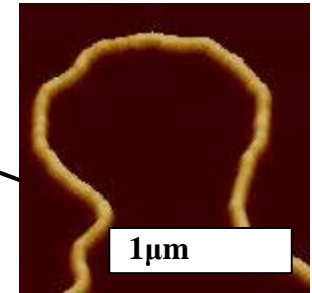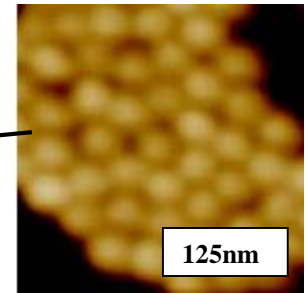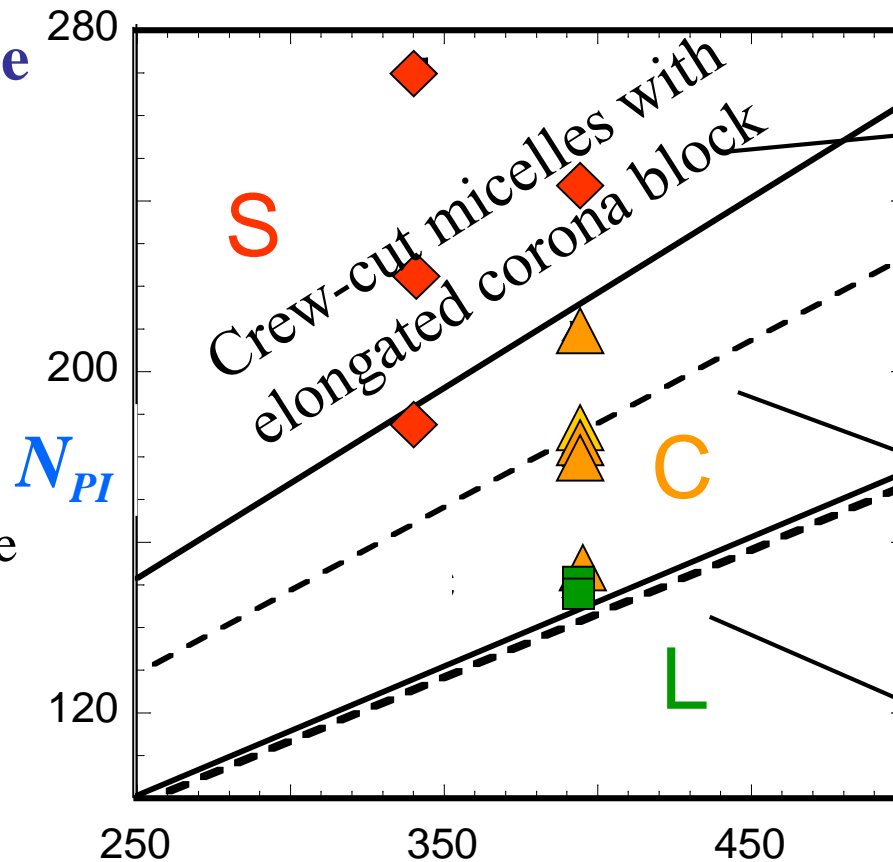
Approximate binodals – – –

Zhulina, E.B.; Adam, M.; LaRue, I.; Sheiko, S.S. Rubinstein, M. *Macromolecules* 2005, *38*, 5330.

Diagram of States for Block-Copolymer Micelles
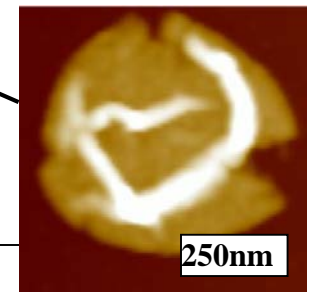

"strong" micelles

Star-like micelles with elongated corona block

Crew-cut micelles with elongated corona blocks

spheres

cylinders

vesicles

"weak" micelles N_{PI}

N_{PS}

125nm

1μm

250nm

- ● Spherical
- ▢ Cylindrical
- ✕ Cylindrical and Spherical
- ＋ Insoluble
- ▲ Vesicle and nano-doughnuts
- — Sphere-cylinder transition
- - - cylinder-lamella transition
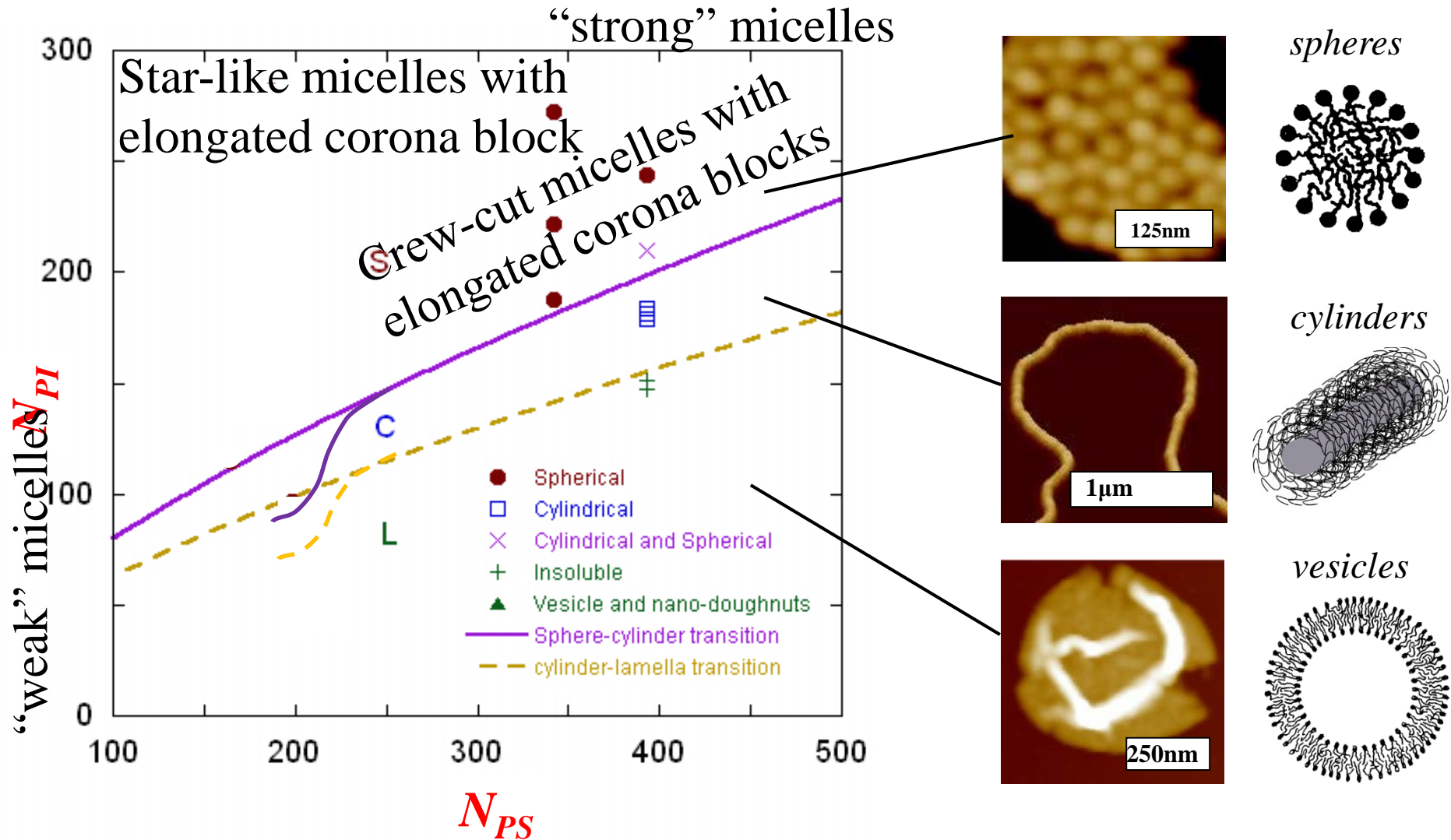
Reversible Morphological Transitions of Polystyrene-*b*-Polyisoprene Micelles in Heptane
Zhulina, E.B.; Adam, M.; LaRue, I.; Sheiko, S.S. Rubinstein, M. *Macromolecules* **2005**, *38*, 5330.
Isaac LaRue, Mireille Adam, Marinos Pitsikalis, Nikos Hadjichristidis, Michael Rubinstein, and
Sergei S. Sheiko *Macromolecules*, **2006**, *39*, 309–314

Micelles Undergo Morphological Transformations in the Crew-Cut Regime ($H_{corona} < R_{core}$)

N_A

Is there a regime with weakly elongated (almost unstretched) corona blocks?

Star-like micelles with elongated corona blocks

Unimers, no micelles

Crew-cut micelles with elongated corona

Other morphologies & sediment

N_B

What are chain properties that make this regime wider?

Reduce surface tension γ

Reduce repulsion in corona
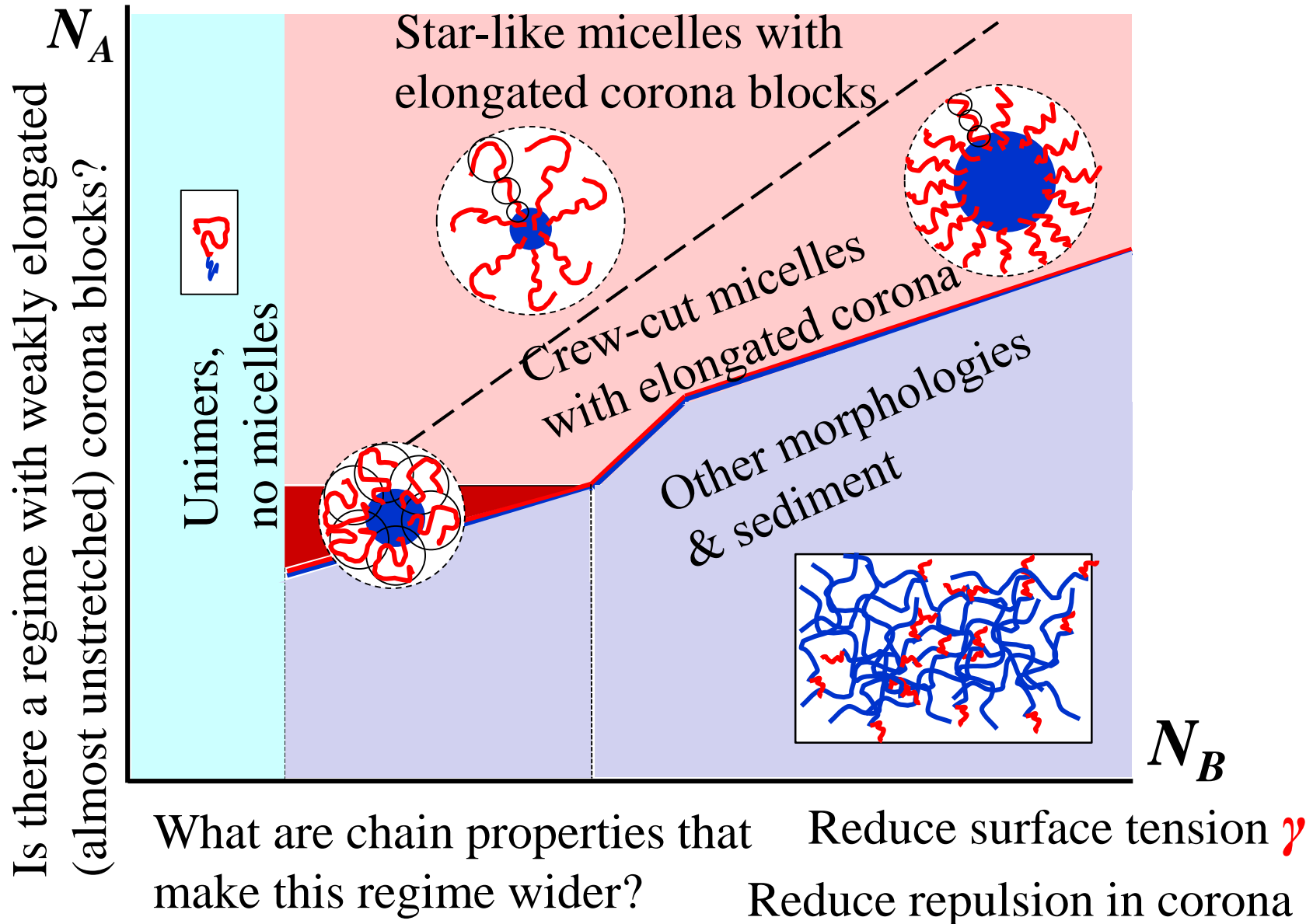
Elastin-Like Polypeptides (ELPs)

[Valine-Proline-Glycine-X-Glycine]$_n$ n = 10-330 pentapeptides
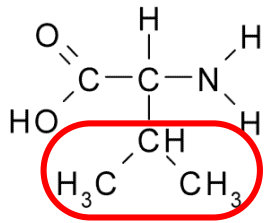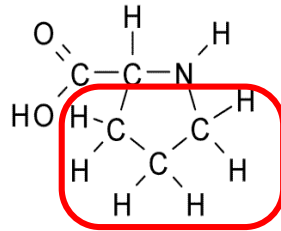
Valine   **Proline**   **Glycine**
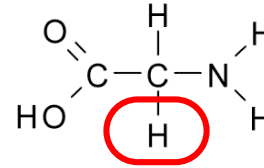
X is any guest amino acid except proline

for example: **Serine**
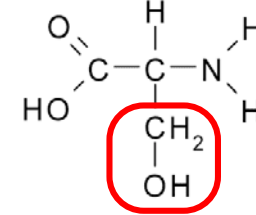
ELPs are perfectly monodispersed structurally disordered polypeptides.

ELPs are synthesized recombinantly by expression of a synthetic gene in E. coli and have complete sequence & molecular weight control.

ELPs phase separate upon heating (LCST)

Unimer   Aggregate

Heat →
← Cool
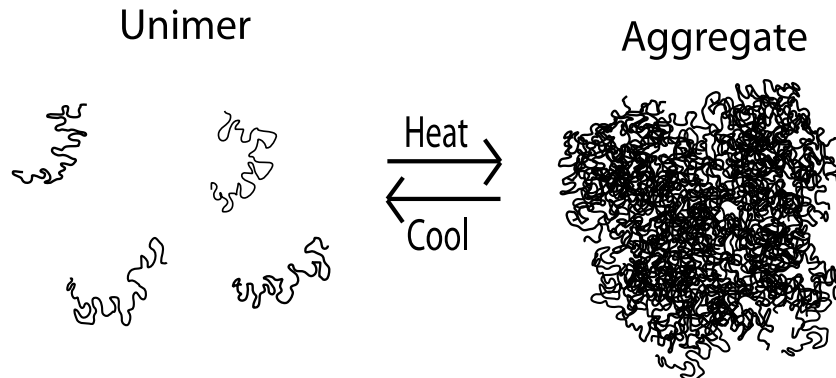
Phase Diagram of Elastin-Like Polypeptides
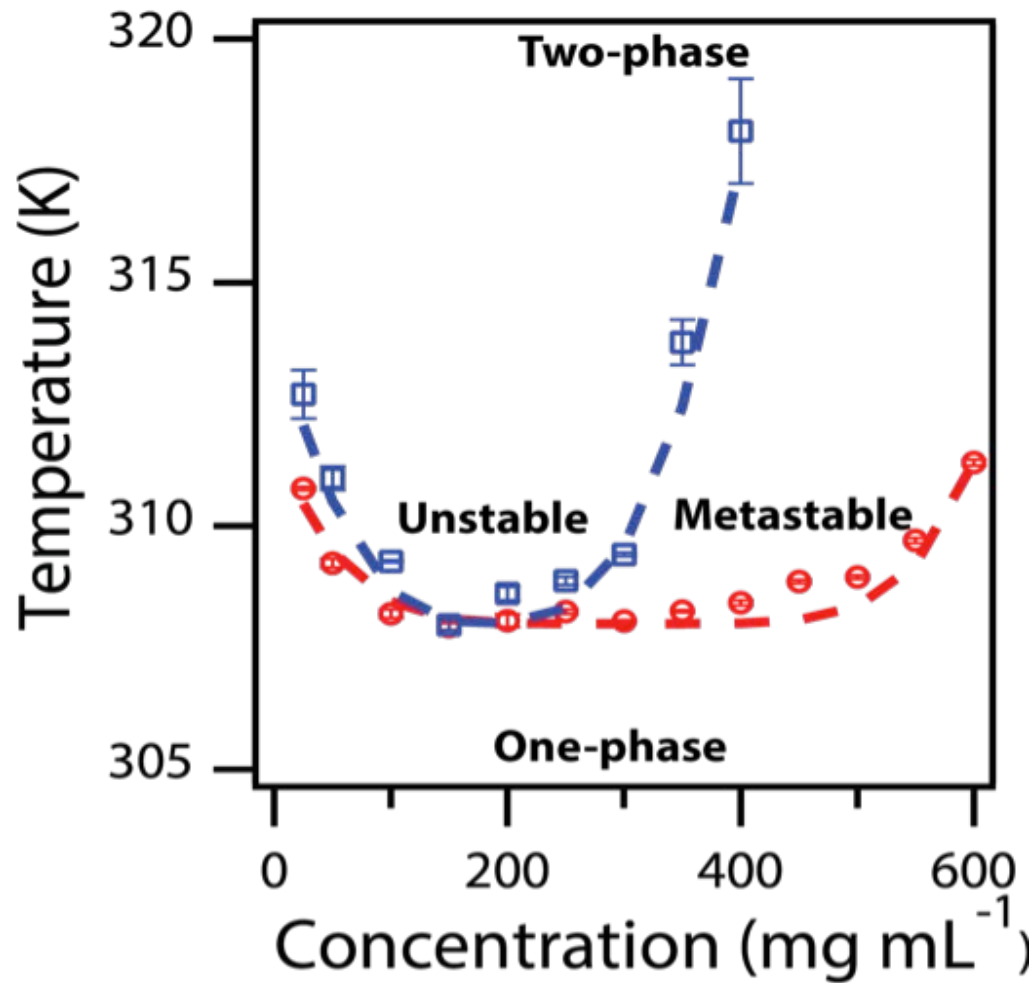
(Val-Pro-Gly-X-Gly)$_n$
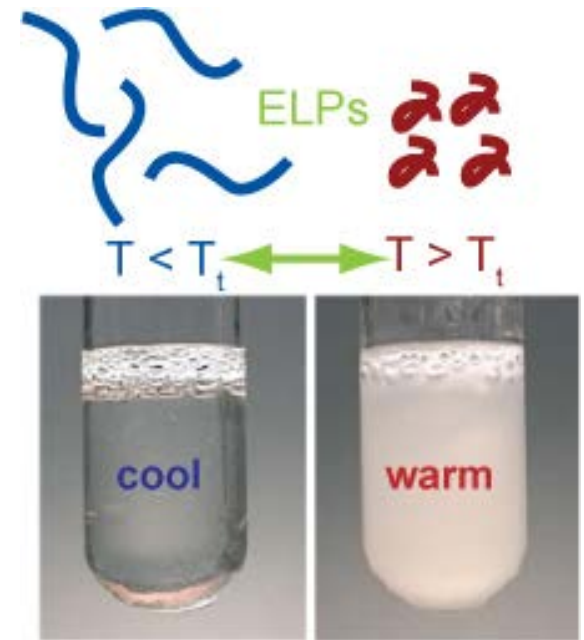
phase diagram of an ELP homopolymer
was obtained by DLS and SLS

Simon   *Carroll*

ELP Block Copolymer Self-Assembly

Each ELP block is **[Valine-Proline-Glycine-X-Glycine]$_n$**
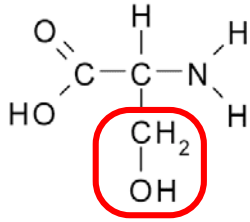
Hydrophilic ELP   Hydrophobic ELP

X =Serine   X =Valine
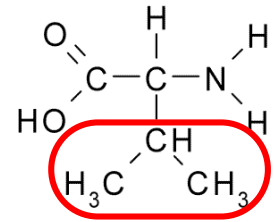
Both blocks share four out of five repeat amino acids.

Unimer   Micelle   Aggregate

Heat →
← Cool
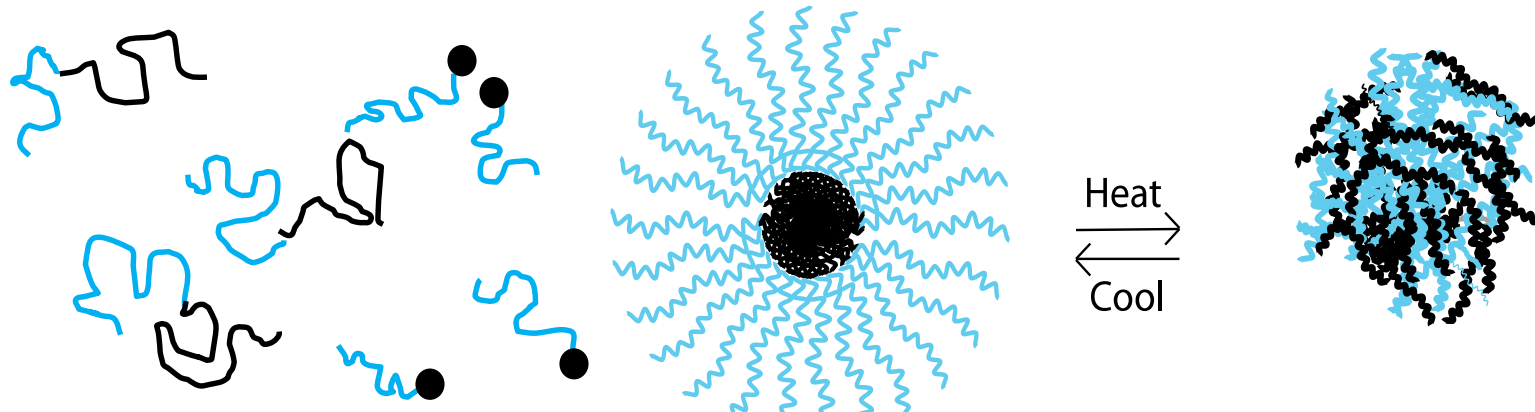
Temperature

CMT   **T$_{aggregation}$**

Critical Micelle Temperature (CMT)

Surface – theoretical prediction of CMT

$$\mu_{unimer} = \mu_{micelle}$$

number of pentapeptides per block
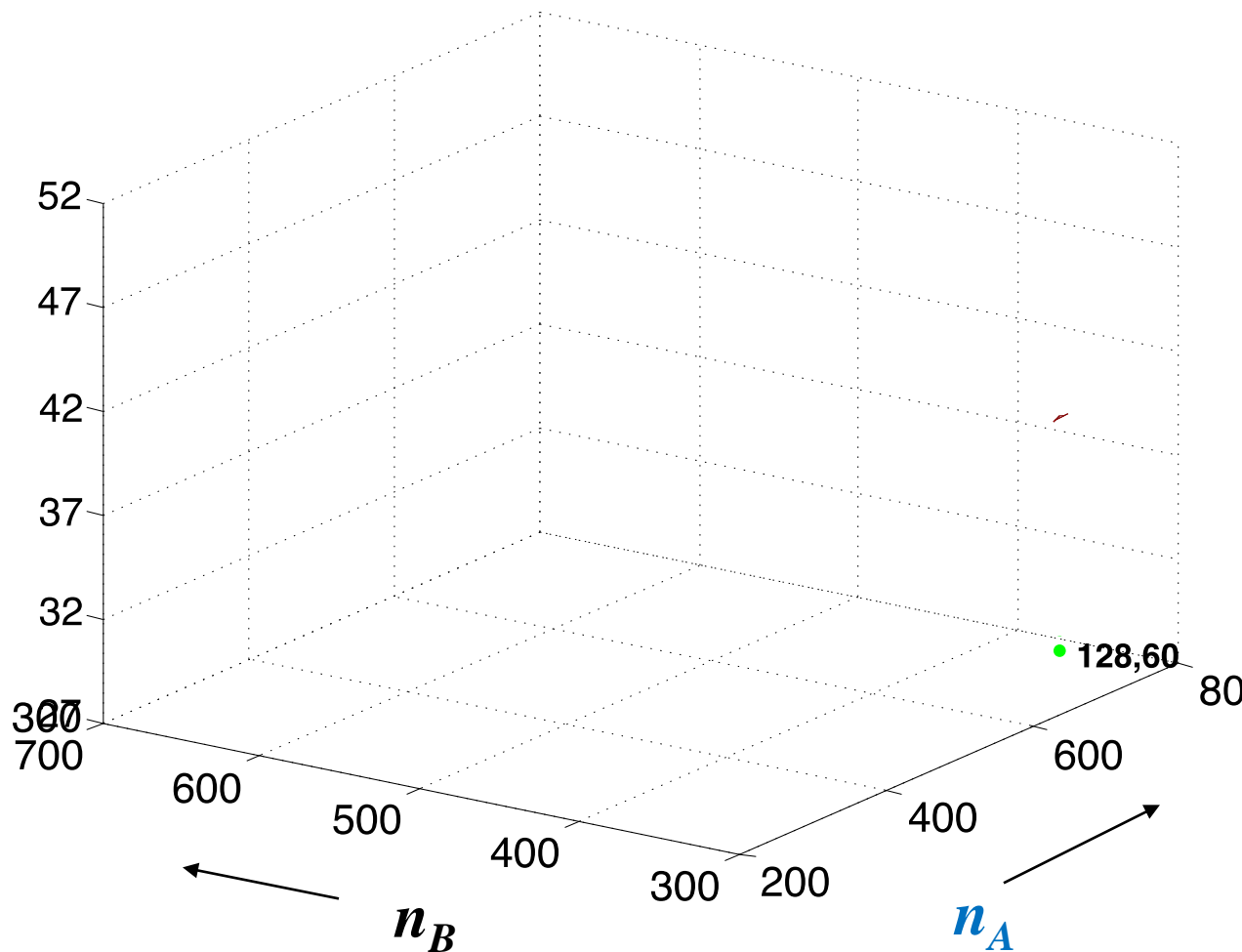
W. Hassouneh, E. B. Zhulina, A. Chilkoti, and M. Rubinstein *Macromolecules 48*, 4183–4195, **2015**

CMT decreases with length n_B of hydrophobic block and is almost independent of the length of hydrophilic block.

Scaling Diagram for Weak Micelles that form at low surface tension (ELPs)
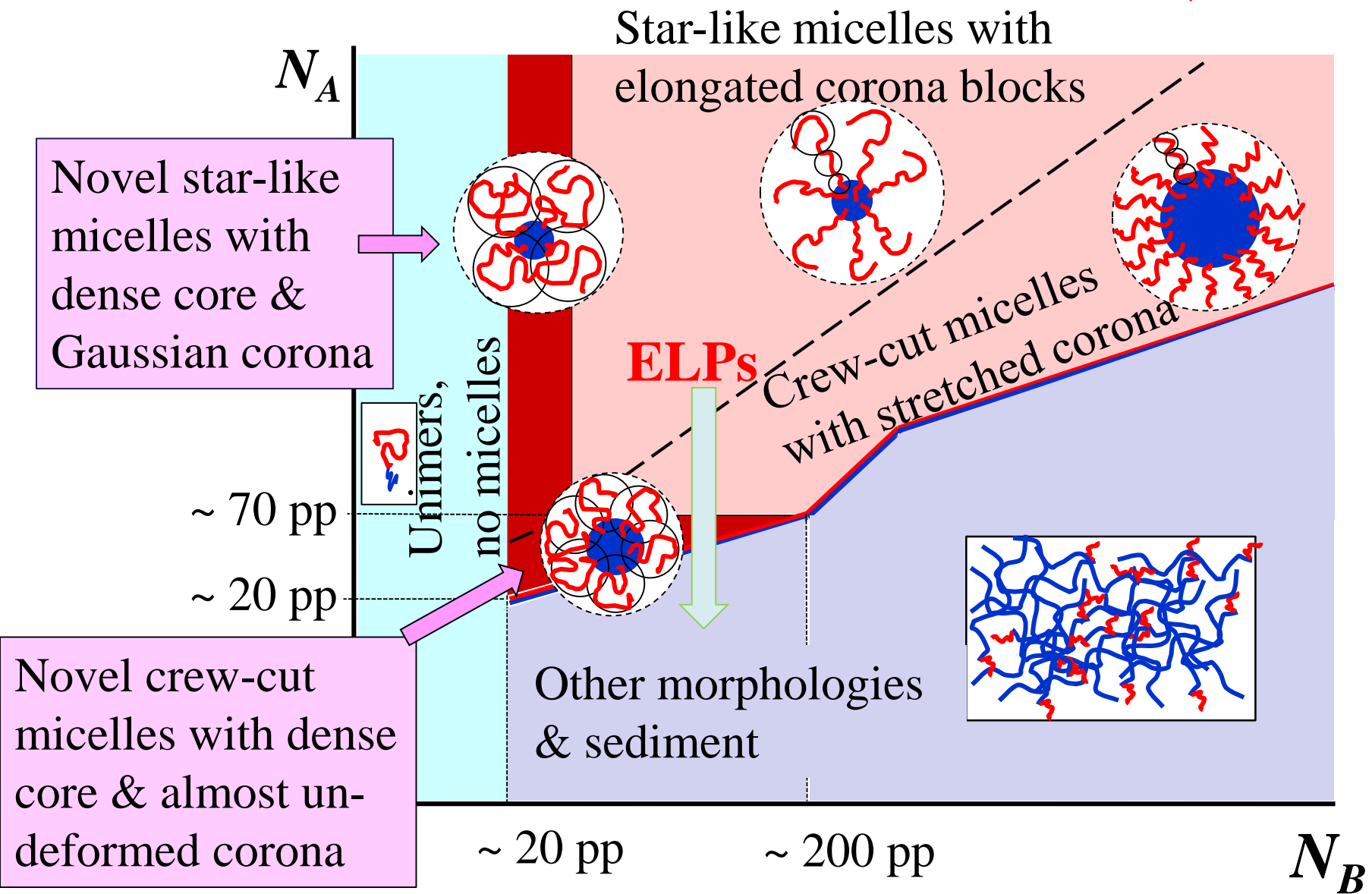
Complexation of Oppositely Charged Polyelectrolytes and Block Polyampholytes

The Story of Love and Hate in Charged Systems

General Rule

Both for Electrostatics and for Life

Stay close

to the ones you Love

and stay away

from the ones you Hate.

Classes of Charged Systems
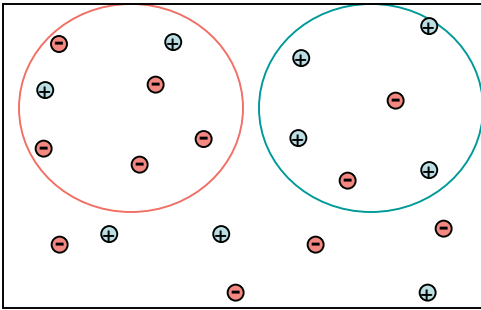
ionic solution
(simple salt)
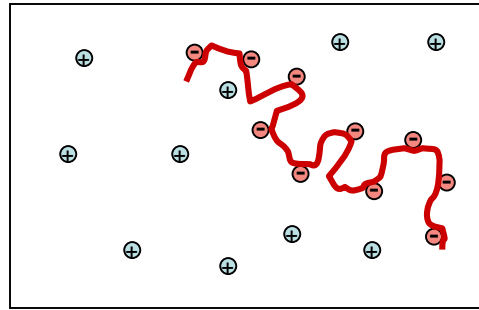
polyelectrolyte
solution
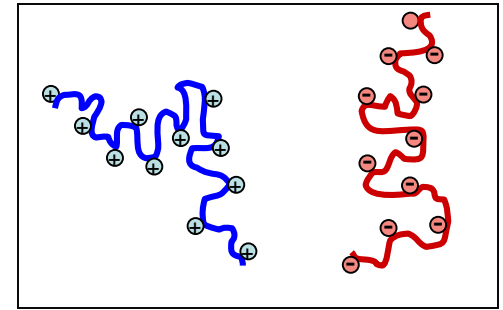
solution of
oppositely charged
polyelectrolytes

Polyampholytes
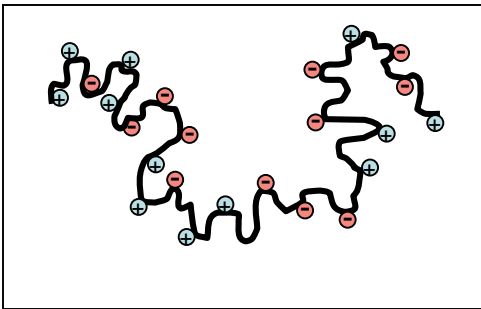
Ionomers

random
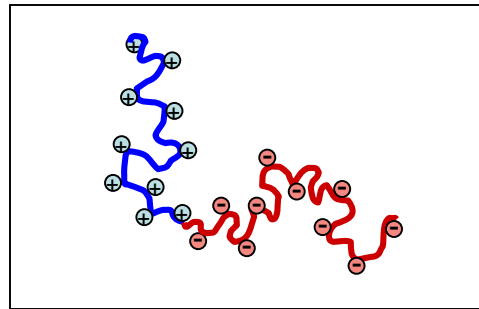
block
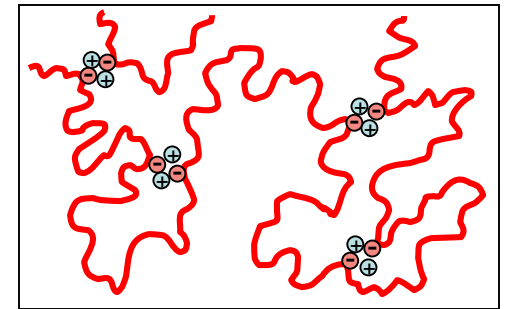
Two Types of Attraction

"Weak" fluctuation-induced attraction

- less than kT per charge
- high T, high ε,
- low valence, low charge density

Flirting regime
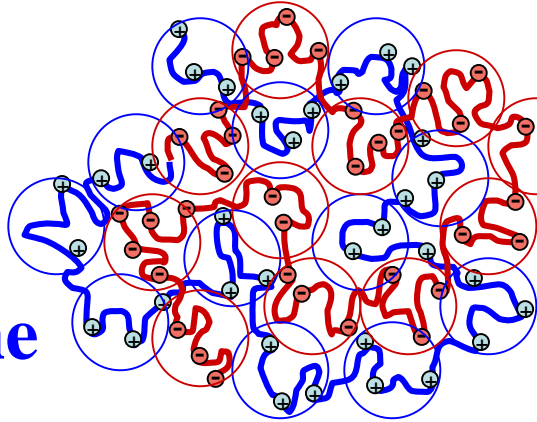
"Strong" binding

- more than kT per charge
- low T, low ε,
- high valence, high charge density

Marriage and beyond
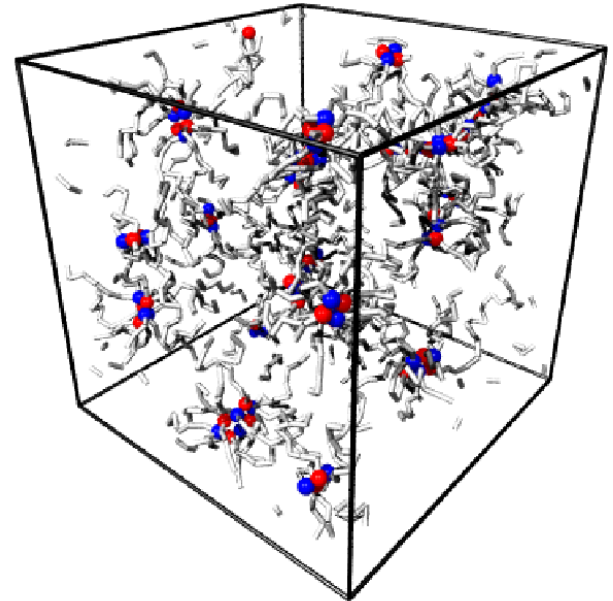
Coil-Globule Transition of a Symmetric Block Polyampholyte
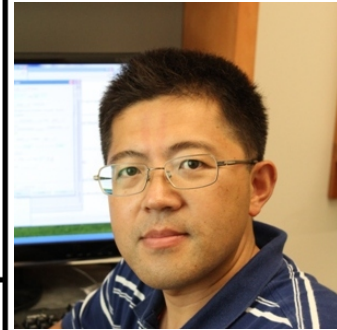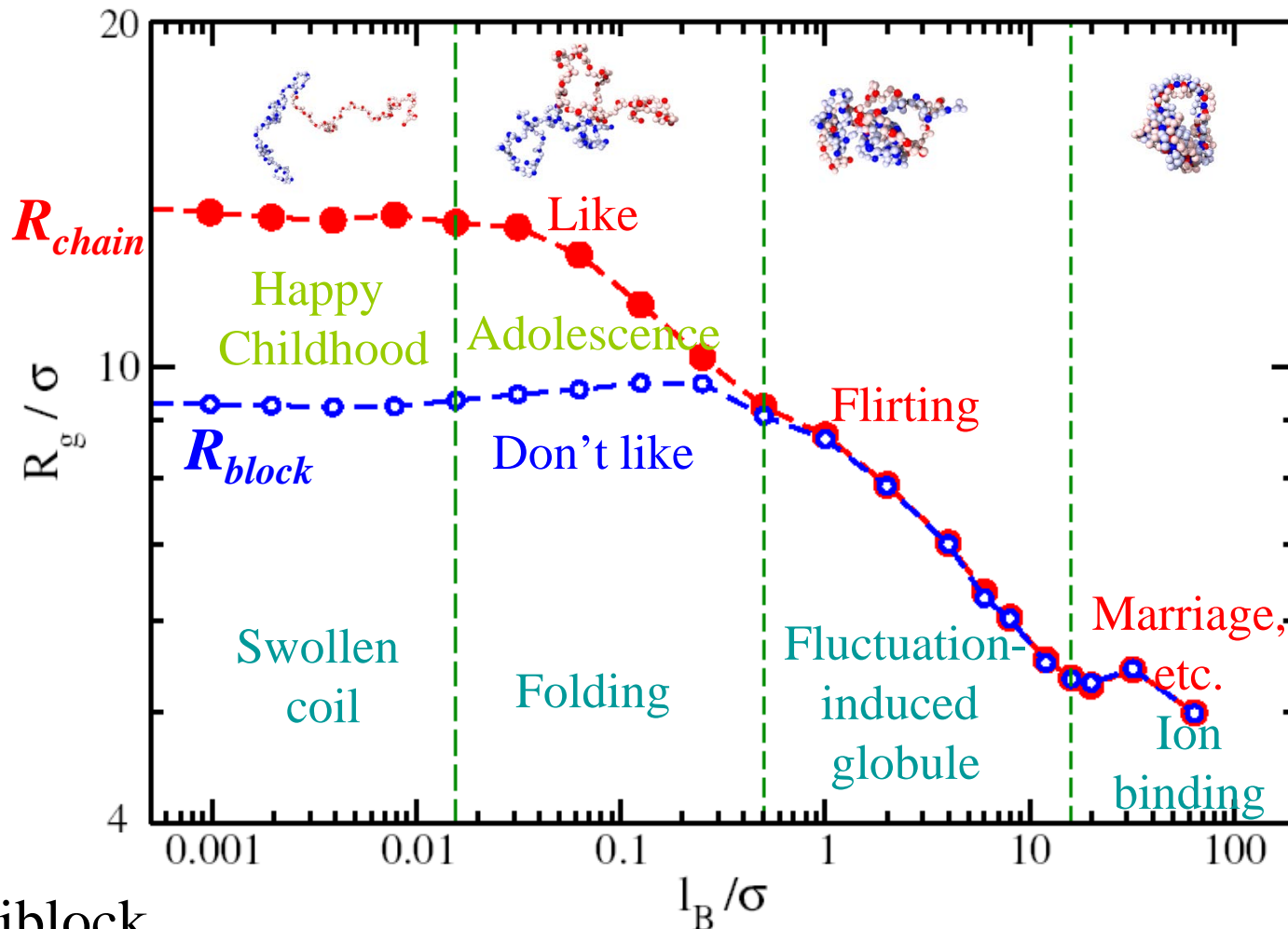
Zuowei Wang University of Reading, UK

- diblock
- individual blocks

$N = 256, f = 1/4$

Bjerrum length $l_B = \dfrac{e^2}{kT\varepsilon}$

Weak Association – "Flirting" Regime

"Flirting" globule – dense packing of electrostatic attraction blobs. Electrostatic blob with size ξ_e is a section of the chain with electrostatic energy kT.

Distance to the Nearest Opposite Charge
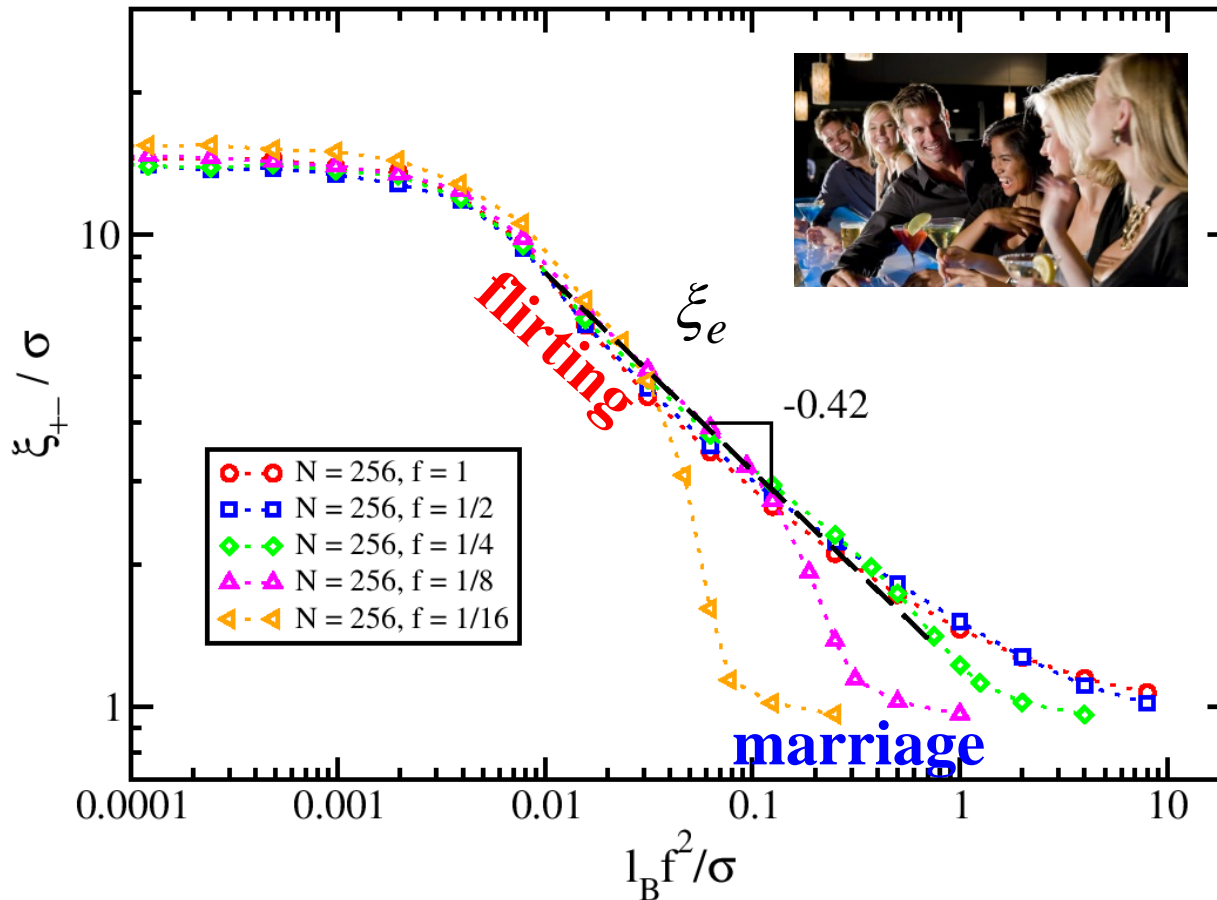
de Gennes et al 1976

$$\xi_e \approx b \left(\frac{l_b f^2}{b} \right)^{-\frac{\upsilon}{2-\upsilon}}$$
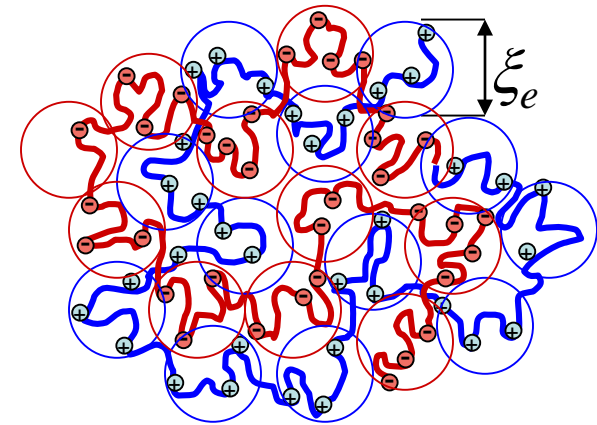
f – fraction of charged monomers

For $\upsilon = 0.588$, the "flirting" exponent $-\upsilon/(2-\upsilon) = -0.42$.

Boundary of the "Flirting" Regime

Upper boundary of the "flirting" regime is one charge per blob

$$\xi_{+-} \approx \xi_{++} \quad \rightarrow \quad \xi_e \approx bf^{-\upsilon} \approx l_B$$

- ▲ 4th nearest opposite
- ◆ 3rd nearest opposite
- ■ 2nd nearest opposite
- ● 1st nearest opposite

- ◇ 3rd nearest same sign
- □ 2nd nearest same sign
- ○ 1st nearest same sign

ξ_{+-}

$\xi_{++(--)}$

ξ / σ

quadrupole

octupole

dipole

l_B / σ
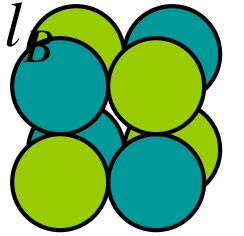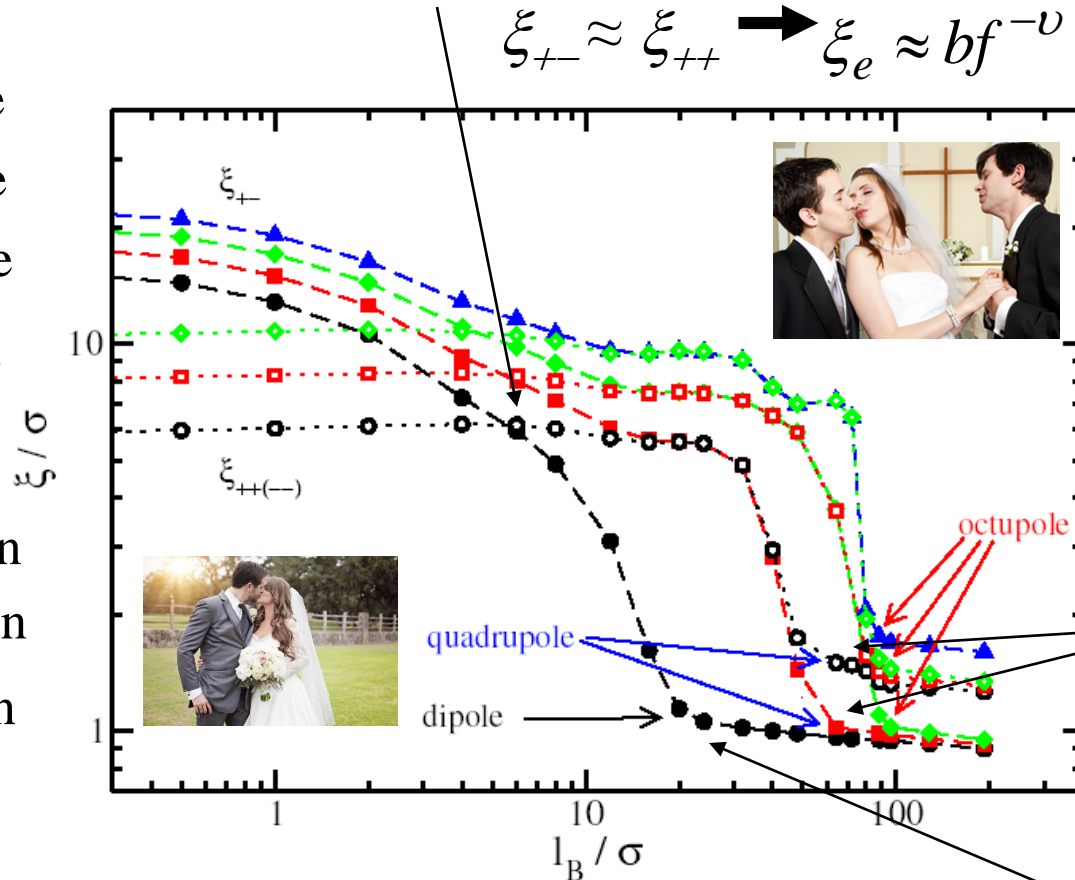
octupole
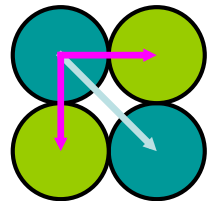
dipole
binding
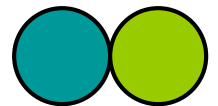
charge binding
(wedding)

N = 256, f = 1/16, good solvent

Probability of Finding a Charged Monomer in a Multiplet

single

"middle-age crisis"

married
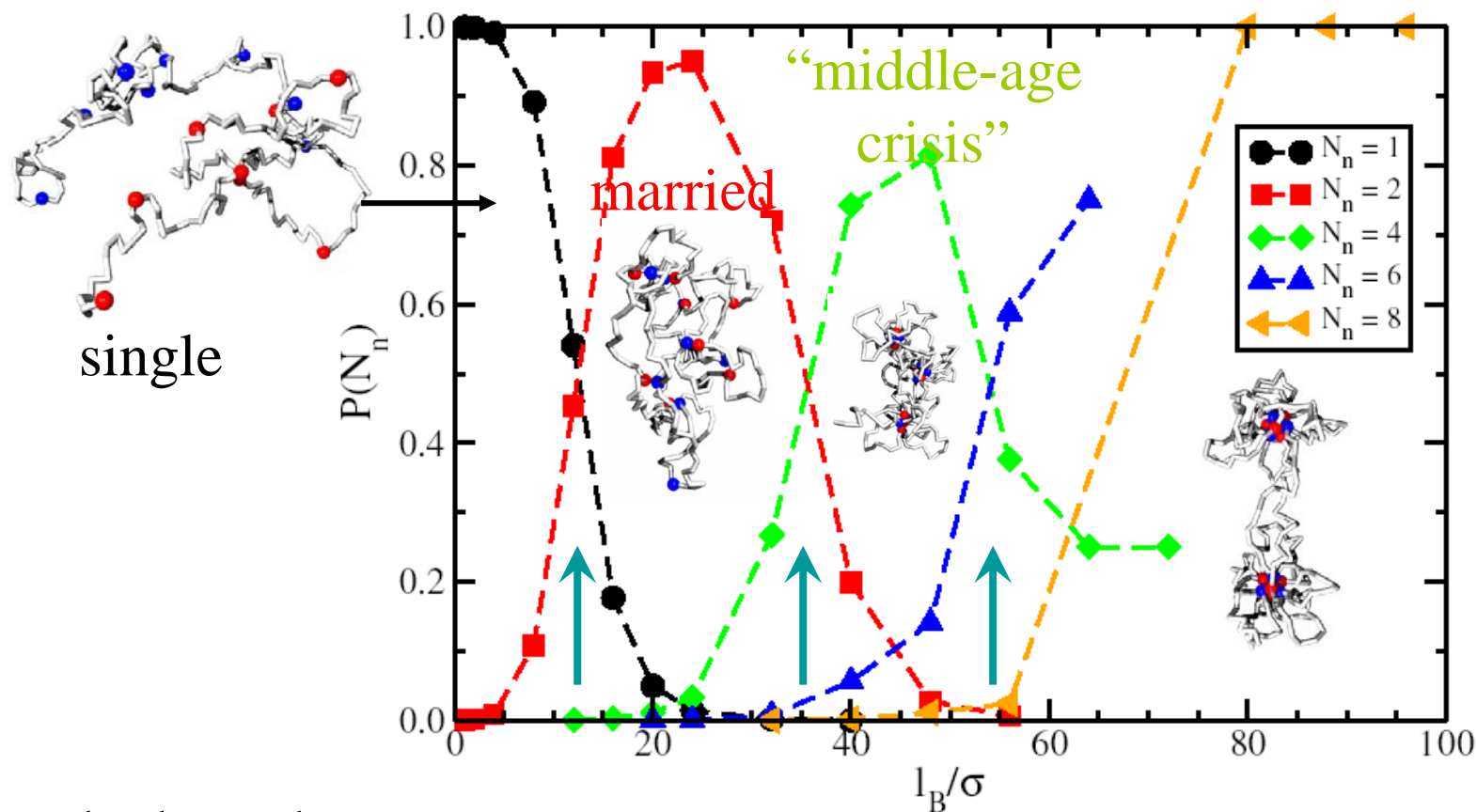
polyelectrolyte – ionomer transition

$N = 256$, $f = 1/16$, good solvent

Diagram of Conformational States

Z. Wang and M. Rubinstein,
Macromolecules **39**, 5897-5912 (2006)
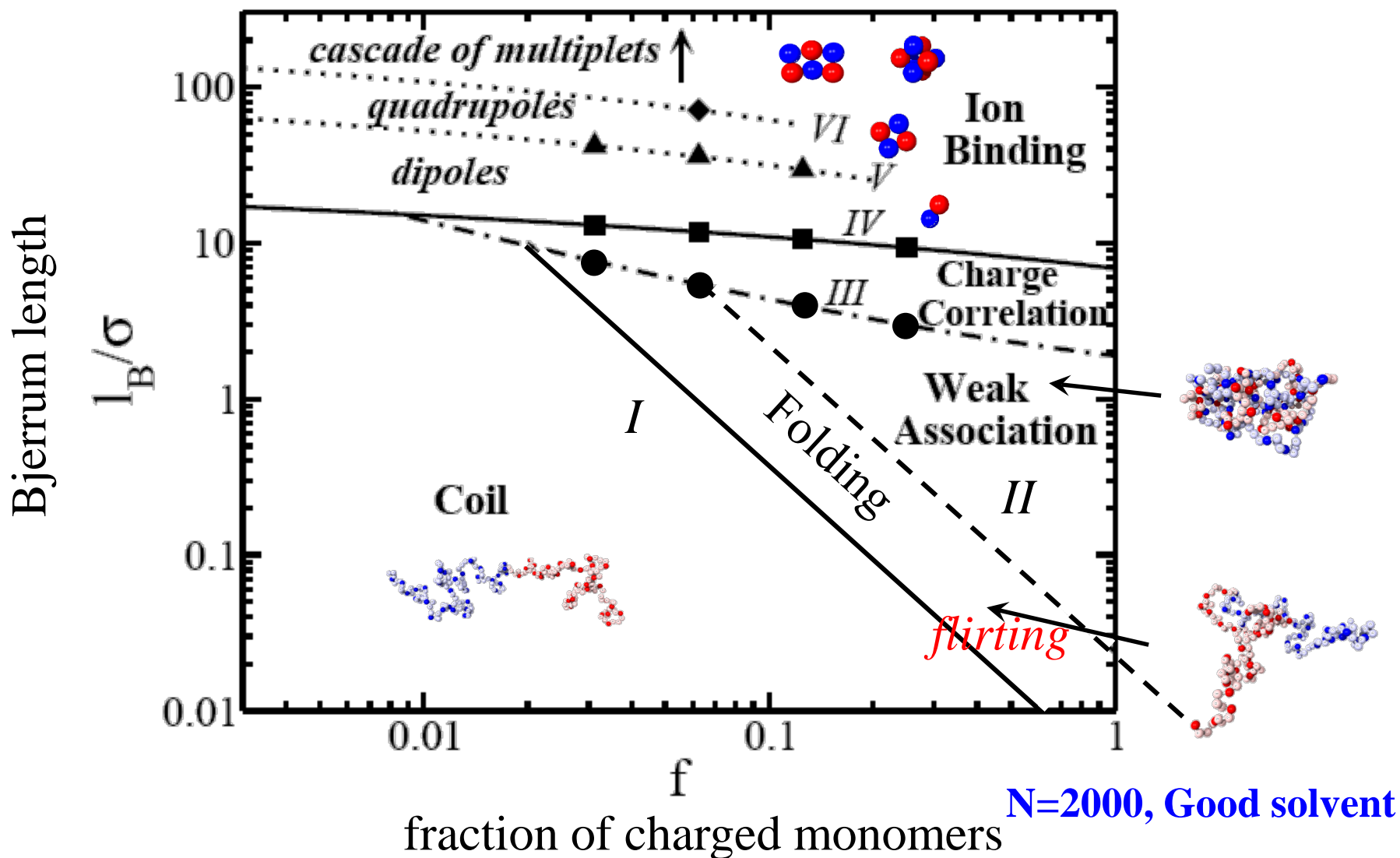
Asymmetric Block Polyampholytes

On the issue of equality

I. Asymmetry in Block Charge

$$Q_- < Q_+ \qquad f_- = f_+$$

II. Asymmetry in Charge Density

$$f_- > f_+ \qquad Q_- = Q_+$$
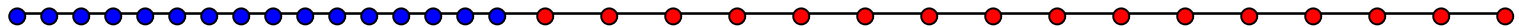
Asymmetry in Block Charge
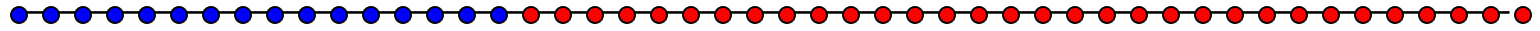
For small charge difference $\Delta N = N_+ - N_-$ both blocks are confined in a globule.

For large charge difference extra charge cannot be confined in a globule.

What will it do?

A. **Hate:** Extra section of the long block will form a tail of a tadpole.
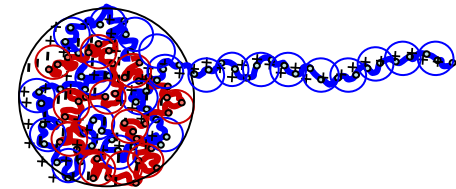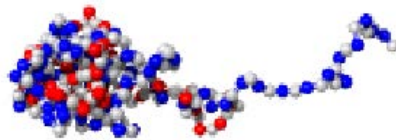
B. **Love:** A smaller section of the shorter block will accompany longer section of the larger block in a double-tail.

C. **Compromise:** Globule will elongate

D. All of the above.

E. None of the above.

Asymmetry in Block Charge

$N = 256$

$f = 1/2$

$l_B = 2\sigma$
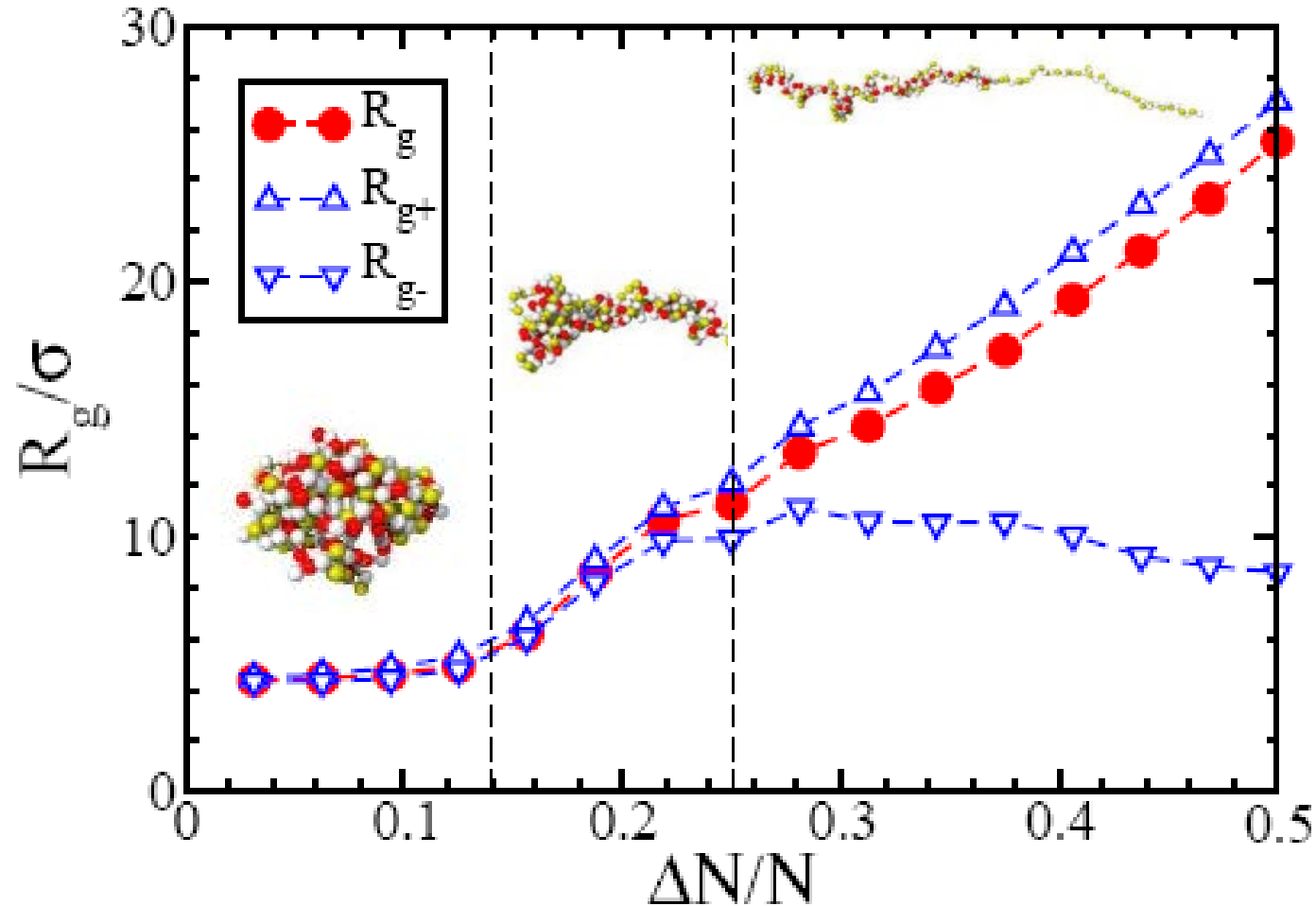
B. **Love:** A smaller section of the shorter block accompanies longer section of the larger block in a double-tail.

Why?

Appearance of a Single-Stranded Tail

$$L_{head} \sim N_- \qquad\qquad L_{tail} \sim N_{tail}$$
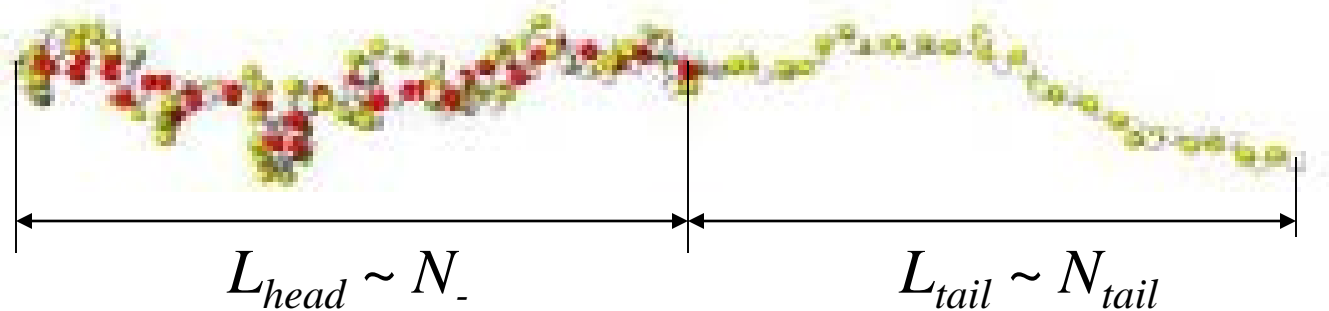
Charge of the head $Q_{head} \sim f(N_+ - N_- - N_{tail})$ **Shklovski & Hu**

Coulomb energy of the head $F_{head}/kT \sim l_B Q_{head}^2/L_{head}$

Coulomb energy of the tail $F_{tail}/kT \sim l_B (fN_{tail})^2/L_{tail}$

Minimization of the free energy **$N_{tail} = N_+ - 3N_-/2$**

**No single-stranded tail (love holds the two strands together)
for $N_+ < 1.5N_-$ ($\Delta N = N_+ - N_- < N/5$)**

Single-stranded tail grows linearly with ΔN for larger charge asymmetry.

Number of Monomers in a Single-Stranded Tail

$N = 256$

$u = l_B/\sigma$

Plot legend:
- $f = 1, u = 2$ (red circles)
- $f = 1/2, u = 2$ (blue squares)
- $f = 1/2, u = 1$ (orange diamonds)
- $f = 1/4, u = 1$ (green triangles)
- Shklovskii (dashed line)

Hate

$N_{tail} = N_+ - 3N_-/2$

Love

$N_{tail} = (5\Delta N - N)/4$

Axis labels: Number of Monomers N_{tail} (vertical), ΔN (horizontal)
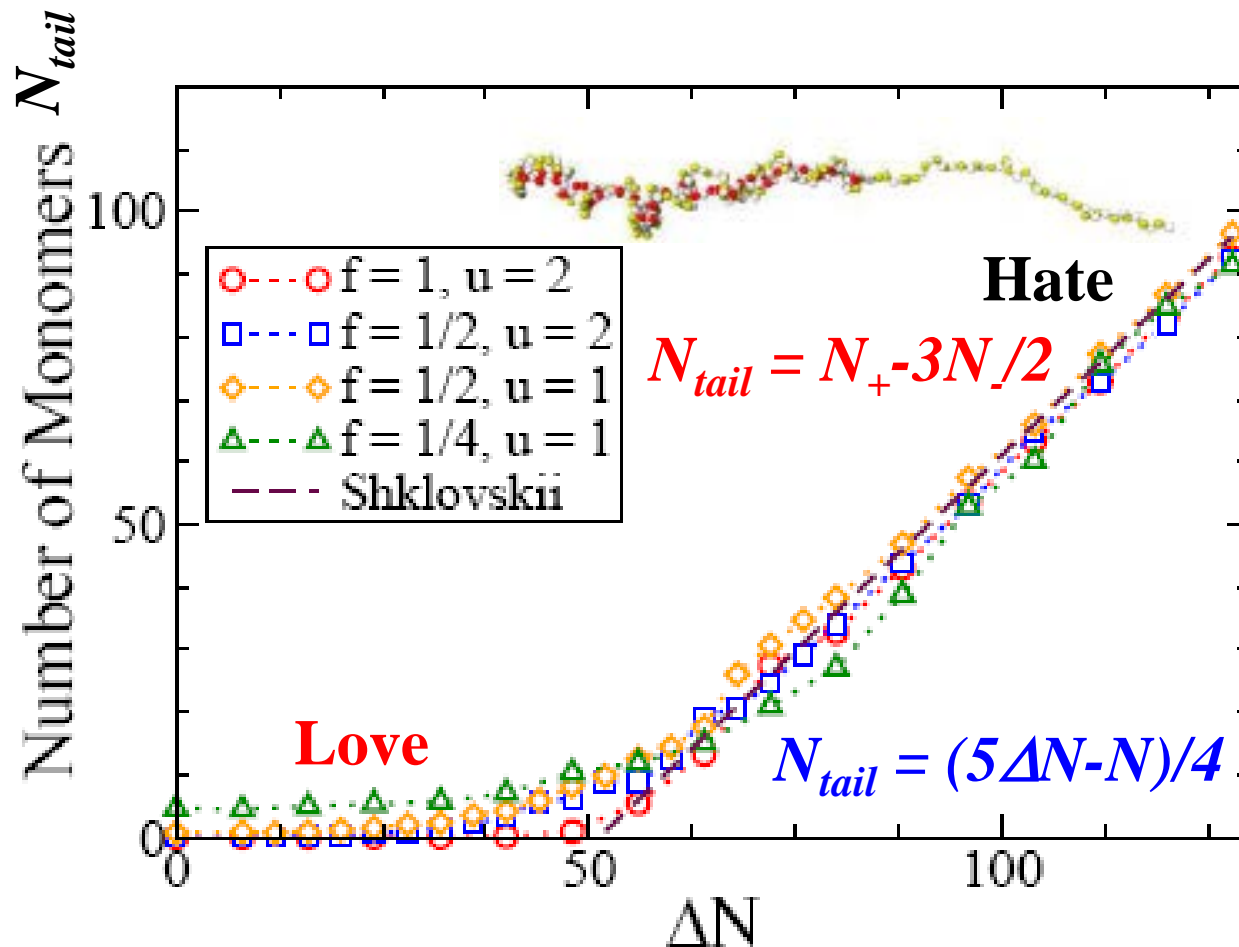
Disproportionation in Micelles of Asymmetric Block Polyampholytes
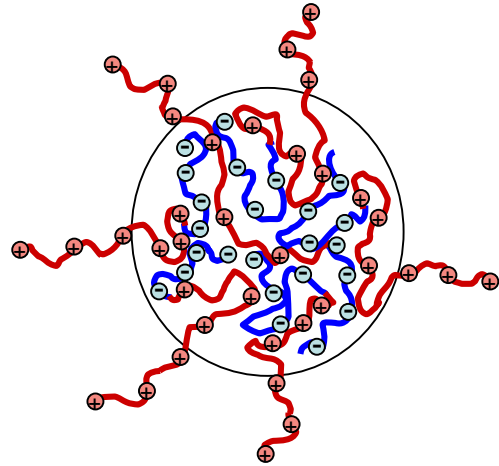
Instead of all blocks being in the same conformation with charge-compensated sections in the core and parts of all blocks with extra charge in corona **block polyampholytes in micelles split into two populations**.
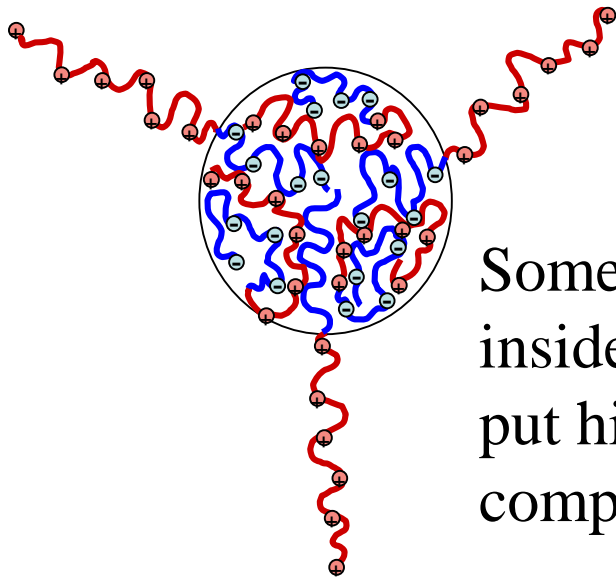
Some chains are completely inside the core, while others put higher charged block completely into the corona.
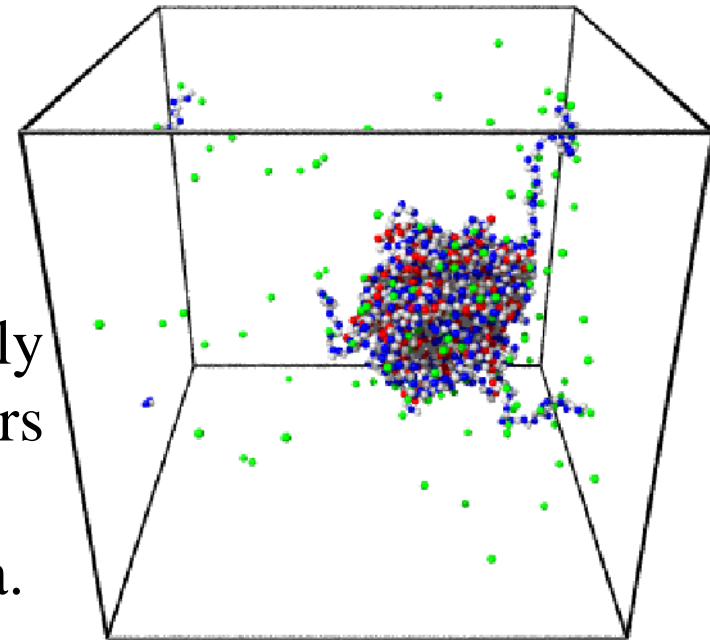
Block Polyampholytes with an Asymmetric Charge Density

Consider block polyampholyte with the fraction of positive charges f_+ much lower than the fraction of negative charges f_-, but with equal number of charges per block $f_+ N_+ = f_- N_-$.

Graph legend:
- $N_+ = 512$, $f_+ = 1/32$
- $N_- = 32$, $f_- = 1/2$

Axes: R_g/σ versus l_B/σ

R_+ R_-

Adsorption of long block on short one

Ion binding

Stretching of short block

1/8   1/2   2   8   32
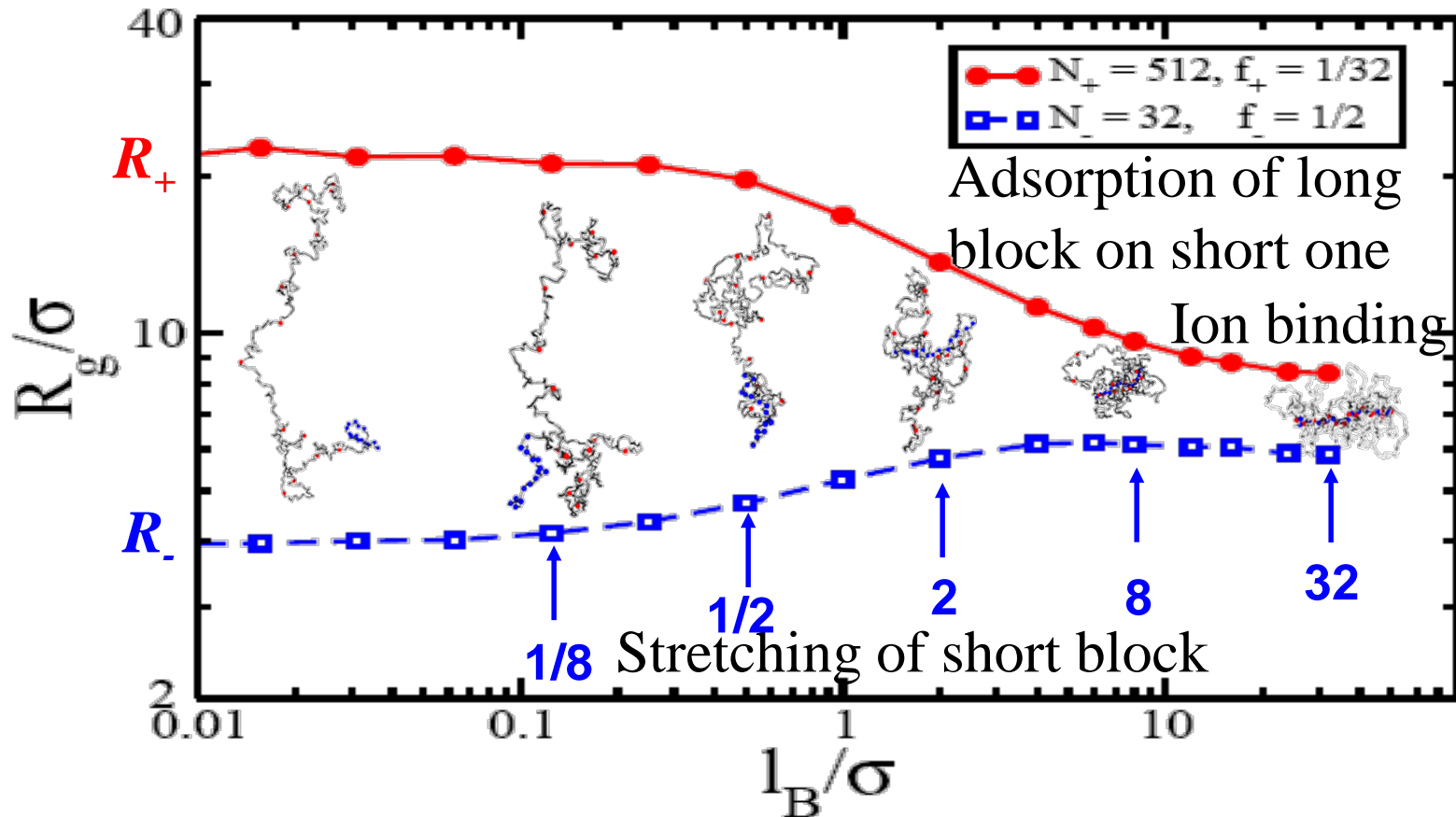
Love Soothes Tension of Short Block

$$l_B \frac{(f_+ N_+)^2}{b N_+^\nu} < 1 < l_B \frac{(f_- N_-)^2}{b N_-^\nu}$$

Shorter block with higher charge density becomes strongly elongated,
while the other block is unperturbed.
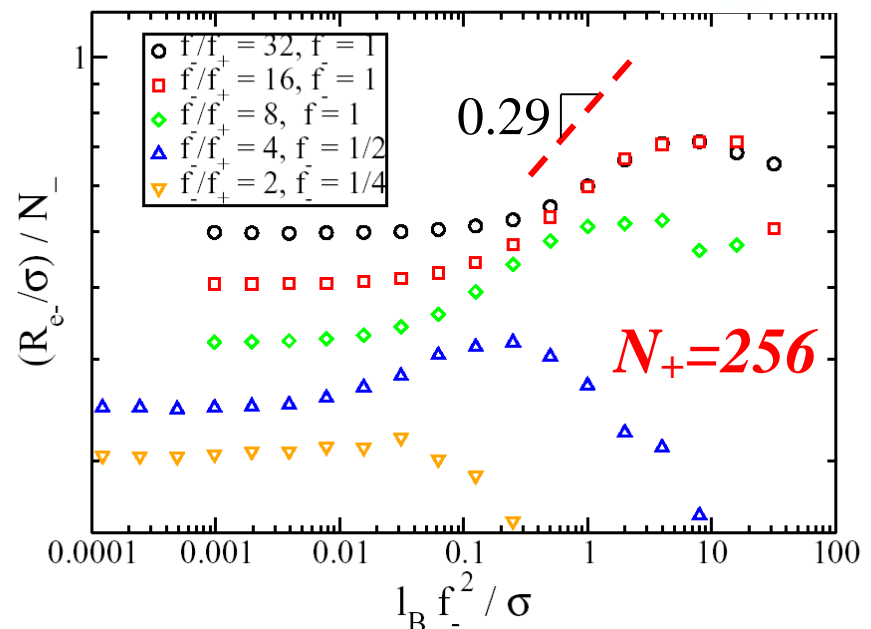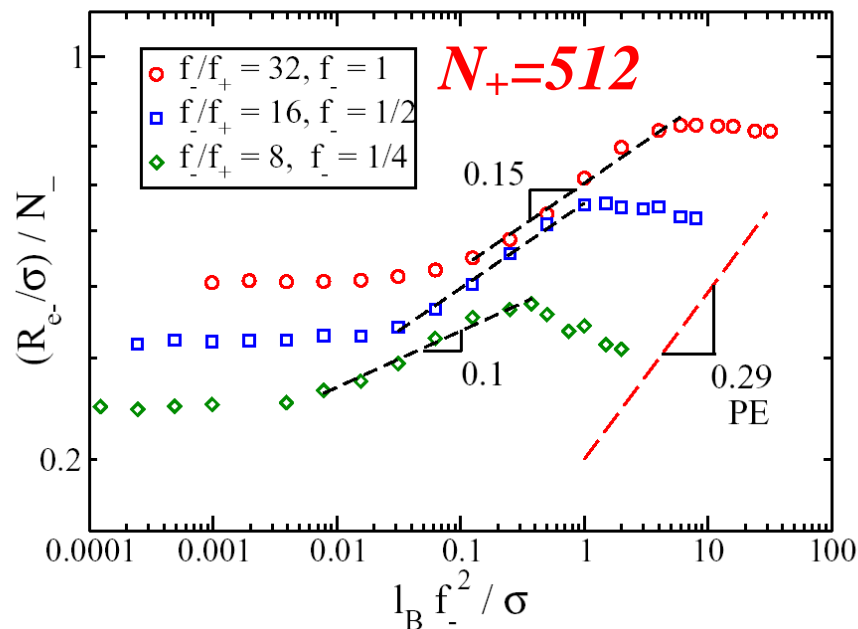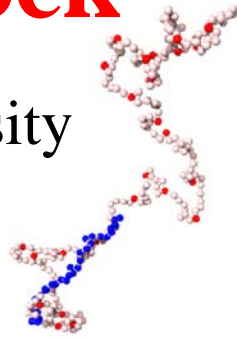
End-to-end distance of polyelectrolytes

$$R_e \approx N (l_B f^2 / \sigma)^{(1-\nu)/(2-\nu)} \qquad (1-\nu)/(2-\nu)=0.29$$

Screening of self-hate by loving oppositely charged block

Block Polyampholytes with an Asymmetric Charge Density
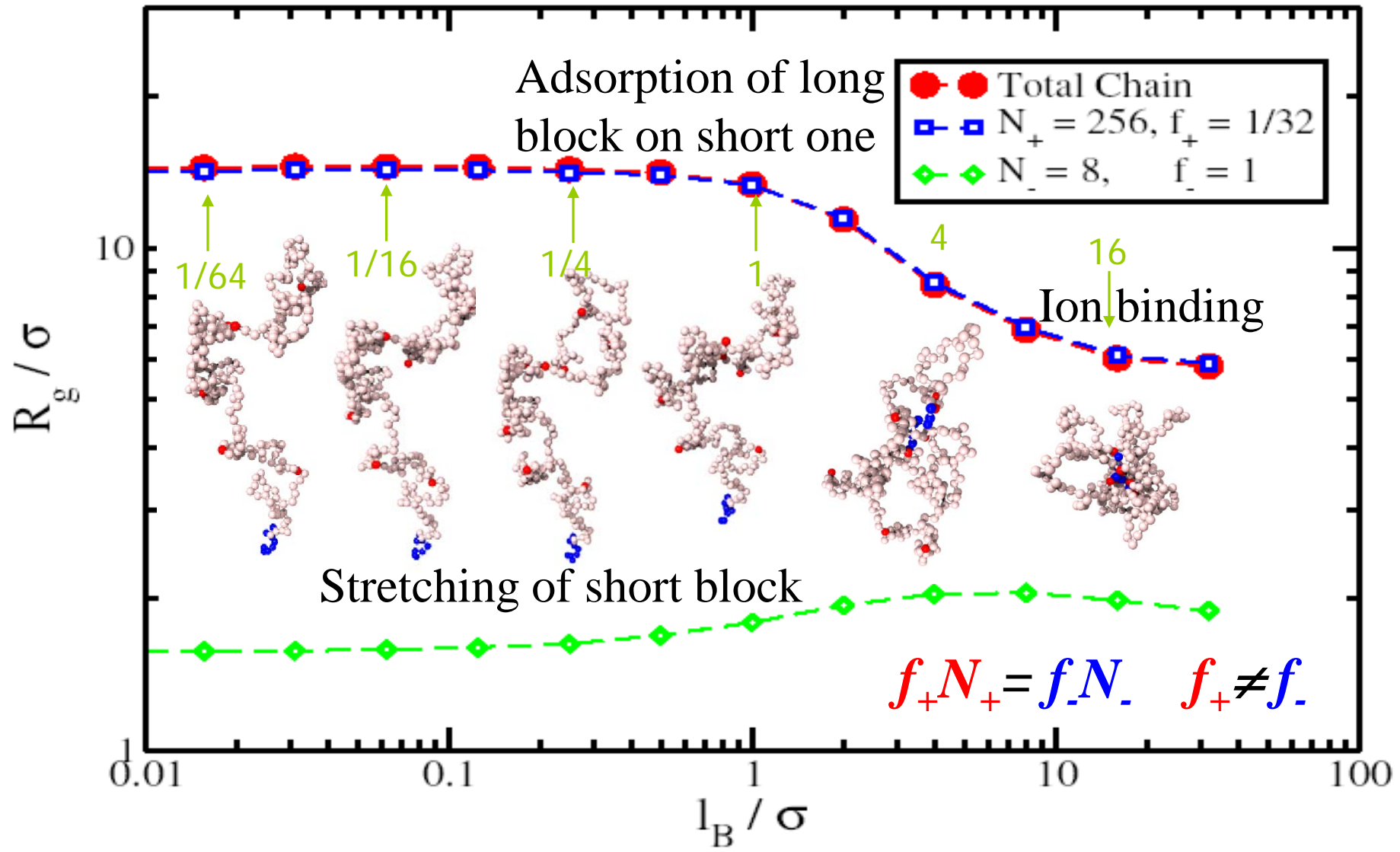
Fatal Attraction: Collapse of Weaker Charged Block on Stronger Charged Block
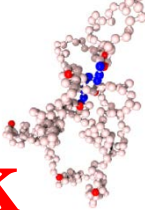
Adsorption starts if electrostatic attraction ~ *kT*: $l_B Q^2/R_{g0+} \approx 1$

$N_+ = 512$

-0.35

- ○ $f_-/f_+ = 32,\ f_- = 1$
- □ $f_-/f_+ = 16,\ f_- = 1/2$
- ◇ $f_-/f_+ = 8,\ \ f_- = 1/4$

$N_+ = 256$

-0.35

- ○ $f_-/f_+ = 32,\ f_- = 1$
- □ $f_-/f_+ = 16,\ f_- = 1$
- ◇ $f_-/f_+ = 8,\ f_- = 1$
- △ $f_-/f_+ = 4,\ f_- = 1/2$
- ◁ $f_-/f_+ = 2,\ f_- = 1/4$
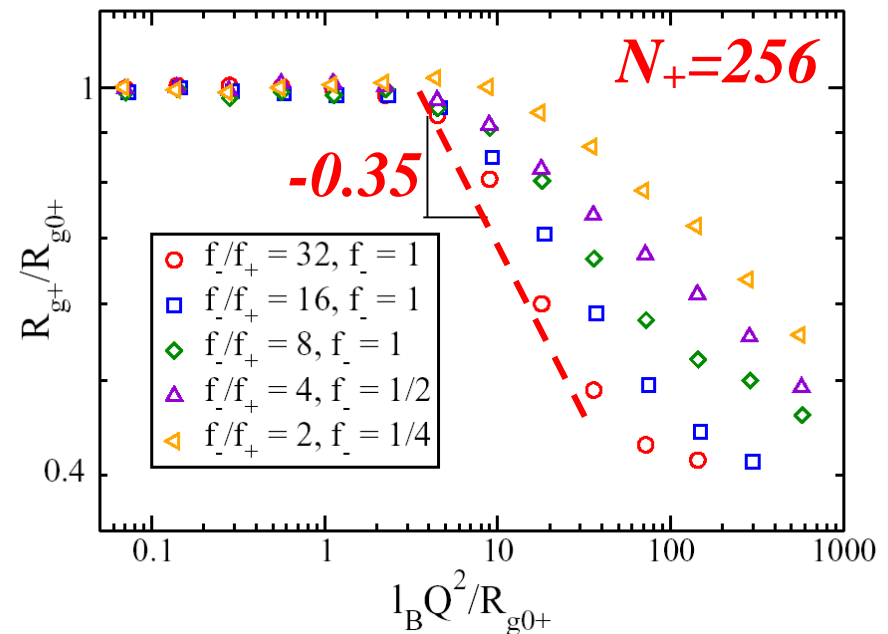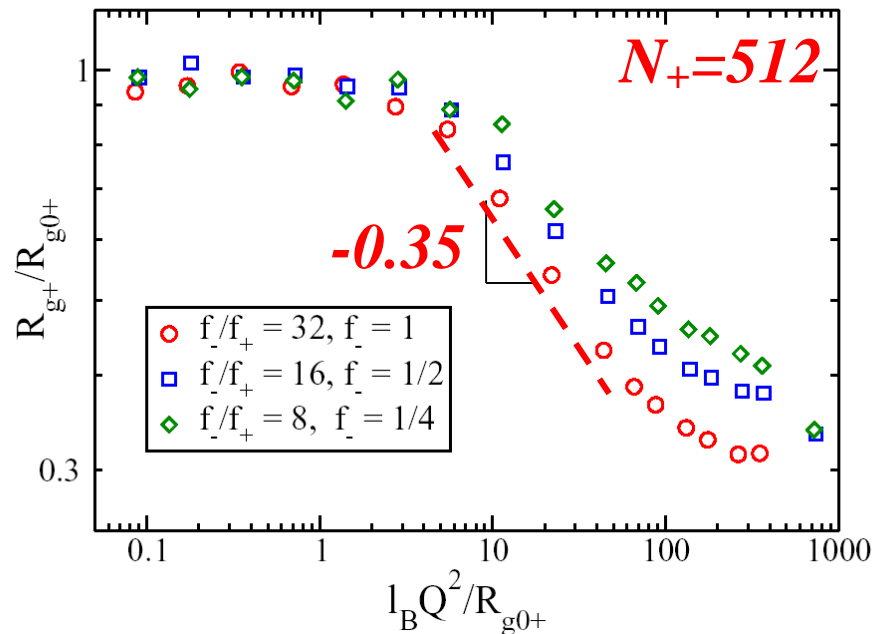
"Atomic" Globule: Electrostatic attraction is stabilized by steric repulsion (osmotic pressure $\Pi \sim c^{9/4}$)

R_{g+}

$$kTl_B Q^2/R_{g+} \approx \Pi R_{g+}^3 \qquad \frac{R_{g+}}{R_{g0+}} \approx \left(\frac{R_{g0+}}{l_B Q^2}\right)^{\frac{3\nu-1}{4-3\nu}} \qquad (3\nu-1)/(4-3\nu)\approx 0.35$$
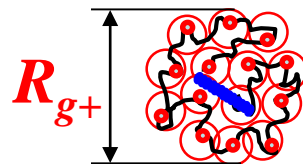
Block Polyampholytes Asymmetric Charge Density

Adsorption of long block on short one

Legend:
- Total Chain
- $N_+ = 256$, $f_+ = 1/8$
- $N_- = 32$, $f_- = 1$

$f_+ N_+ = f_- N_-$ $f_+ \neq f_-$

R_g / σ

1/64   1/16   1/4   1   4   16

Stretching of short block

Ion binding

l_B / σ
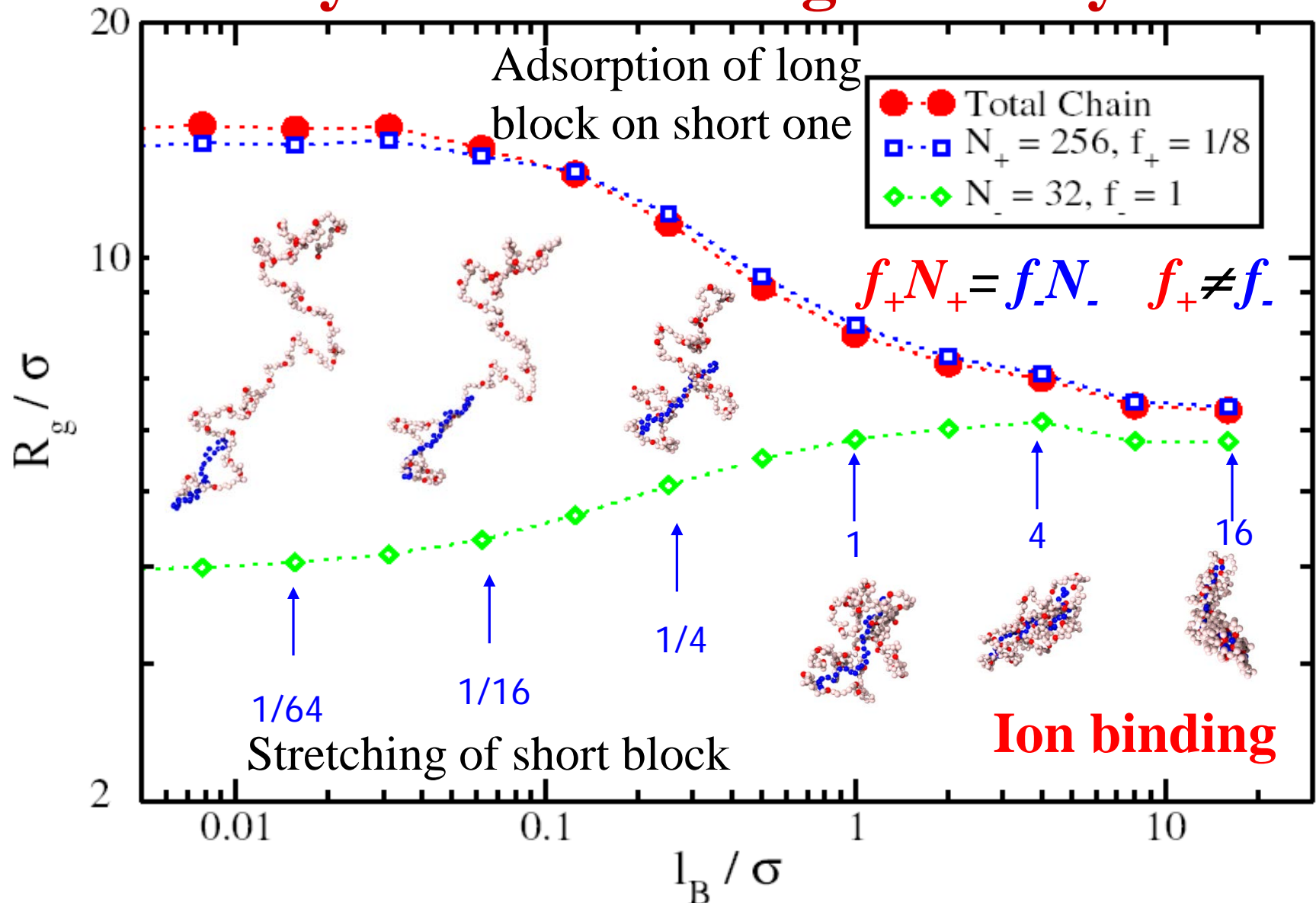
Ion Binding – Formation of Bottlebrush

Correlation length increases with distance from the center of the globule with decreasing electrostatic potential due to screening of short block charge by inner parts of long block.
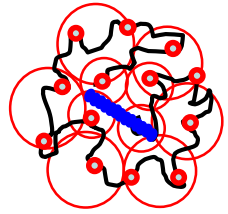
Flirting globule – bottlebrush "wedding" transition at one charge per inner blob
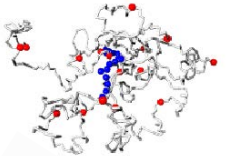
Crew-cut bottlebrush – cylindrical micelle with loop sizes of strands between charges $bf_+^{-2v/(1+v)}f_-^{(1-v)/(1+v)}$ smaller than the length of shorter block bN_-
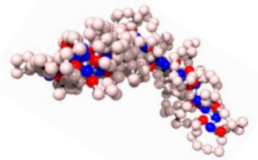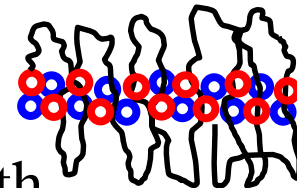
Hairy bottlebrush with loop sizes $bf_+^{(1-3v)/2}N_+^{(1-v)/2}$ longer than the size of short block bN_-
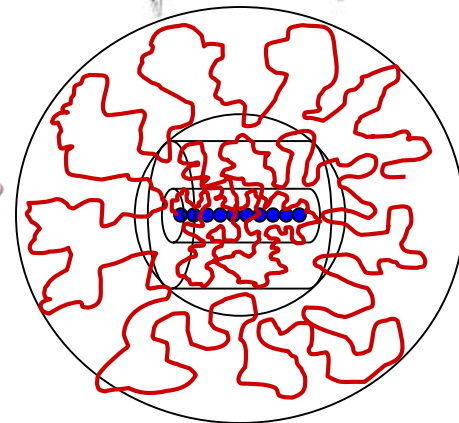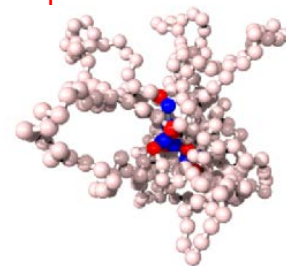
Ion Binding From Distance Between Charges

Distance Between Same Sign Charges

long block

short block
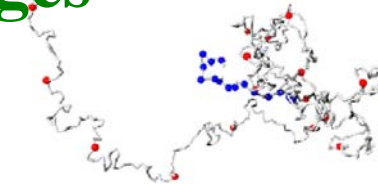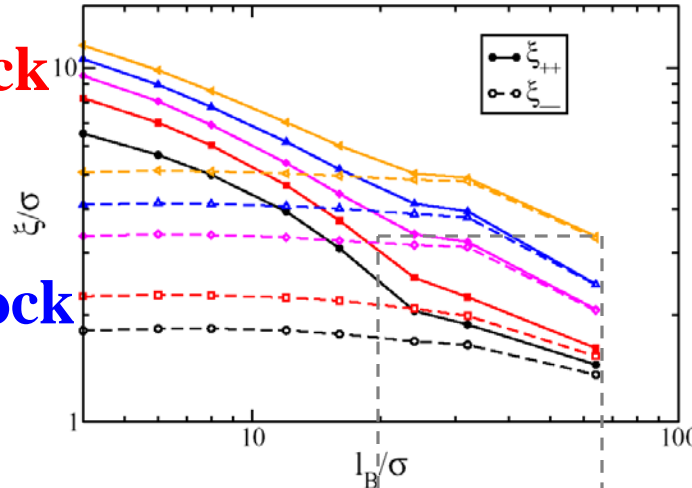
Short block stretching $l_B \sim \sigma$
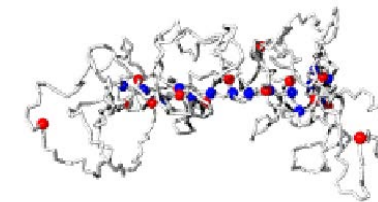
Flirting – long block adsorption $l_B \sim 10\sigma$

Distance between

opposite sign charges

same sign charges on short bock
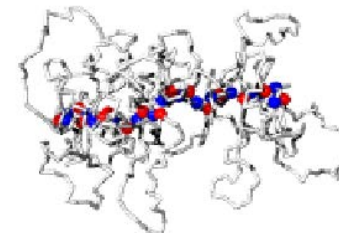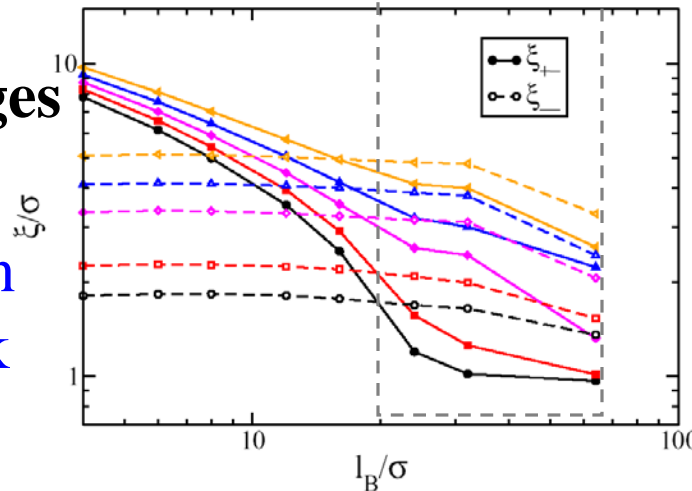
Marriage – ion binding $l_B \sim 20\sigma$
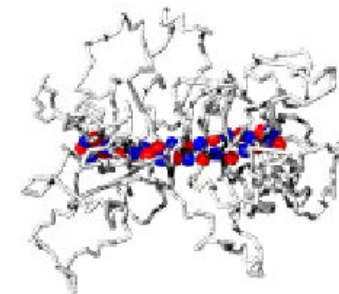
Bottlebrush of loops $l_B \sim 60\sigma$

$N_+ = 512,\ f_+ = 1/32,\ N_- = 32,\ f_- = 1/2$

Conclusions

I.   There are two classes of association for all charged systems including **block and random polyampholytes**, **polyelectrolytes**, and their transition to ionomers:

  1. Weak fluctuation-induced association (less than kT per charge) leading to the "flirting" globule.

  2. Strong ion-binding association (marriage) stabilized by neutral strands with a cascade of multiplet transitions
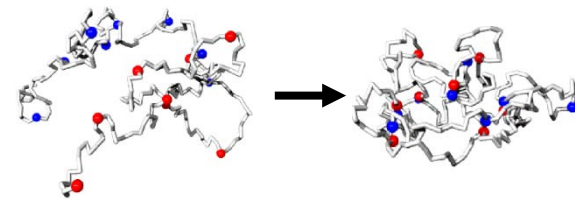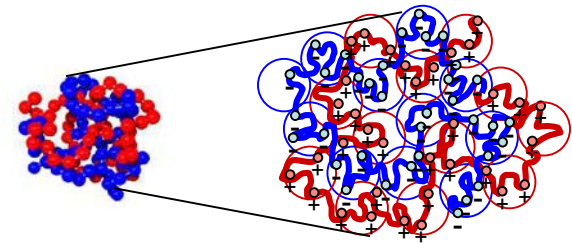
II. Two regimes for **charge asymmetry**:
love holding the overcharged pair together up to $Q_+=1.5Q_-$ and **hate** (expulsion) for $Q_+>1.5Q_-$

III. **Charge density asymmetry** leads through flirtation ("atomic" globule) and marriage (ion binding) to **crew-cut or hairy loopy bottle brushes.**
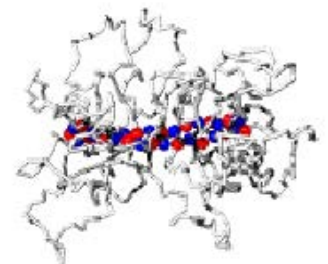
Self-Assembled Wrath of Flower Micelles

A. N. Semenov and M. Rubinstein

Associating Polymers
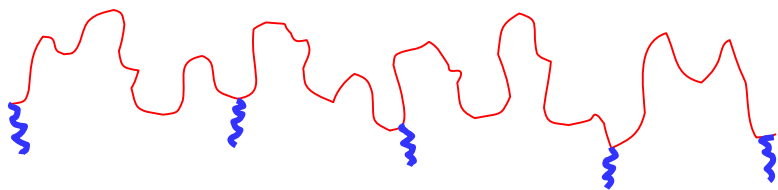
Solvable backbone with f stickers $f >> 1$

n monomers between stickers $n >> 1$

Multi-block copolymer in selective solvent

...-A-A-B-B-...-B-B-A-A-...-A-A-B-B-...

...-$(A)_n$-$(B)_k$-$(A)_n$-$(B)_k$-$(A)_n$-$(B)_k$-$(A)_n$-$(B)_k$-...

Flower Micelle

Polymers aggregate into micelles with m stickers in the core and soluble n-spacers in the corona. $m >> 1$

Association energy per sticker is εkT $\varepsilon >> 1$

Correlation length increases linearly with distance r to the center $\xi \approx r/m^{1/2}$

Volume fraction ϕ decreases with distance r to the center

$$\phi \approx \left(\frac{b\sqrt{m}}{r}\right)^{(3\upsilon-1)/\upsilon}$$
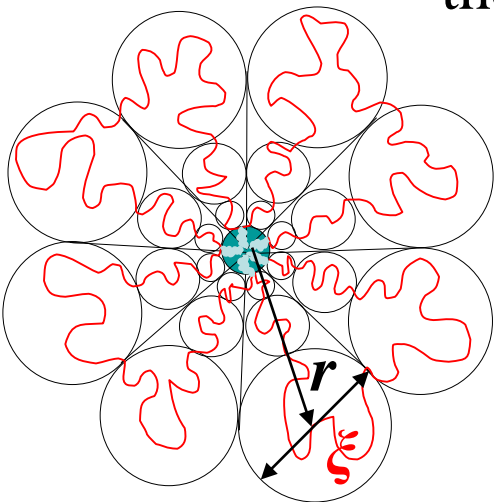
Size & Structure of a Flower Micelle
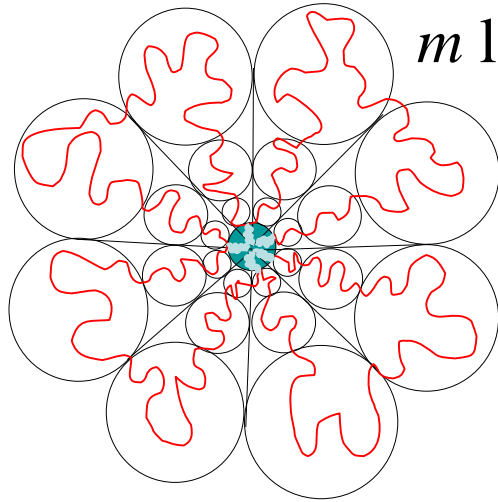
m loops *n* monomers each

Balance of elastic and osmotic parts of free energy

Flory theory

$$F \approx kT\left(m\frac{R^2}{nb^2} + b^3\frac{(mn)^2}{R^3}\right) \qquad R^* \approx bm^{1/5}n^{3/5}$$

Size of an uncompressed micelle $\quad R^* = bn^{\nu}m^{(1-\nu)/2}$

Average volume fraction in an isolated micelle $\quad \phi^* = \dfrac{mnb^3}{(R^*)^3} = \left(\dfrac{\sqrt{m}}{n}\right)^{3\nu-1}$

Free energy of an isolated flower micelle

$$F \approx mkT\int_{R_{core}}^{R^*}\frac{dr}{\xi} \approx mkT\int_{R_{core}}^{R^*}m^{1/2}\frac{dr}{r} \approx kTm^{3/2}ln\left(\frac{R^*}{R_{core}}\right)$$

For micelle to be stable, the energy of sticker εkT has to be larger than

$$\varepsilon kT > \partial F/\partial m \approx kT\sqrt{m}$$

Flower micelles attracts each other by forming $m^{5/6}$ bridges each and phase separate in dilute solution into a gel with concentration ϕ^*.

Network of Interconnected Micelles at $\phi > \phi^*$
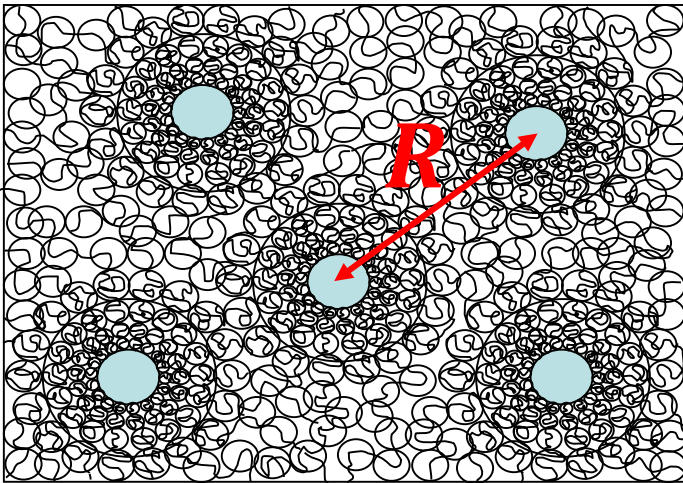
Micelles are compressed $R \approx R^* \left(\dfrac{\phi^*}{\phi} \right)^{1/3}$

Inner parts of coronas still have non-uniform density – same as at ϕ^*.

Density of outer parts (most of the solution) is uniform & controlled by osmotic pressure.

Elastic free energy of the outer part
~ interaction between micelles
~ deformation energy upon displacement of a micelle.

$$\Delta F \approx mkT \left(\frac{R}{R_n} \right)^2 \approx mkT \left(\frac{\tilde{\phi}}{\phi} \right)^{1/[3(3\nu-1)]}$$

$$R_n \approx bn^{1/2} \phi^{-(\nu-1/2)/(3\upsilon-1)}$$ - size of free n-mer at concentration ϕ

ΔF *decreases* with increasing concentration (strands are less extended)

Number of bridges per micelle $N_b \approx \begin{cases} m(\phi/\tilde{\phi})^{1/[9(3\nu-1)]} & \phi^* < \phi < \tilde{\phi} \\ m & \phi > \tilde{\phi} \end{cases}$

Above the concentration $\tilde{\phi} \approx \left(m^2/n \right)^{3\nu-1}$ n-spacers are no longer stretched

Summary of the Structure of the Network of Interconnected Micelles
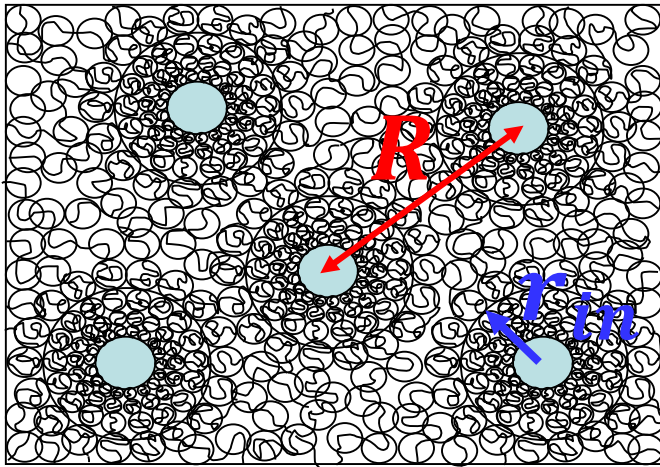
Free energy at $\phi > \phi^*$ is dominated by the osmotic pressure of the outer region

$$\Pi \approx kT\phi^{3\upsilon/(3\upsilon-1)}$$

Size of high concentration inner corona zones

$$r_{in} \approx R^*(\phi^*/\phi)^{3\upsilon/(3\upsilon-1)}$$

decreases faster than spacing between micelles

Most of the gel volume has uniform concentration.

For $\phi^* < \phi < \tilde{\phi}$ spacers are in extended loops and bridges (mostly loops)

Elongation of n-mers decreases with concentration $F_{el} \sim \phi^{-0.43}$

Fraction of bridges increases as $\phi^{0.14}$, they connect neighboring micelles

For $\phi > \tilde{\phi}$ flowers loose their petals; n-strands are undeformed (outside very near-core zone r_{in}) and most of them are bridges connecting distant aggregates ($R_n > R$).

Elastic Modulus of a Reversible Gel

Elastic free energy of the outer part
~ interaction between micelles
~ deformation energy upon displacement of a micelle.

$$\Delta F \approx mkT \left(\frac{\widetilde{\phi}}{\phi} \right)^{1/[3(3\upsilon-1)]}$$

Shear elastic modulus $\quad G \approx \dfrac{\Delta F}{R^3} \approx \dfrac{kT}{b^3} \dfrac{m^{2/3}}{n^{4/3}} \phi^{1-1/[3(3\upsilon-1)]} \sim \phi^{0.57}$

of unentangled gel and at intermediate time scales
(longer than disentanglement time) of entangled gel

Chain Dynamics
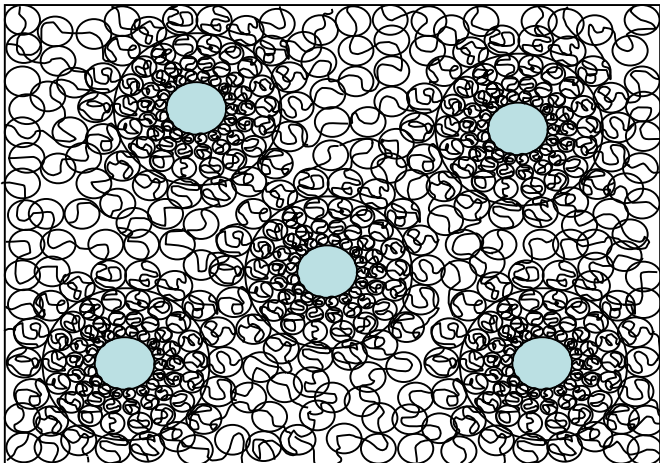
Stickers hop between micellar cores

No renormalization of bond lifetime as aggregation number m can fluctuate around its average value if

$$\sqrt{m} < \varepsilon < m^{4/3}$$

Introduction to Polymer Dynamics
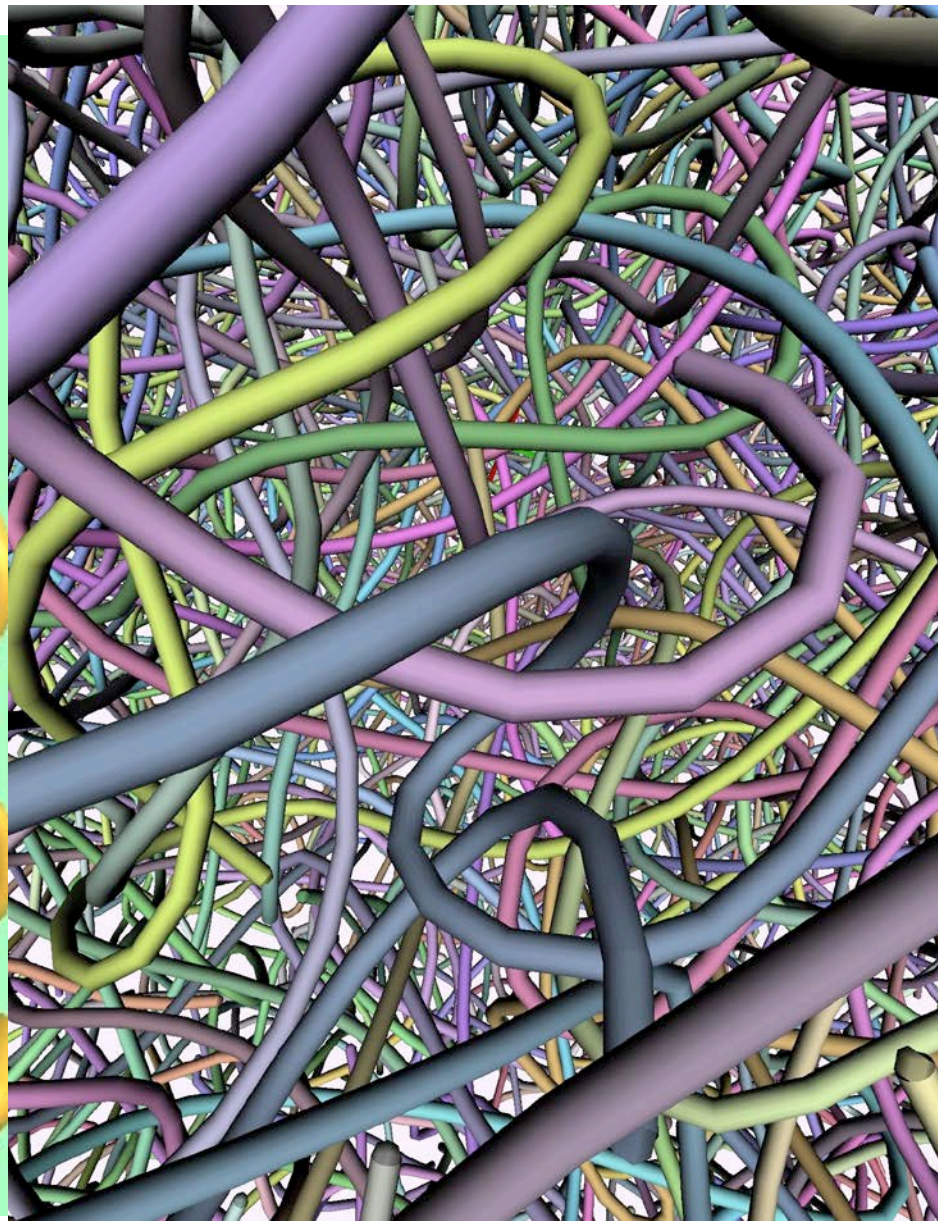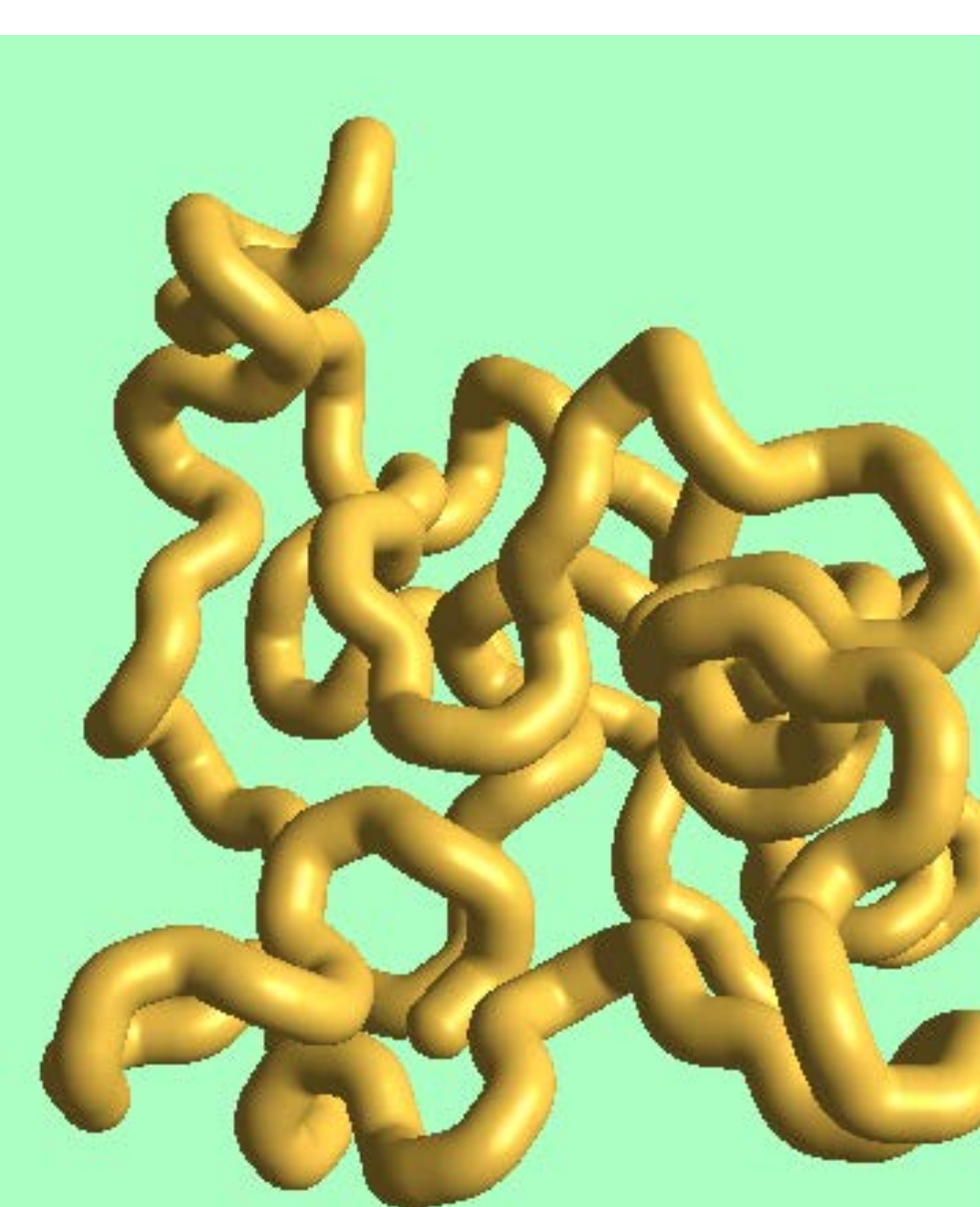
Particle Dynamics

Diffusive Motion

mean-square displacement

$$\left\langle [\vec{r}(t) - \vec{r}(0)]^2 \right\rangle = 6Dt$$

D – diffusion coefficient

$\vec{v}$ – velocity of particle due to applied force

$$\vec{f} = \vec{v}\zeta$$

ζ – friction coefficient

Stokes Law $\quad \zeta = 6\pi\eta R$

R – radius of the particle

η – viscosity of the fluid

viscous drag $-\vec{f}$

Robert Brown (1773–1858)

George Gabriel Stokes (1819-1903)

Einstein relation

$$D = \frac{kT}{\zeta}$$

Stokes-Einstein relation $\quad D = \frac{kT}{6\pi\eta R}$

Time required for a particle to move a distance of order of its size

$$\tau \approx \frac{R^2}{D} \approx \frac{R^2 \zeta}{kT}$$
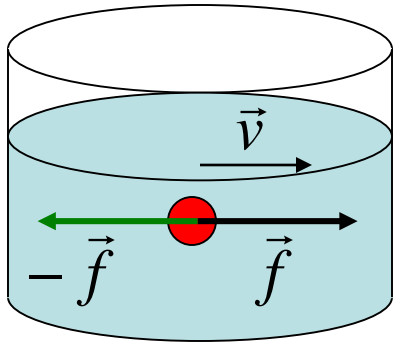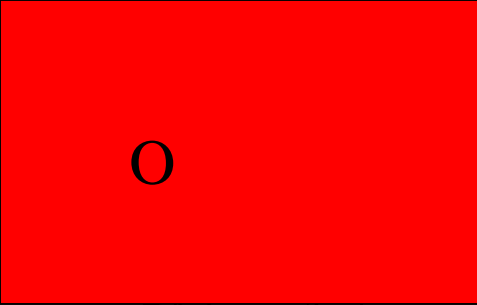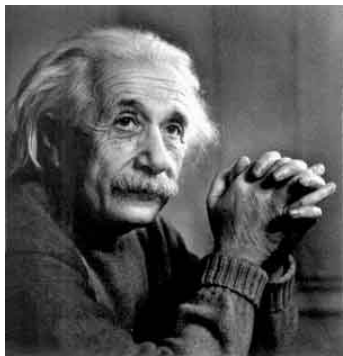
Rouse Model
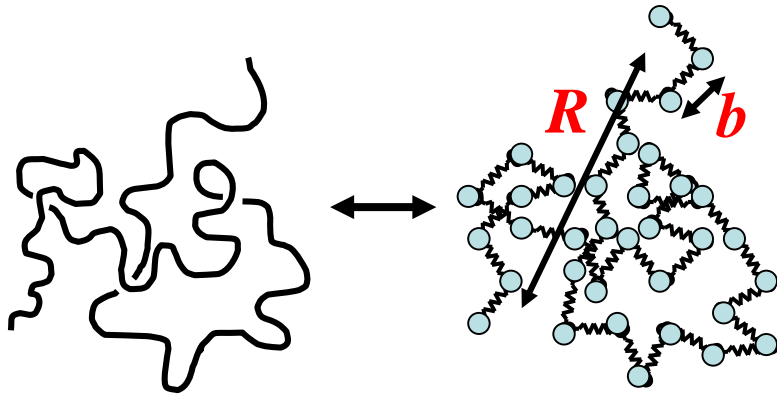
N beads connected by springs with root-mean square size b.

ζ – friction coefficient of a bead

No hydrodynamic coupling between beads

$\zeta_R = N\zeta$ – total friction coefficient of the Rouse chain

$D_R = \dfrac{kT}{N\zeta}$ – diffusion coefficient of the Rouse chain

$\tau_R \approx \dfrac{R^2}{D_R} \approx \dfrac{\zeta}{kT} N R^2$ – Rouse time

for $t < \tau_R$ – viscoelastic modes

for $t > \tau_R$ – diffusive motion

$R \approx bN^\nu \longrightarrow \tau_R \approx \dfrac{b^2\zeta}{kT} N^{1+2\nu} \approx \tau_0 N^{1+2\nu}$

Stokes Law

$\zeta \approx \eta_s b$

$\tau_0 \approx \dfrac{b^2\zeta}{kT}$ – Kuhn monomer relaxation time

$\tau_0 \approx \dfrac{b^3\eta_s}{kT}$

For ideal linear chain $\nu = 1/2$

$$\tau_R \approx \tau_0 N^2$$

Rouse model – draining limit

Zimm Model
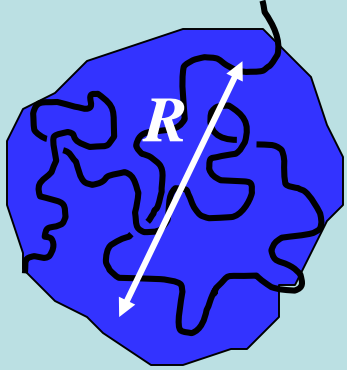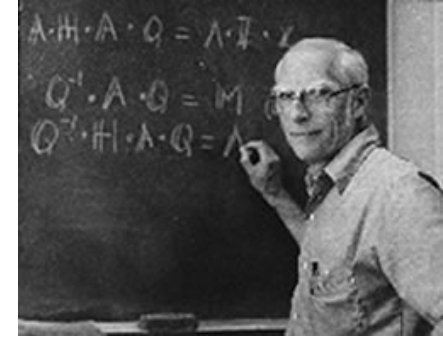
Hydrodynamic interactions couple the motion of monomers with the motion of solvent.

Chain drags with it the solvent in its pervaded volume.

Friction coefficient of chain of size R in a solvent with viscosity η_s

$$\zeta_Z \approx \eta_s R$$

Zimm diffusion coefficient

$$D_Z = \frac{kT}{\zeta_Z} \approx \frac{kT}{\eta_s R}$$

Zimm time

$$\tau_Z = \frac{R^2}{D_Z} \approx \frac{\eta_s}{kT} R^3 \approx \frac{\eta_s b^3}{kT} N^{3\nu} \approx \tau_0 N^{3\nu}$$

in θ-solvent $\nu=1/2$

$$\tau_z \sim N^{3/2}$$

in good solvent $\nu=3/5$

$$\tau_z \sim N^{9/5}$$

$3\nu < 1+2\nu$ for $\nu<1$ Zimm time is shorter than Rouse time in dilute solutions.

Hydrodynamic interactions are important in dilute solutions.

Self-Similar Dynamics

Chains are fractal – they look the same on different length scales and move in the same way on different time scales.

Rouse Model   ## Zimm Model

Longest relaxation time

Rouse time $\tau_R \approx \tau_0 N^2$ Zimm time $\tau_Z \approx \tau_0 N^{3\nu}$

p-th mode involves relaxation of N/p monomers.
Sections of the chain with $g=N/p$ monomers relax like a g-mer.

$$\tau_p \approx \tau_0 \left(\frac{N}{p}\right)^2 \qquad\qquad \tau_p \approx \tau_0 \left(\frac{N}{p}\right)^{3\nu}$$

At time τ_p modes with index higher than p have relaxed, while modes with index lower than p have not relaxed.

At time τ_p there are p un-relaxed modes per chain each contributing energy of order kT to the stress relaxation modulus. $G(\tau_p) \approx \dfrac{kT}{b^3} \dfrac{\phi}{N} p$
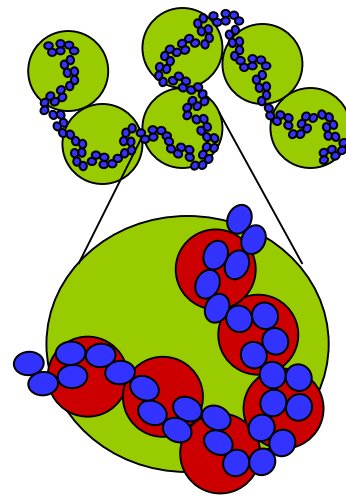
Self-Similar Dynamics

Rouse Model   Zimm Model

$$G(\tau_p) \approx \frac{kT}{b^3} \frac{\phi}{N} p$$

Index p of the mode that relaxes at $t = \tau_p \approx \tau_0 \left(\dfrac{N}{p}\right)^{\alpha}$

$$p \approx \left(\frac{t}{\tau_0}\right)^{-1/2} N \qquad\qquad p \approx \left(\frac{t}{\tau_0}\right)^{-1/3\nu} N$$

Stress relaxation modulus at $t < \tau_{relax}$

$$G(t) \approx \frac{kT}{b^3} \phi \left(\frac{t}{\tau_0}\right)^{-1/2} \qquad\qquad G(t) \approx \frac{kT}{b^3} \phi \left(\frac{t}{\tau_0}\right)^{-1/3\nu}$$

Stress relaxation modulus approximation for all $t > \tau_0$

$$G(t) \approx \frac{kT}{b^3} \phi \left(\frac{t}{\tau_0}\right)^{-1/2} \exp\left(-\frac{t}{\tau_R}\right) \qquad G(t) \approx \frac{kT}{b^3} \phi \left(\frac{t}{\tau_0}\right)^{-1/3\nu} \exp\left(-\frac{t}{\tau_Z}\right)$$

Stress Relaxation Modulus
Rouse Model

Scaling approximation $G(t) \approx \dfrac{kT}{b^3} \phi \left(\dfrac{t}{\tau_0} \right)^{-1/2} \exp\left(-\dfrac{t}{\tau_R} \right)$ (points)

Exact solution

$$G(t) = kT \frac{\phi}{Nb^3} \sum_{p=1}^{N} \exp\left(-\frac{t}{\tau_p} \right)$$

(solid line)

relaxation time
of p-th mode

$$\tau_p = \frac{b^2 \zeta}{6\pi^2 kT} \left(\frac{N}{p} \right)^2$$

$N = 10^3$
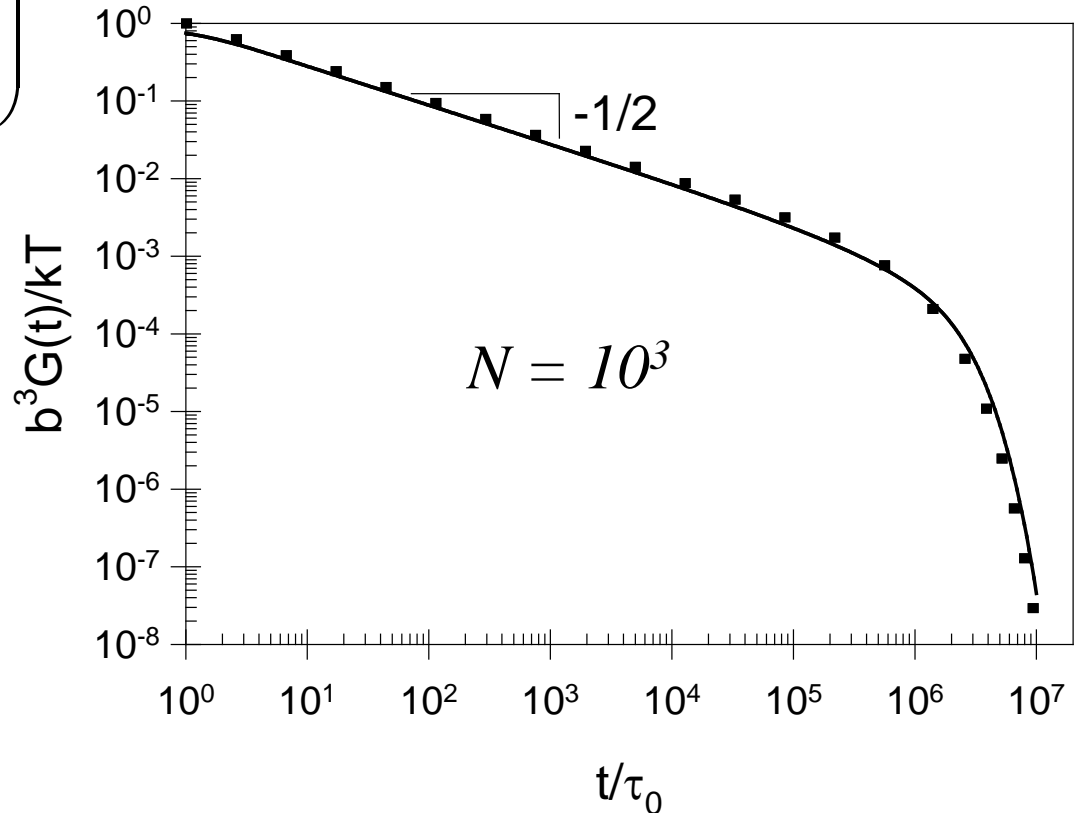
Rouse Relaxation Modes

Stress relaxation modulus $G(t) \approx \dfrac{kT}{b^3} \phi \left(\dfrac{t}{\tau_0} \right)^{-1/2} \exp \left(- \dfrac{t}{\tau_R} \right)$

$G'(\omega) \approx G''(\omega) \sim \omega^{1/2}$ in the frequency range $1/\tau_R << \omega << 1/\tau_0$

Rouse Viscosity

$\eta \approx G(\tau_R)\tau_R \approx \dfrac{kT}{b^3} \dfrac{\phi}{N} \dfrac{b^2 \zeta}{kT} N^2$

$\eta \approx \dfrac{\zeta}{b} N\phi$

Rouse model applies to melts of short unentangled chains

$\eta \approx \dfrac{\zeta}{b} N$
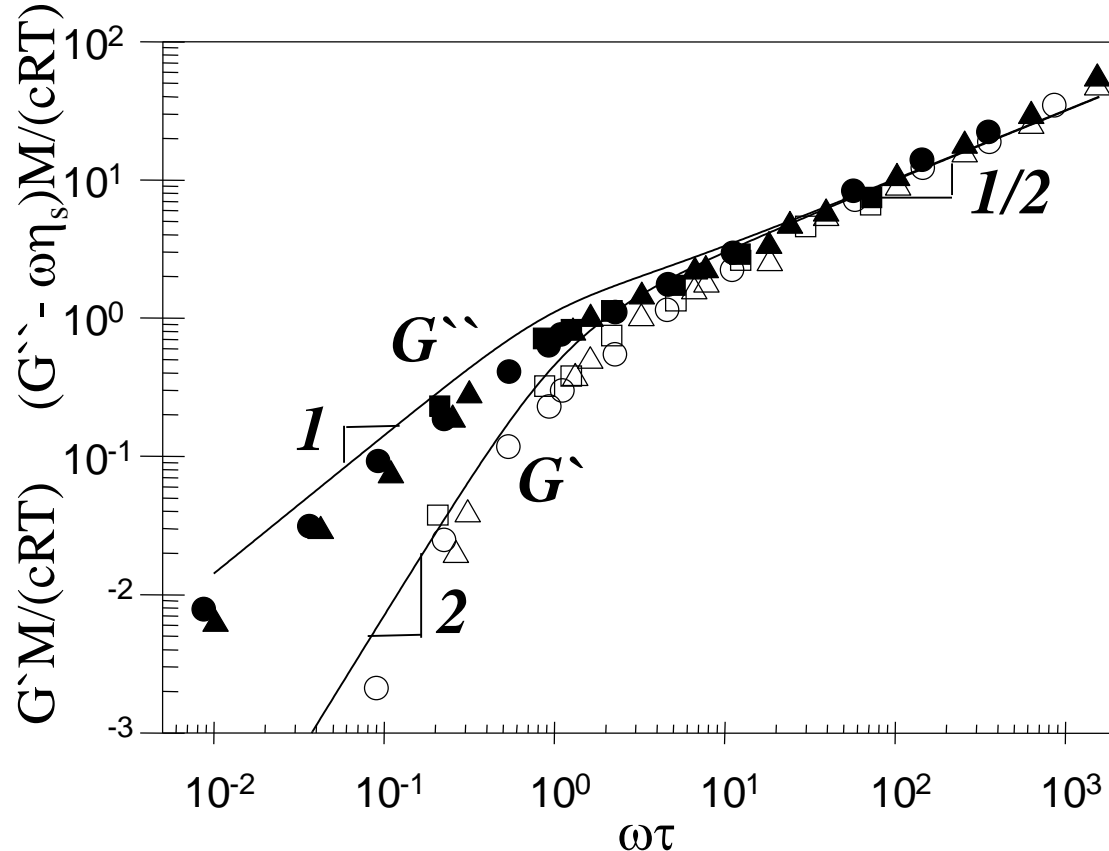
Zimm Relaxation Modes

Stress relaxation modulus
$$G(t) \approx \frac{kT}{b^3} \phi\left(\frac{t}{\tau_0}\right)^{-1/3\nu} \exp\left(-\frac{t}{\tau_Z}\right)$$

$G'(\omega) \approx G''(\omega) \sim \omega^{1/3\nu}$ in the frequency range $1/\tau_Z << \omega << 1/\tau_0$

in θ-solvents $\nu=1/2$

$G'(\omega) \approx G''(\omega) \sim \omega^{2/3}$

Zimm model is valid in dilute solution and is used for polymer characterization using intrinsic viscosity

dilute solutions of polystyrene in θ-solvents
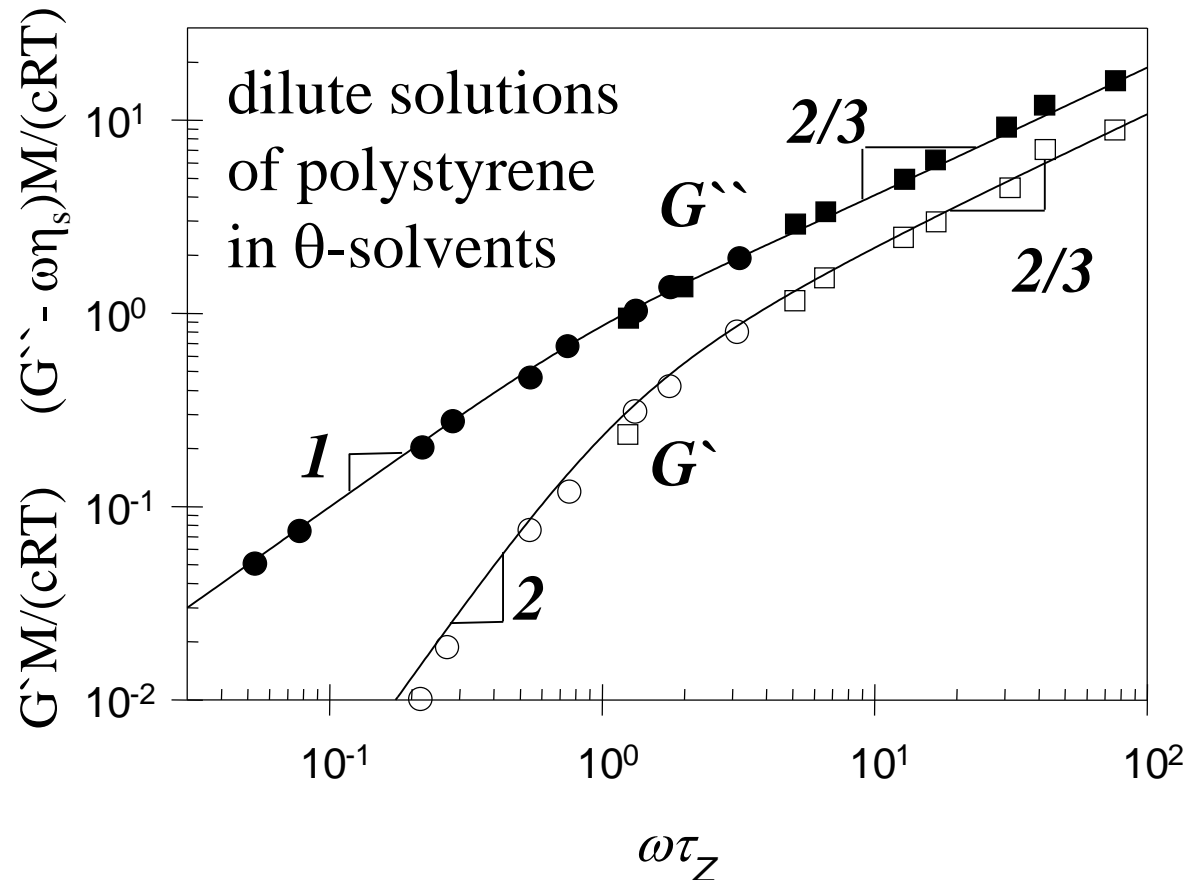
Mean Square Displacement of Monomers

Rouse Model   Zimm Model

Section of N/p monomers moves by its size during its relaxation time τ_p

ok for melts

$$\left\langle \left[\vec{r}_j(\tau_p) - \vec{r}_j(0) \right]^2 \right\rangle \approx b^2 \left(\frac{N}{p} \right)^{2\nu}$$

ok for dilute solutions

for ideal chain $\nu = 1/2$

$$p/N = (t/\tau_0)^{-1/2} \qquad\qquad p/N = (t/\tau_0)^{-1/3\nu}$$

Mean square monomer displacement for $\tau_0 < t < \tau_{relax}$

$$\left\langle \left[\vec{r}_j(t) - \vec{r}_j(0) \right]^2 \right\rangle \approx b^2 (t/\tau_0)^{1/2} \qquad \left\langle \left[\vec{r}_j(t) - \vec{r}_j(0) \right]^2 \right\rangle \approx b^2 (t/\tau_0)^{2/3}$$

Sub-diffusive motion

log – log plot

Sections of N/p monomers move coherently on time scale τ_p

Monomer motion in Zimm model is faster than in Rouse model
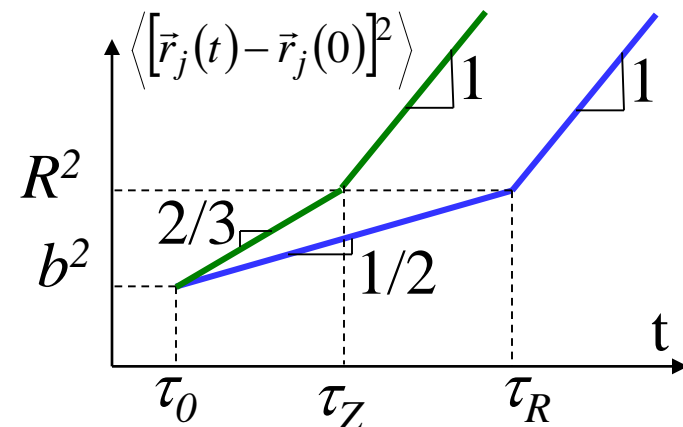
Quiz # 5

Which model is better in dilute solutions?

A. Rouse model with chain friction $\zeta = \zeta_0 N$

B. Zimm model with chain friction $\zeta \sim \eta R$

C. Reptation model

D. None of the above

E. All of the above

Summary of Single Chain Dynamics

Rouse model – local monomer friction ζ and no hydrodynamic interactions. It is applicable to unentangled polymer melts.

Rouse friction coefficient of an N-mer is $N\zeta$ and diffusion coefficient

$$D_R = kT/(N\zeta)$$

Zimm model – motion of monomers is hydrodynamically coupled. Polymer drags solvent in its pervaded volume. It is applicable to dilute solutions. Diffusion coefficient $\quad D_Z = kT/(\eta_s R)$

Polymer diffuses distance of order of its size during its relaxation time.

$$\tau_R \approx \frac{\zeta}{kT} N R^2 \qquad\qquad \tau_Z \approx \frac{\eta_s}{kT} R^3$$

Self-similar structure of stress relaxation function

$$G(t) \approx \frac{kT}{b^3}\phi\left(\frac{t}{\tau_0}\right)^{-1/2}\exp\left(-\frac{t}{\tau_R}\right) \qquad G(t) \approx \frac{kT}{b^3}\phi\left(\frac{t}{\tau_0}\right)^{-1/3\nu}\exp\left(-\frac{t}{\tau_Z}\right)$$

Rheology – Dilute Solutions
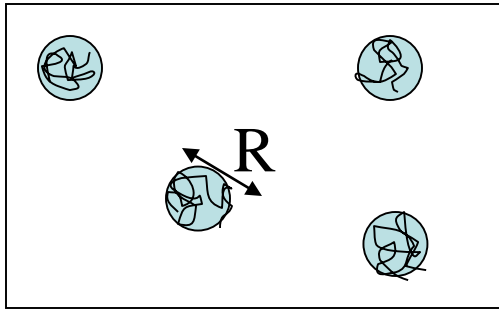
Chains are far apart and move independently of each other, dragging solvent with them.

non-draining (Zimm) dynamics

relaxation time $\tau \sim R^3$ modulus $G(\tau) \sim kT\phi/N$

$\phi < \phi^* \approx Nb^3/R^3$ viscosity $\eta \sim G(\tau)\tau \sim \phi R^3/N$ $\eta_{sp} = (\eta - \eta_s)/\eta_s \sim \phi/\phi^*$

Unentangled Semidilute Solutions

$\phi > \phi^*$

R

ξ

g monomers
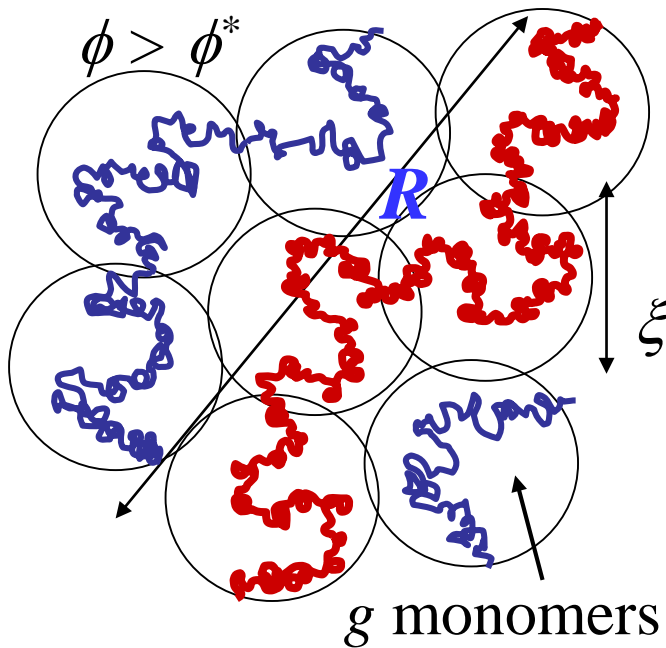
For $r < \xi$ dynamics are the same as in dilute solutions – non-draining (Zimm).

$\tau_\xi \sim \xi^3$

For $r > \xi$ overlapping chains screen hydrodynamics.

draining (Rouse) dynamics

hydrodynamic screening length ~ correlation length

relaxation time $\tau \sim \tau_\xi (N/g)^2$

Unentangled Semidilute Solutions
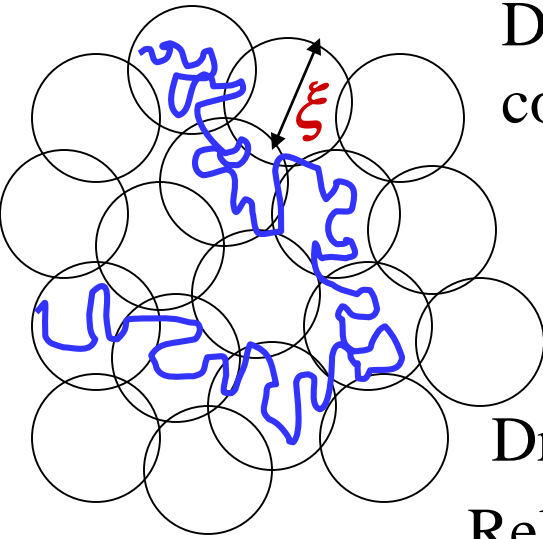
Dilute-like Zimm dynamics on length scales up to correlation length ξ (~hydrodynamic screening length)

$$\xi \approx b g^{\nu} \quad \phi \approx \frac{g b^3}{\xi^3} \qquad \xi \approx b \phi^{-\nu/(3\nu-1)} \qquad g \approx \phi^{-1/(3\nu-1)}$$

Relaxation time of a correlation blob $\tau_{\xi} \approx \dfrac{\eta_s}{kT} \xi^3$

Draining (Rouse-like) on scales > correlation length ξ

Relaxation time of the chain – Rouse time of N/g blobs

$$\tau_{chain} \approx \tau_{\xi} \left(\frac{N}{g}\right)^2 \approx \frac{\eta_s}{kT} \xi^3 \left(\frac{N}{g}\right)^2 \approx \frac{\eta_s b^3}{kT} N^2 \phi^{(2-3\nu)/(3\nu-1)}$$

In θ-solvents $\quad \tau_{chain} \sim \phi \qquad\qquad$ In good solvents $\quad \tau_{chain} \sim \phi^{0.31}$

Polymer size in semidilute solutions $\quad R \approx \xi \left(\dfrac{N}{g}\right)^{1/2} \approx b N^{1/2} \phi^{-(2\nu-1)/(6\nu-2)}$

Diffusion coefficient decreases with ϕ in semidilute solutions

$$D \approx \frac{R^2}{\tau_{chain}} \approx \frac{kT}{\eta_s b} \frac{\phi^{-(1-\nu)/(3\nu-1)}}{N} \approx D_Z \left(\frac{\phi}{\phi^*}\right)^{-(1-\nu)/(3\nu-1)}$$

In good solvents
$D \sim \phi^{-0.54}$

Concentration Dependence of Diffusion Coefficient in Semidilute Solutions

Unentangled semidilute good solvent

$$D \approx D_Z \left(\frac{\phi}{\phi^*} \right)^{-0.54}$$

Entangled semidilute at $\phi > 10\, \phi^*$
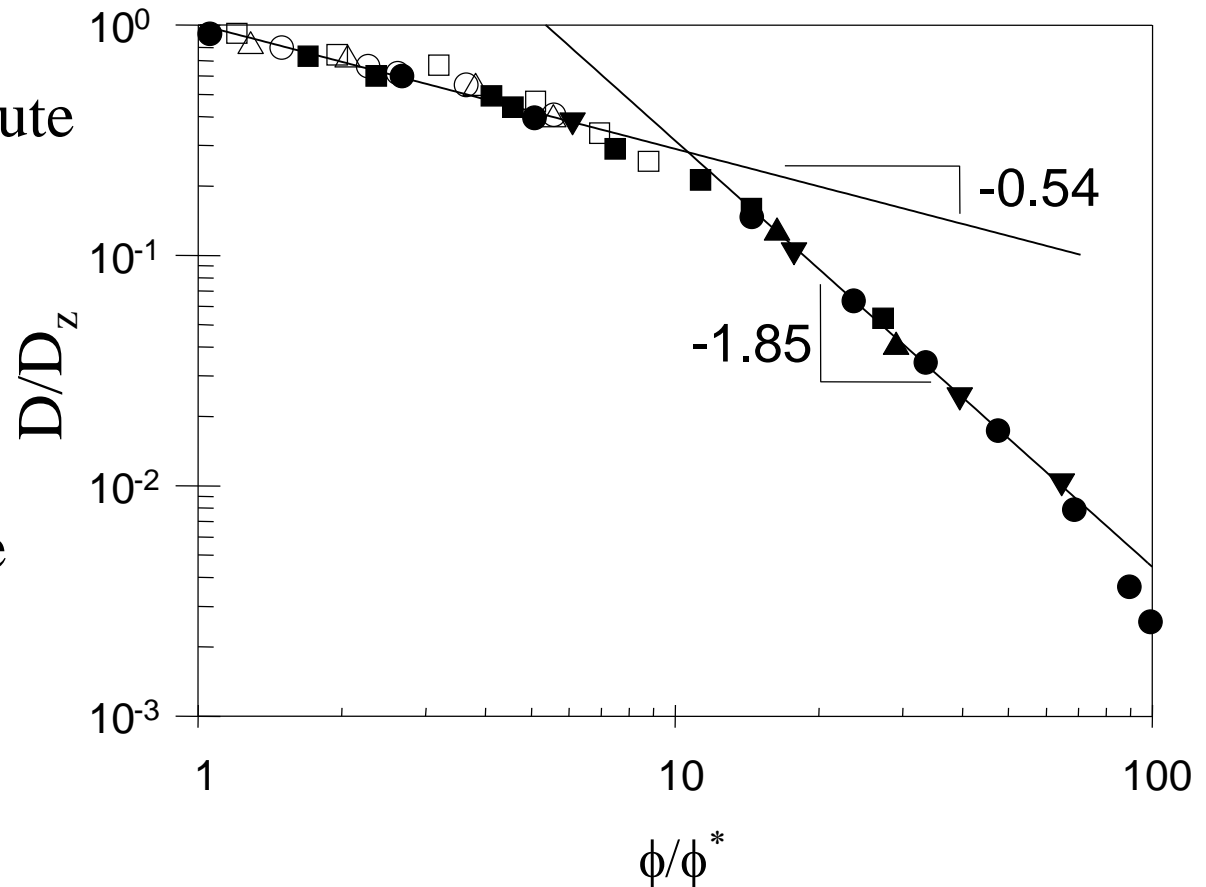
Filled symbols – polystyrene in benzene
Open symbols – poly(ethylene oxide) in water

Quiz # 1

How does relaxation time τ_{chain} vary with polymer concentration ϕ in semidilute unentangled regime for different values of exponent ν?

A. Increases

B. Decreases

C. All of the above

D. None of the above

$$\tau_{chain} \sim \phi^{(2-3\nu)/(3\nu-1)}$$

A. for $1/3 < \nu < 2/3$

B. for $\nu > 2/3$

Correct answer – C

Concentration Dependence of Viscosity

Viscosity at ϕ^* is approximately twice the solvent viscosity η_s

Viscosity in semidilute solutions $\quad \eta - \eta_s \approx \eta_s \left(\dfrac{\phi}{\phi^*} \right)^x$

$$\phi^* \approx Nb^3 / R^3 \approx N^{1-3\nu} \quad \longrightarrow \quad \eta - \eta_s \approx \eta_s N^{(3\nu-1)x} \phi^x$$

In semidilute solutions: modes shorter than correlation blobs are Zimm-like, while long-time modes are Rouse like $\quad \eta - \eta_s \sim N$

$x = 1/(3\nu\text{-}1)$

Specific viscosity $\quad \eta_{sp} = \dfrac{\eta - \eta_s}{\eta_s} \approx \left(\dfrac{\phi}{\phi^*} \right)^{1/(3\nu-1)}$

In θ-solvents $\nu = 1/2$ and $\quad \eta_{sp} \approx N\phi^2 \approx \left(\phi / \phi^* \right)^2$

In good solvents $\nu = 0.588$ and $\quad \eta_{sp} \approx N\phi^{1.3} \approx \left(\phi / \phi^* \right)^{1.3}$
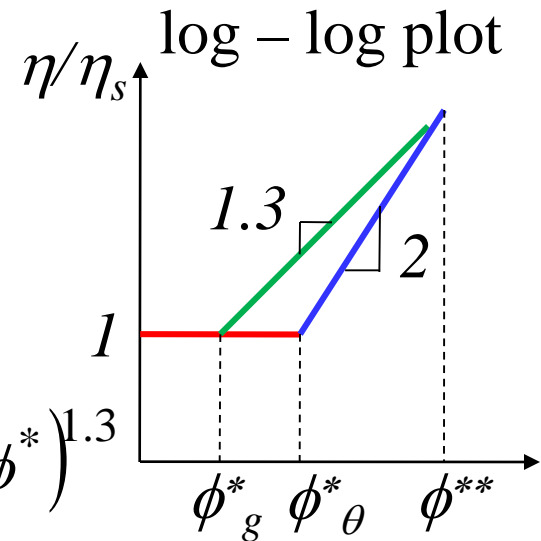
Concentration Dependence of Specific Viscosity

$$\eta_{sp}=(\eta-\eta_s)/\eta_s$$
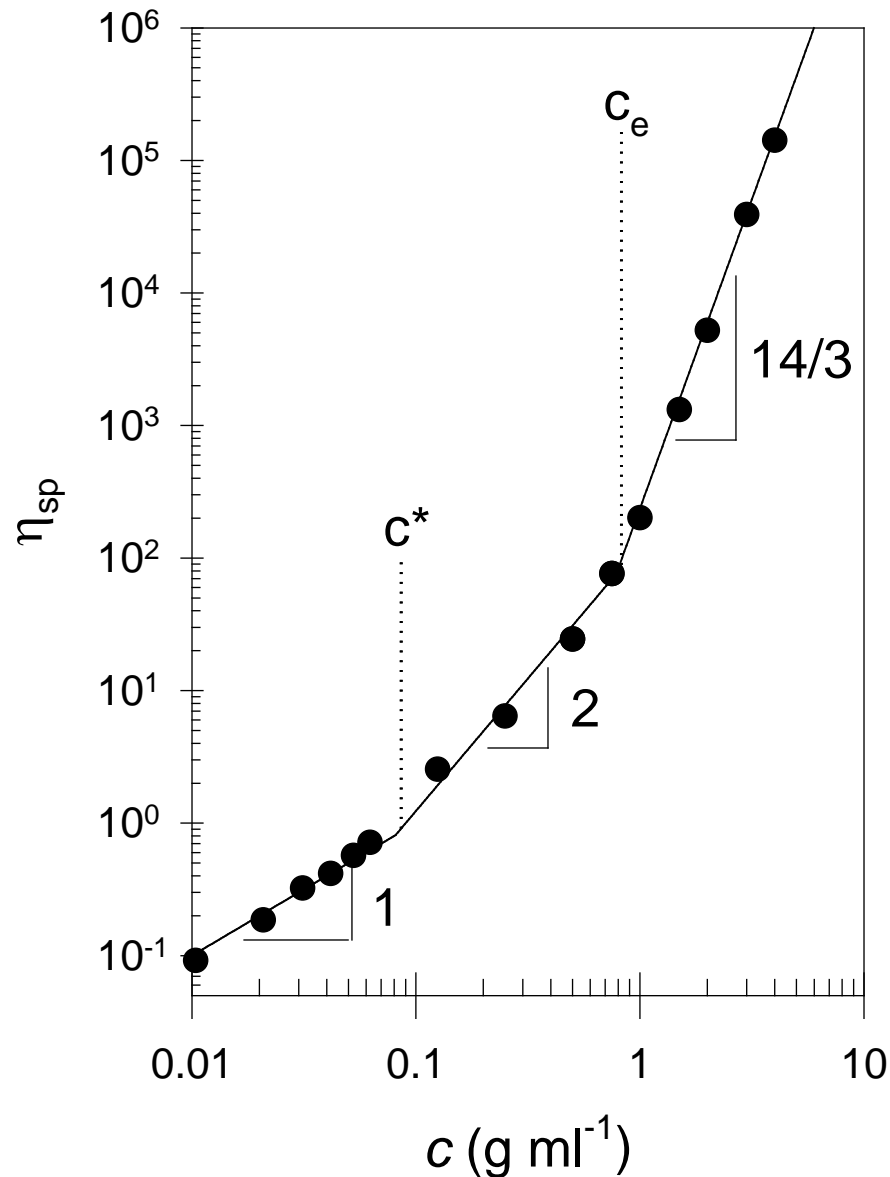
Polyethylene oxide in water at 25°C

Summary of Semidilute Unentangled Dynamics

Hydrodynamic interactions in semidilute solutions are important up to the scales of hydrodynamic screening length (Zimm non-draining modes).

On larger length scales both excluded volume and hydrodynamic interactions are screened by surrounding chains (Rouse draining modes).

Dynamics of Entangled Polymers

Entanglements!

Multi-chain effects due to topological interactions (e.g. knots).

Entanglements dramatically effect polymer properties e.g. viscosity, elasticity - **viscoelasticity**.

Visco   -   elastic

"Silicone bouncing putty appeals to people of superior intellect" (Peter Hodgson)

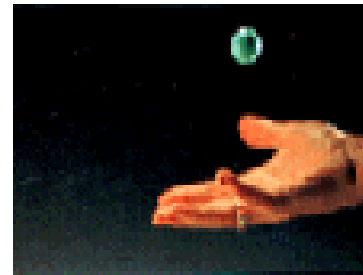# Tube Model of Polymer Entanglements

Edwards 1967

kT

a

free energy

0

transverse distance
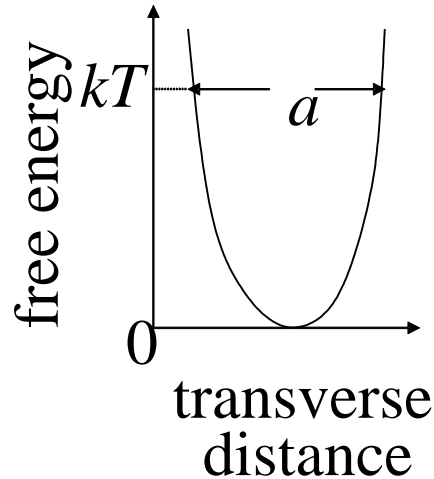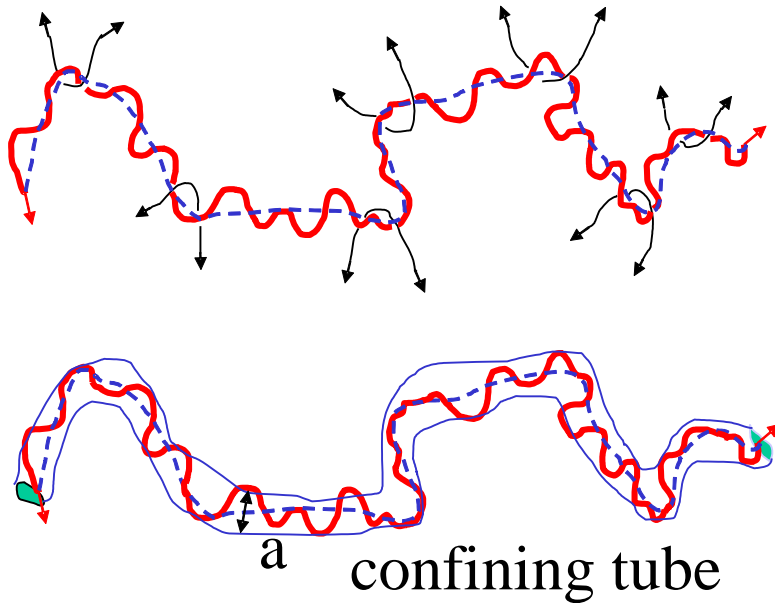
a – tube diameter

N_e – number of Kuhn monomers in an entanglement strand

$$a \approx b\sqrt{N_e}$$

a

confining tube

Confining tube consists of N/N_e entanglement strands of size a

$$R \approx a\sqrt{\frac{N}{N_e}} \approx b\sqrt{N}$$

The center of confining tube is called primitive path of length L

$$\langle L \rangle \approx a\frac{N}{N_e} \approx \frac{b^2 N}{a} \approx \frac{bN}{\sqrt{N_e}}$$

Overlap criterion for entanglements: number of chains in volume a^3 is $P_e = const$

$$P_e \approx \frac{a^3}{v_0 N_e} \approx \frac{b^3}{v_0}\sqrt{N_e} \cong 20$$

Reptation in Polymer Melts
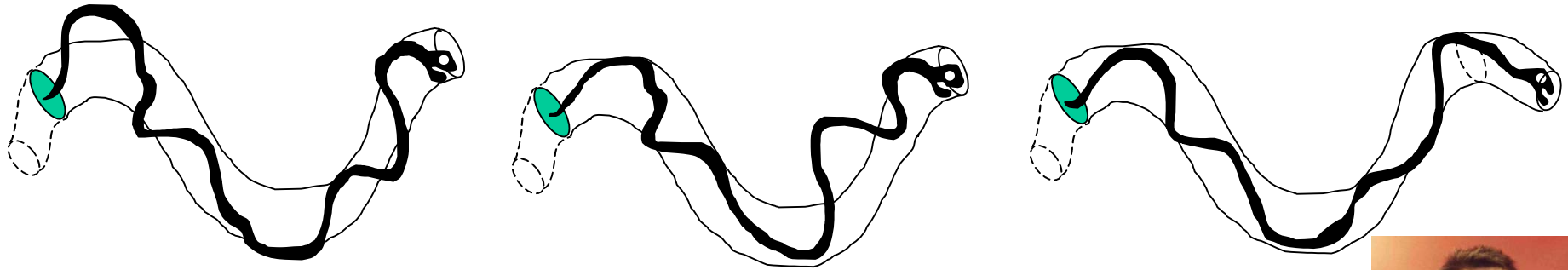
Motion of chain along the contour of the tube is unhindered by topological constraints.

Curvilinear diffusion coefficient along the primitive path is Rouse diffusion $D_c = kT/(N\zeta)$

de Gennes 1971

Time it takes chain to diffuse out of its original tube is reptation time

$$\tau_{rep} \approx \frac{\langle L \rangle^2}{D_c} \approx \tau_e \left(\frac{N}{N_e} \right)^3$$

Rouse relaxation time of an entanglement strand $\tau_e \approx \frac{b^2 \zeta}{kT} N_e^2$

Experimentally $\tau_{rep} \sim M^{3.4}$
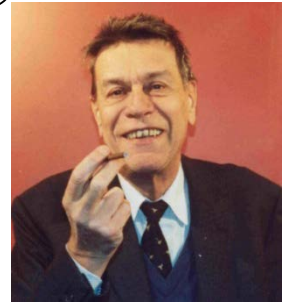
Diffusion Coefficient in Entangled Melts

Reptation time $\qquad \tau_{rep} \approx \dfrac{b^2 \zeta}{kT} \dfrac{N^3}{N_e} \approx \tau_e \left(\dfrac{N}{N_e} \right)^3$

Diffusion coefficient $\quad D \approx \dfrac{R^2}{\tau_{rep}} \approx \dfrac{kT}{\zeta} \dfrac{N_e}{N^2}$

Experimentally $\ D \sim M^{-2.3}$

hydrogenated
polybutadiene at 175 °C

Stress Relaxation of Entangled Melts

On length scales between Kuhn b and tube diameter a sections of chain do not "feel" entanglements and relax by Rouse modes.

$$G(t) \approx G_0 \left(t / \tau_0 \right)^{-1/2}$$
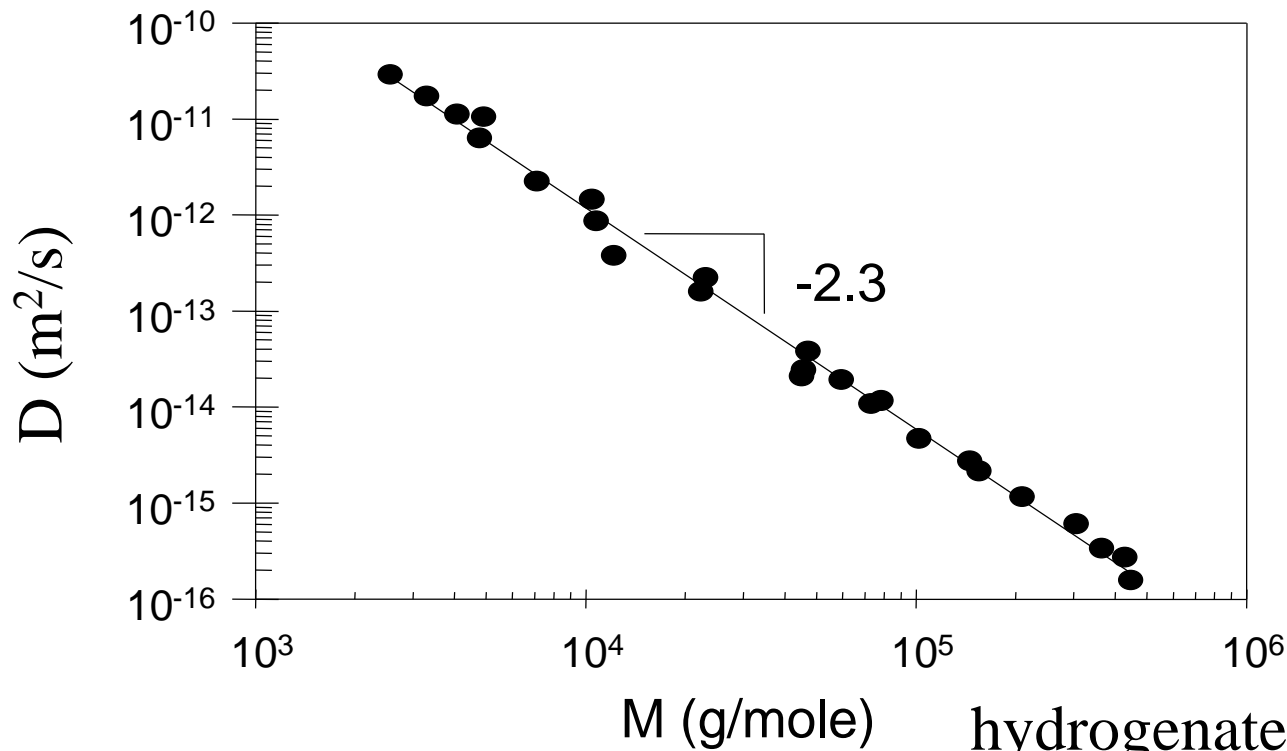
$$\text{for } \tau_0 < t < \tau_e$$

Relaxation time of a Kuhn segment $\quad \tau_0 \approx b^2 \zeta / kT$

Relaxation time of an entanglement strand $\quad \tau_e \approx \tau_0 N_e^2$

Stress relaxation modulus at τ_e is kT per entanglement strand

$$G_e \approx G(\tau_e) \approx \frac{G_0}{N_e} \approx \frac{kT}{v_0 N_e}$$
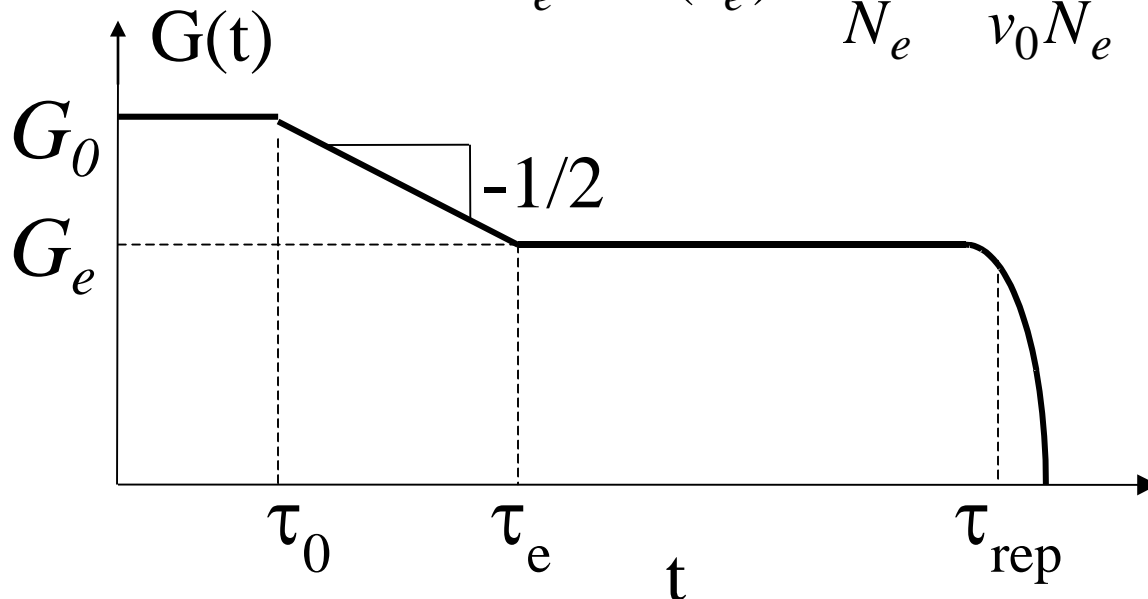
There is a delay in relaxation between τ_e and reptation time τ_{rep}. Melt acts as a rubber. G_e – rubbery plateau modulus.

$$\tau_{rep} \approx \tau_0 \frac{N^3}{N_e} \approx \tau_e \left(\frac{N}{N_e} \right)^3$$

Oscillatory Shear Data for Polybutadiene Melt

$1/\tau_{rep}$ $1/\tau_R$ $1/\tau_e$ $1/\tau_0$

y-axis: $b_T G'$ and $b_T G''$ (Pa)

x-axis: ωa_T (rad/s)

$M = 130\ kg/mol$

25^0 C
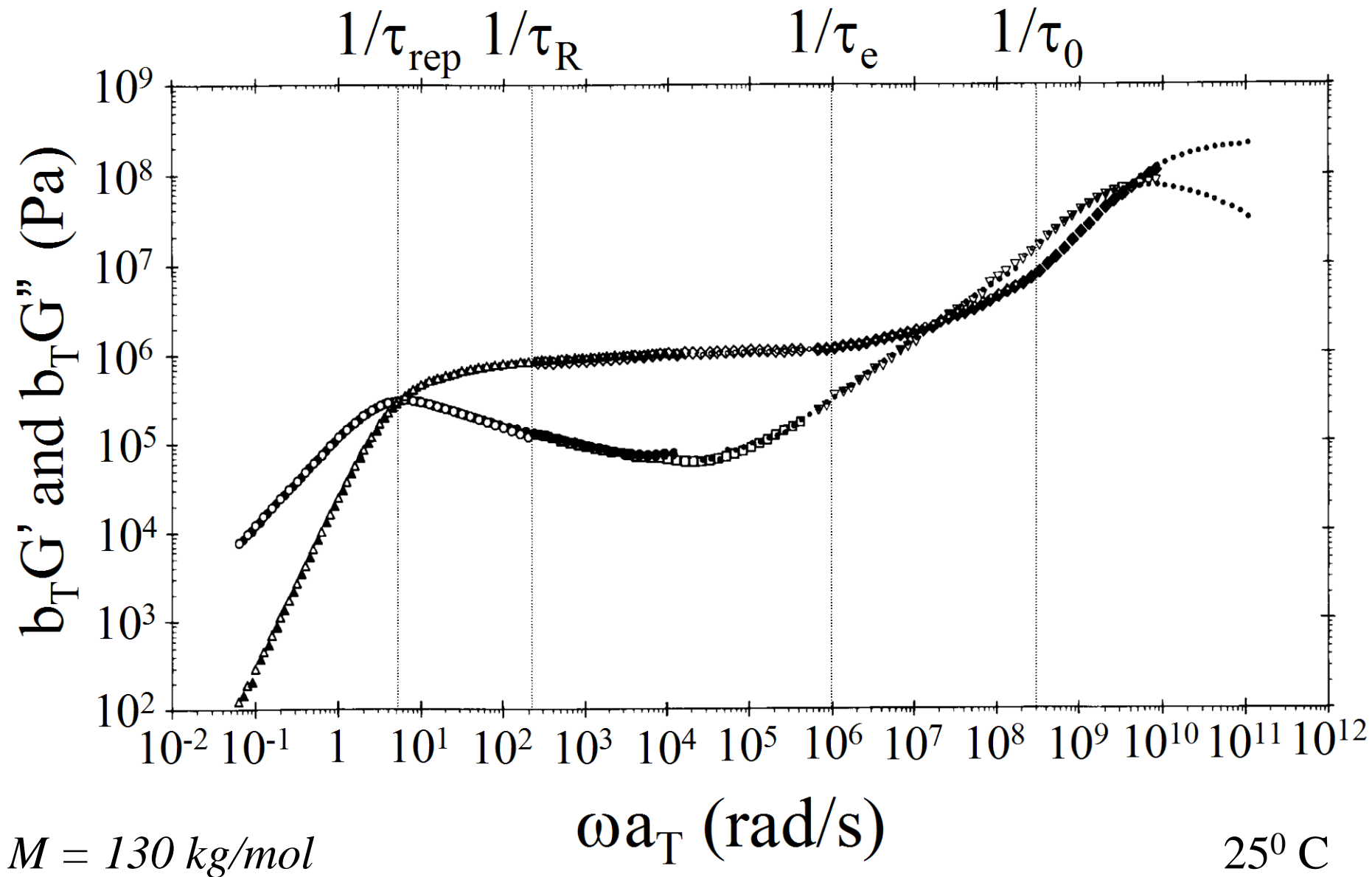
Viscosity of Entangled Melts

$$\eta \approx G_e \tau_{rep} \approx G_e \tau_e \left(\frac{N}{N_e} \right)^3 \approx \frac{b^2 \zeta}{v_0} \frac{N^3}{N_e^2}$$

Viscosity of polymer melts

$$\eta \sim \begin{cases} M & \text{for } M < M_e \\ M^3 & \text{for } M > M_e \end{cases}$$

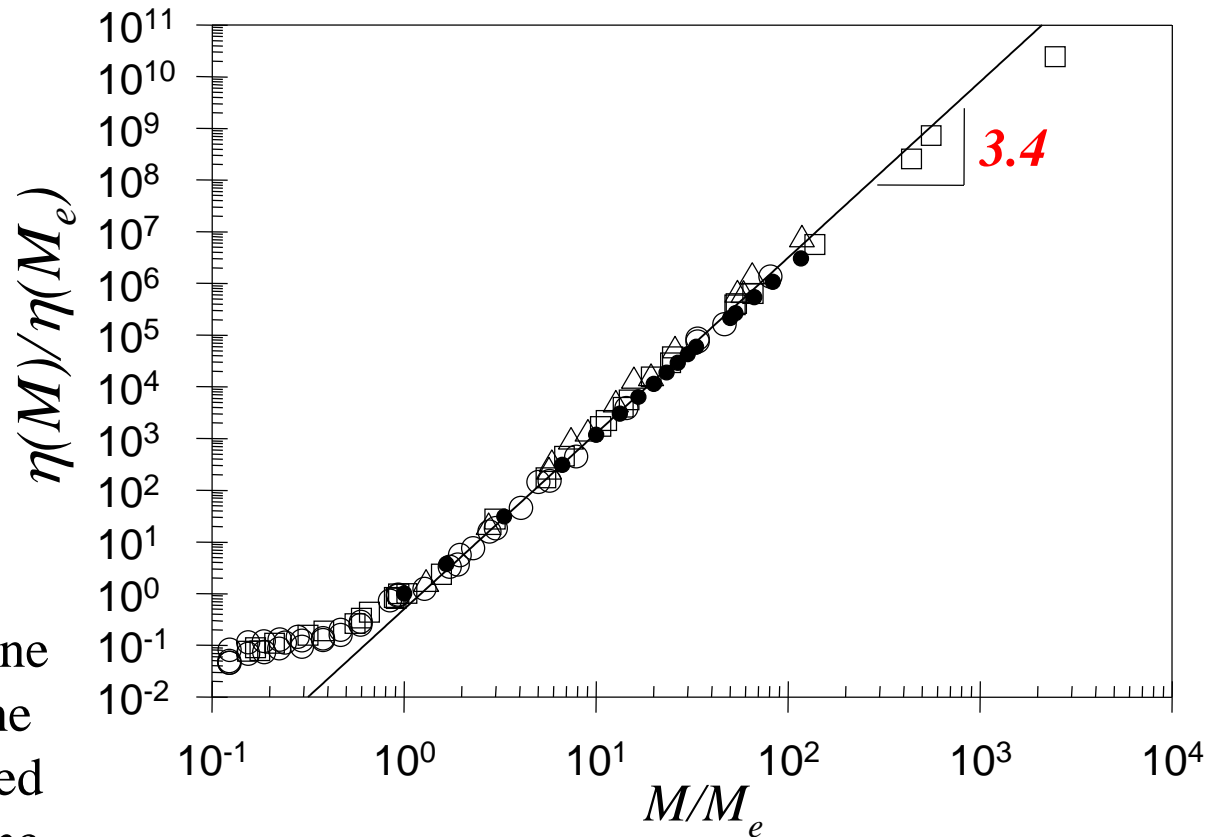Experimentally

$$\eta \approx G_e \tau_{rep} \sim M^{3.4}$$

open circles – polyisobutylene
open squares – polybutadiene
open triangles – hydrogenated
polybutadiene
filled circles – repton model

Semidilute Entangled Solutions
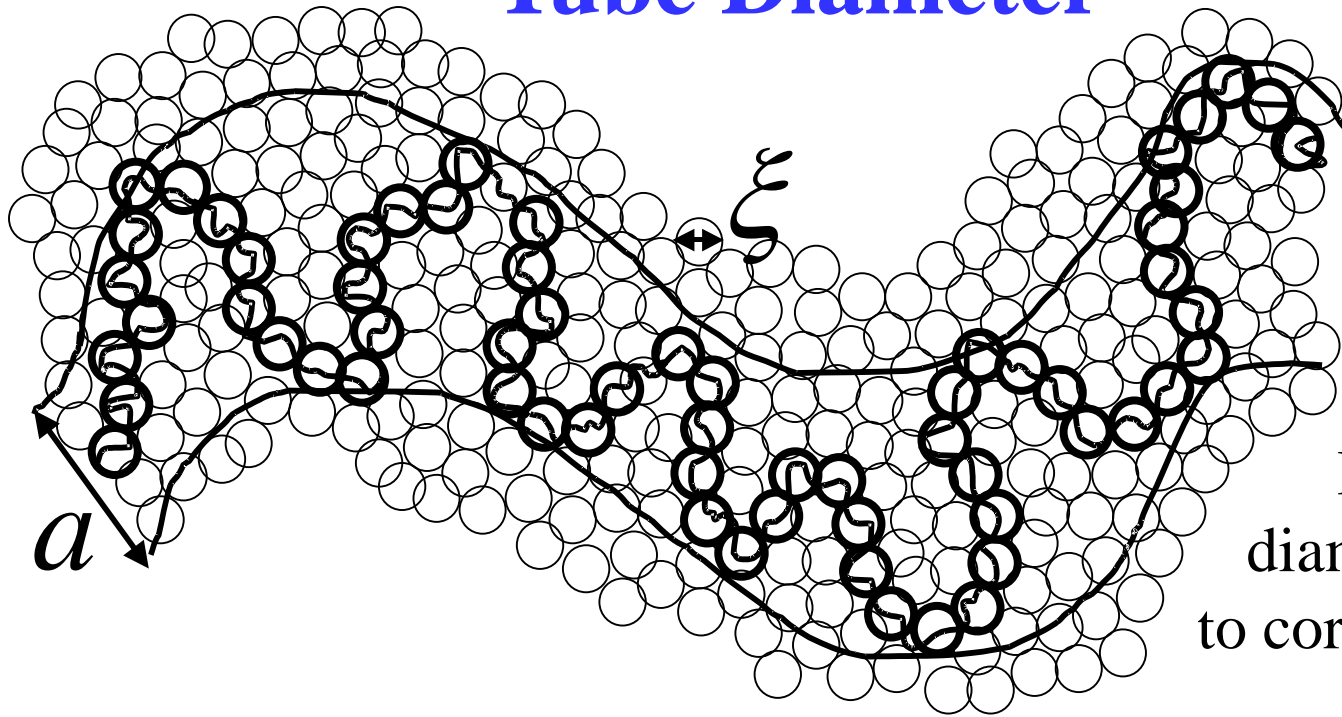
Tube Diameter

Fixed number of binary contacts per a^3

In good solvent tube diameter is proportional to correlation length $a \sim \xi$

$$a(\phi) \approx a(1)\phi^{-\nu/(3\nu-1)} \approx a(1)\phi^{-0.76}$$

In θ-solvents the distance between 2-body contacts $\sim \phi^{2/3}$, while correlation length is proportional the distance between 3-body contacts.

$$a(\phi) \approx a(1)\phi^{-2/3} \qquad \text{in θ-solvents}$$

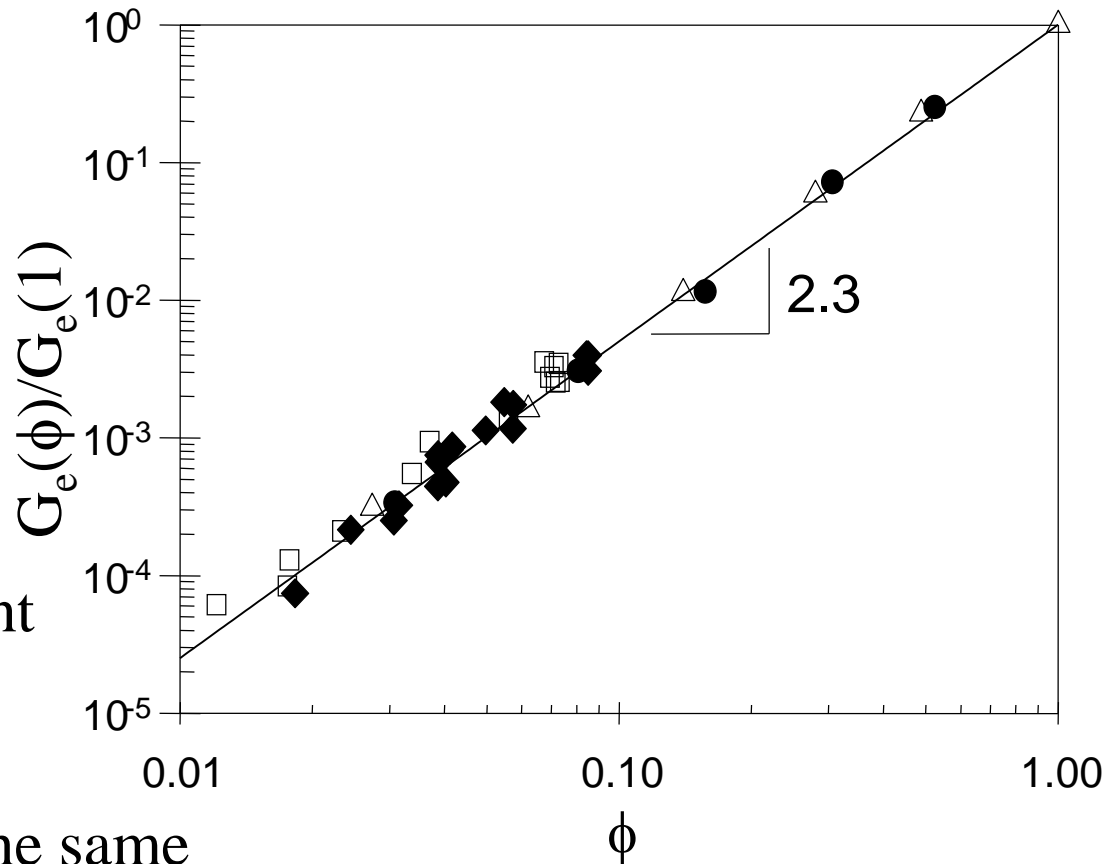# Plateau Modulus in Entangled Solutions

Tube diameter is a random walk of correlation volumes $\quad a \approx \xi \sqrt{\dfrac{N_e}{g}}$

Number of monomers in an entanglement strand
$$N_e(\phi) \approx g\left(\frac{a}{\xi}\right)^2 \approx N_e(1) \begin{cases} \phi^{-1.3} & \text{for good solvent} \\[2mm] \phi^{-4/3} & \text{for } \theta\text{-solvent} \end{cases}$$
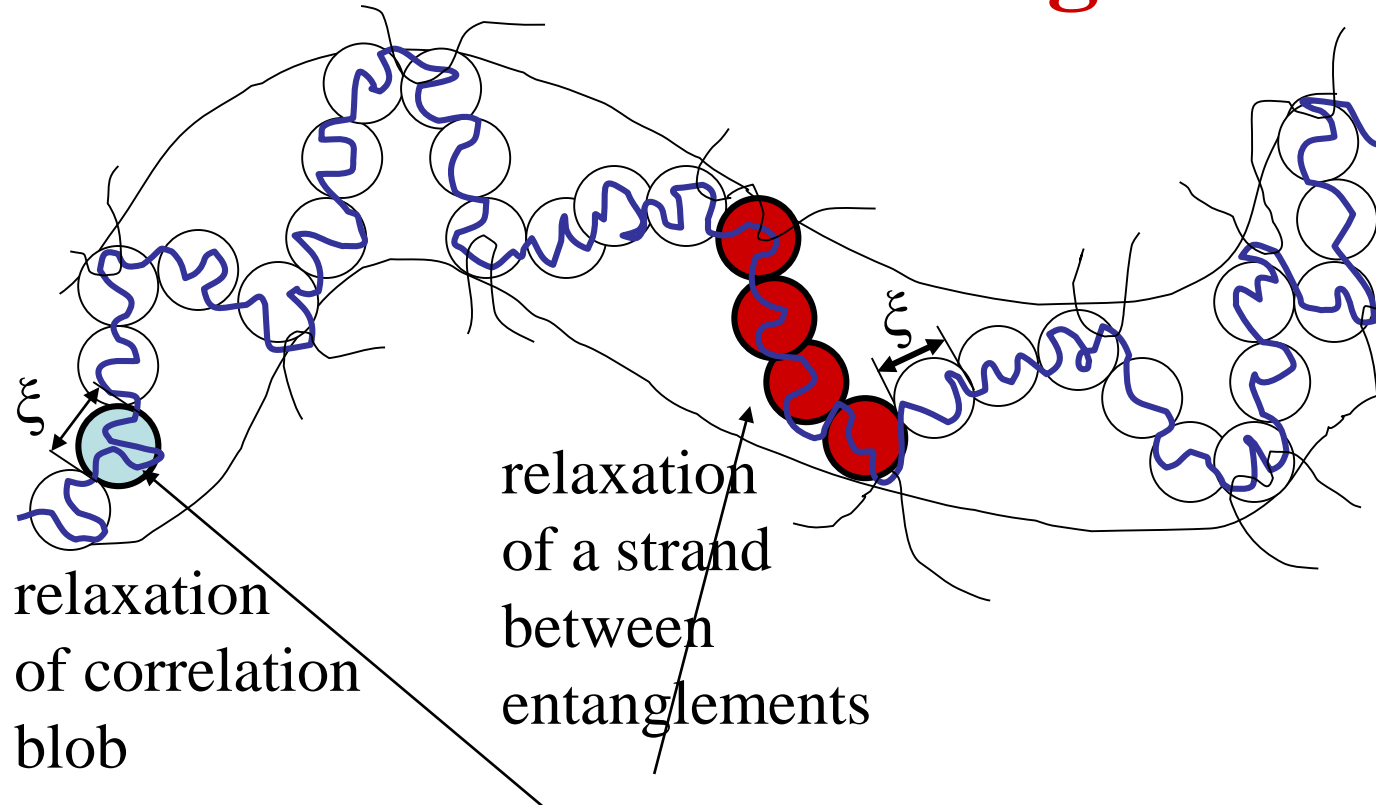
Plateau modulus is kT per entanglement strand

$$G_e(\phi) \approx \frac{kT\phi}{b^3 N_e(\phi)} \approx$$

$$\approx G_e(1) \begin{cases} \phi^{2.3} & \text{for good solvent} \\[2mm] \phi^{7/3} & \text{for } \theta\text{-solvent} \end{cases}$$

predictions are essentially the same

Relaxation Time of Entangled Solutions

relaxation of correlation blob

relaxation of a strand between entanglements

$$\tau_{\text{rep}} = \tau_\xi (N_e/g)^2 (N/N_e)^3$$

$$\tau_{rep} \approx \tau_0 \left(\frac{\xi}{b}\right)^3 \left(\frac{N_e}{g}\right)^2 \left(\frac{N}{N_e}\right)^3 \approx \tau_0 \frac{N^3}{N_e(1)} \begin{cases} \phi^{1.6} \text{ for good solvent} \\ \phi^{7/3} \text{ for } \theta-\text{solvent} \end{cases}$$
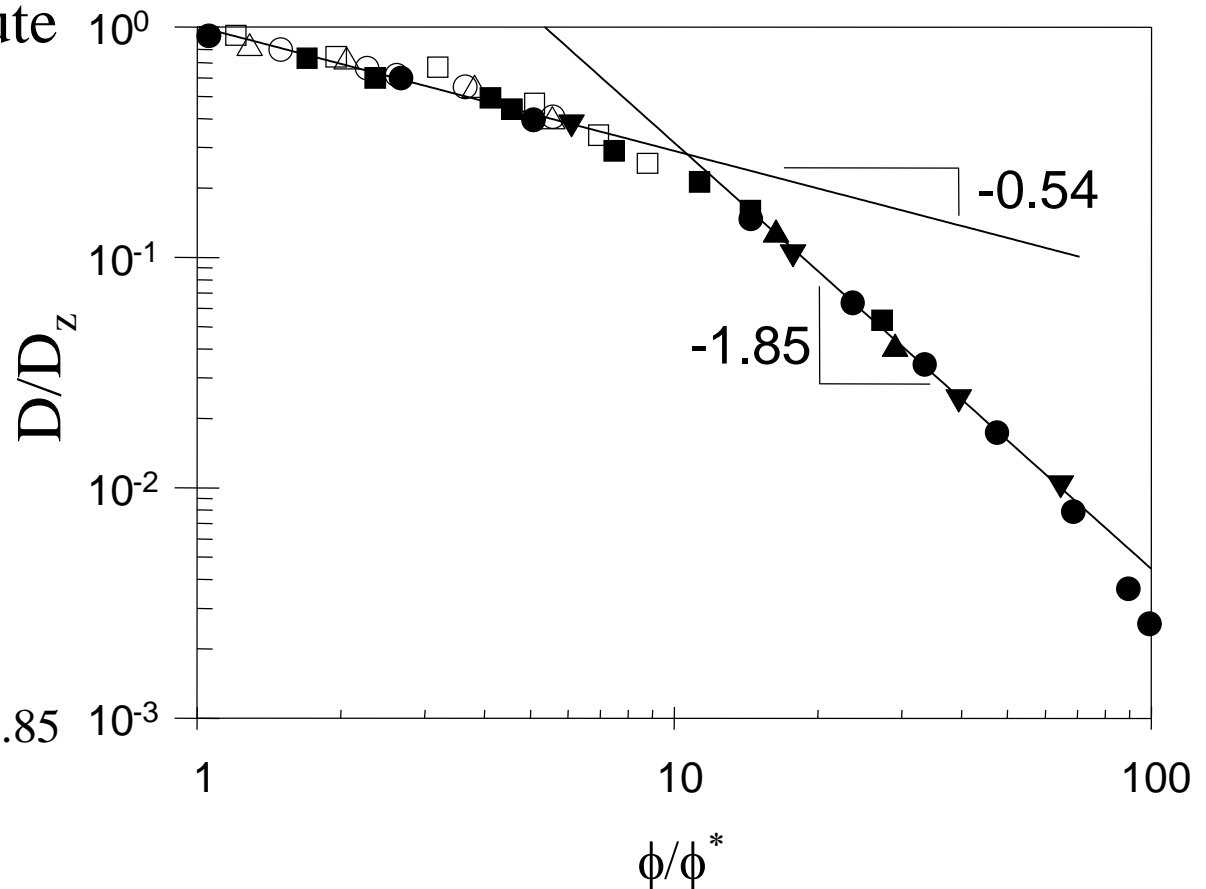
Diffusion Coefficient in Semidilute Solutions

Unentangled semidilute good solvent

$$D \approx D_Z \left(\frac{\phi}{\phi^*} \right)^{-0.54}$$

Entangled semidilute

$$D \approx \frac{R^2}{\tau_{rep}} \approx \frac{b^2}{\tau_0} \frac{N_e(1)}{N^2} \phi^{-1.85}$$
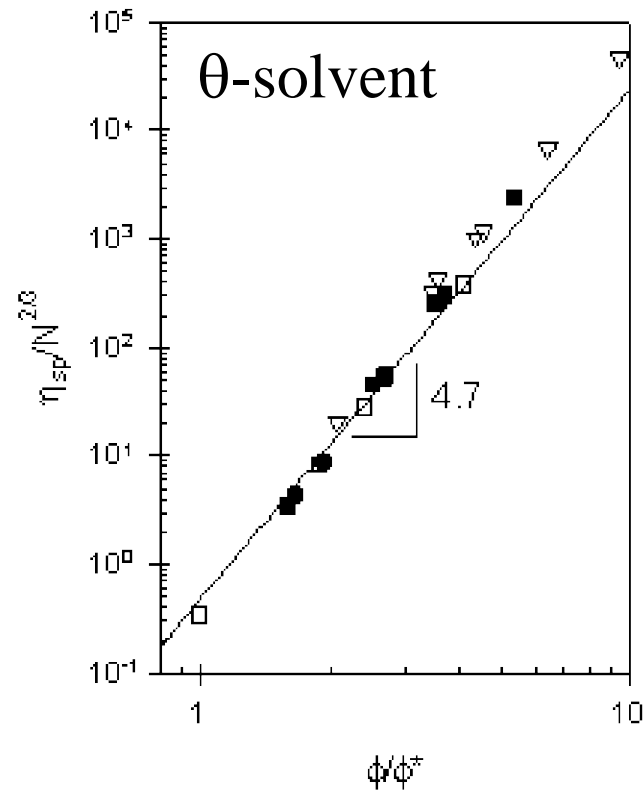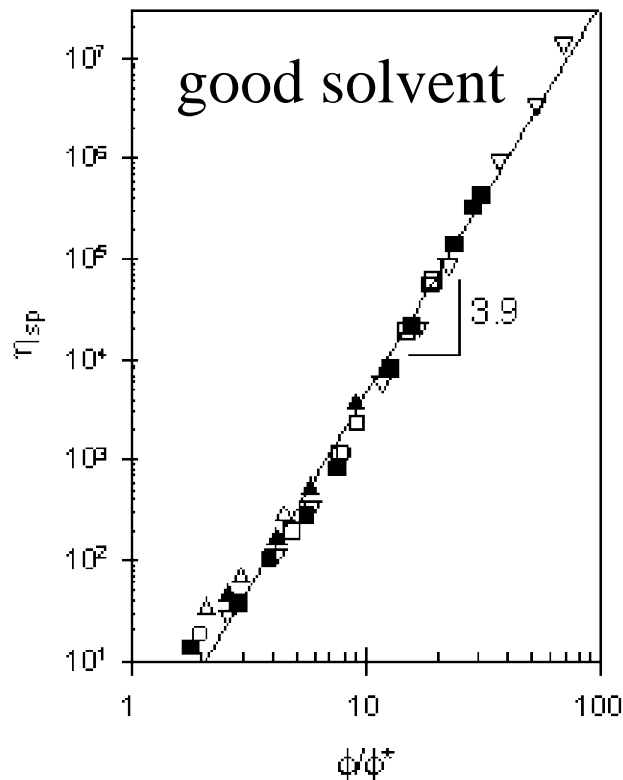

Filled symbols – polystyrene in benzene
Open symbols – poly(ethylene oxide) in water

Viscosity of Entangled Solutions

$$\eta - \eta_s \approx G_e \tau_{rep} \approx \eta_s \frac{N^3}{[N_e(1)]^2} \begin{cases} \phi^{3.9} \text{ for good solvent} \\ \\ \phi^{4.7} \text{ for } \theta-\text{solvent} \end{cases}$$

$$\eta_{sp} = (\eta - \eta_s)/\eta_s \approx \begin{cases} (\phi/\phi^*)^{3.9}/[N_e(1)]^2 & \text{ for good solvent} \\ (\phi/\phi^*)^{14/3}N^{2/3}/[N_e(1)]^2 & \text{ for } \theta\text{-solvent} \end{cases}$$

Dynamics of Networks of Flower Micelles
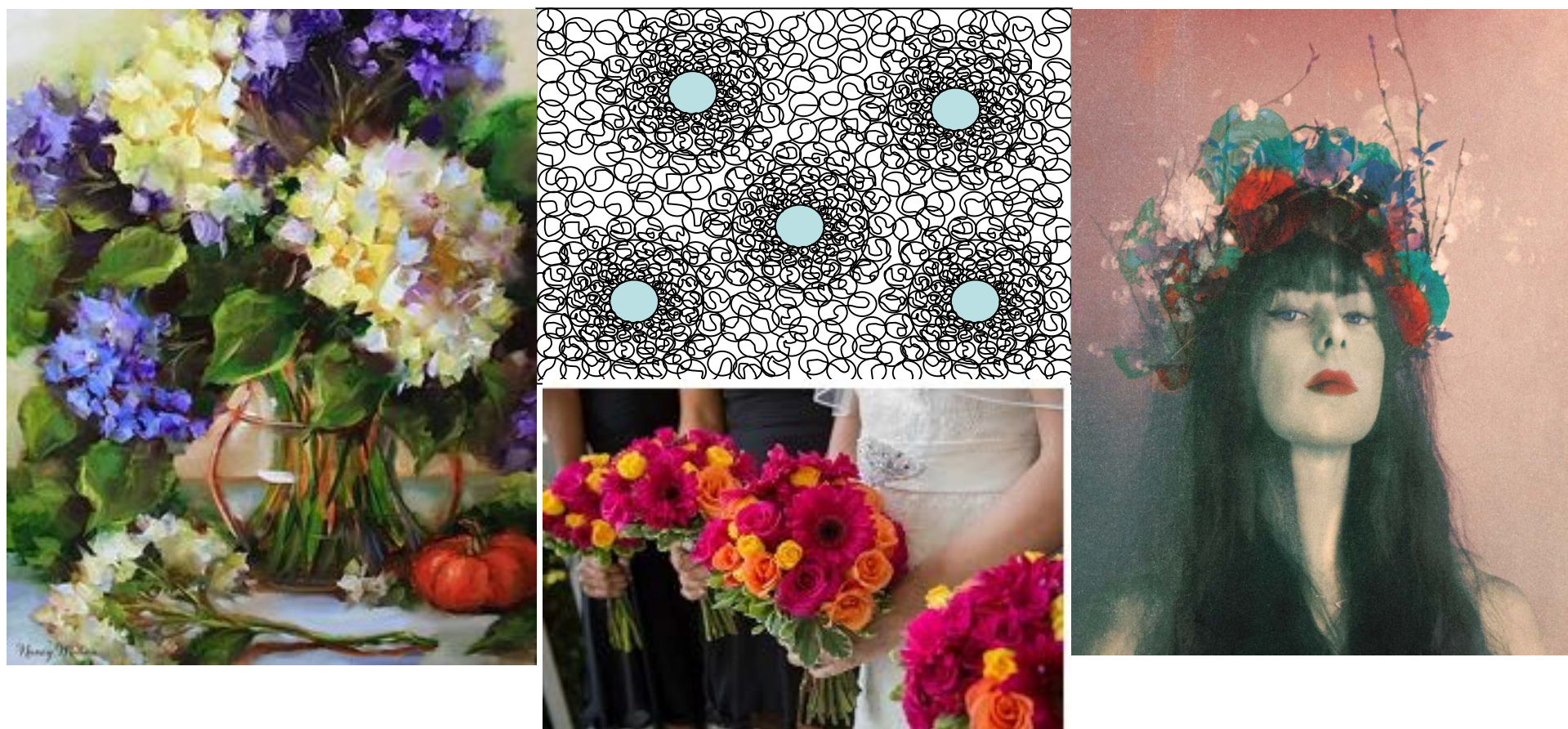
A. N. Semenov and M. Rubinstein

Chain Dynamics

Sticker lifetime

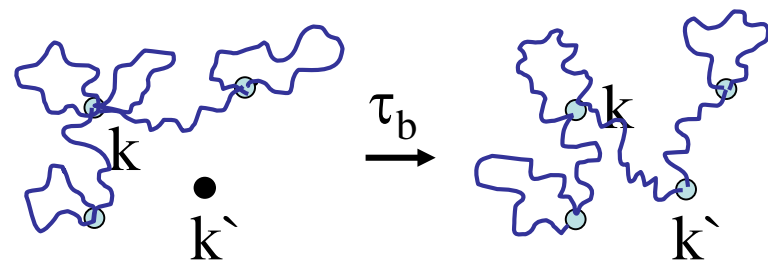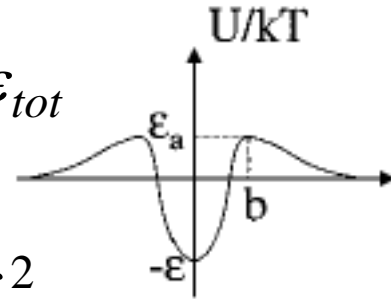$$\tau_b \approx \tau_0 \exp(\varepsilon + \varepsilon_a) \approx \tau_0 \exp\varepsilon_{tot}$$

$kT\varepsilon_a$ – energy barrier

Sticky Rouse time of a chain with f stickers $\quad \tau_R \approx \tau_b f^2$

I. Weakly entangled regime (unentangled n-spacers) $\quad n < N_e(\phi) < N$

entanglements do not affect spacer hops

Sticky reptation time $\quad \tau_{rept} \approx \tau_R N / N_e(\phi)$

II. Strongly Entangled Regime

Transport by unentangled n-loops (n-hernias)
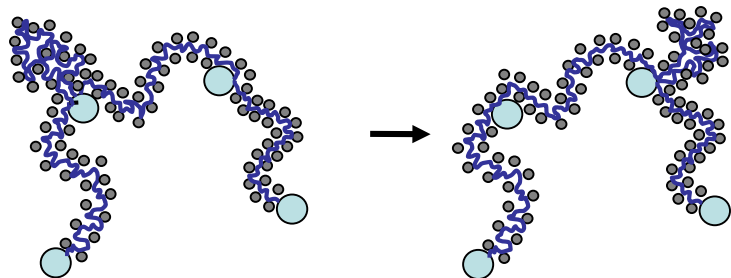
$\exp(-F_e/kT)$ - probability of an n-loop to be unentangled

$$F_e \approx kTn / N_e(\phi) \approx kT(\phi / \phi_e)^{1/(3\nu-1)} \sim \phi^{1.3}$$

Reptation by n-hernias $\quad \tau_{rept} \approx \tau_b f^3 \exp(F_e / kT) \approx \tau_b f^3 \exp\left[(\phi / \phi_e)^{1/(3\nu-1)}\right]$

Strongly Entangled Regime
Collective Tube Leakage

At concentrations higher than

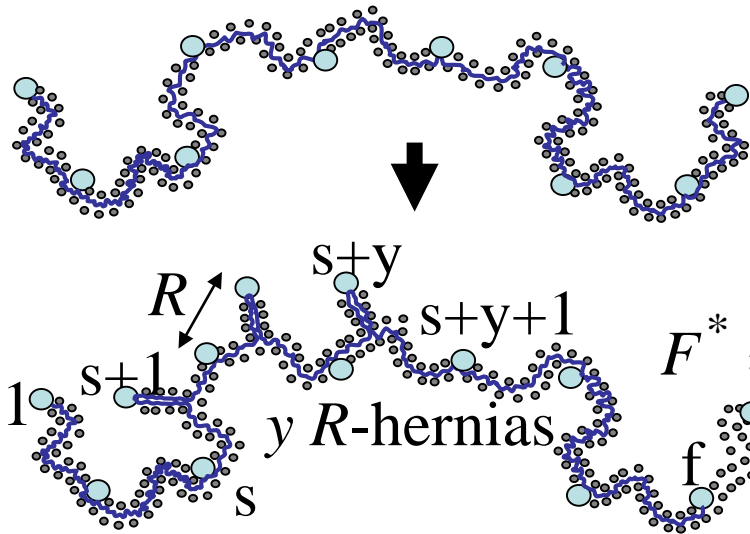$$\phi_{kink} \approx \tilde{\phi}\left(N_{e0}/m^2\right)^{3(3\nu-1)/4}$$

the free energy of a collective kink

$$F^* \approx kT\left(\phi_{kink}/\phi_e\right)^{1/(3\nu-1)}\left(\phi/\phi_{kink}\right)^{2/[3(3\nu-1)]} \sim \phi^{0.87}$$

is lower than that of an unentangled n-loop

Entanglement concentration of n-loop $\quad \phi_e \approx (N_{e0}/n)^{3\nu-1}$
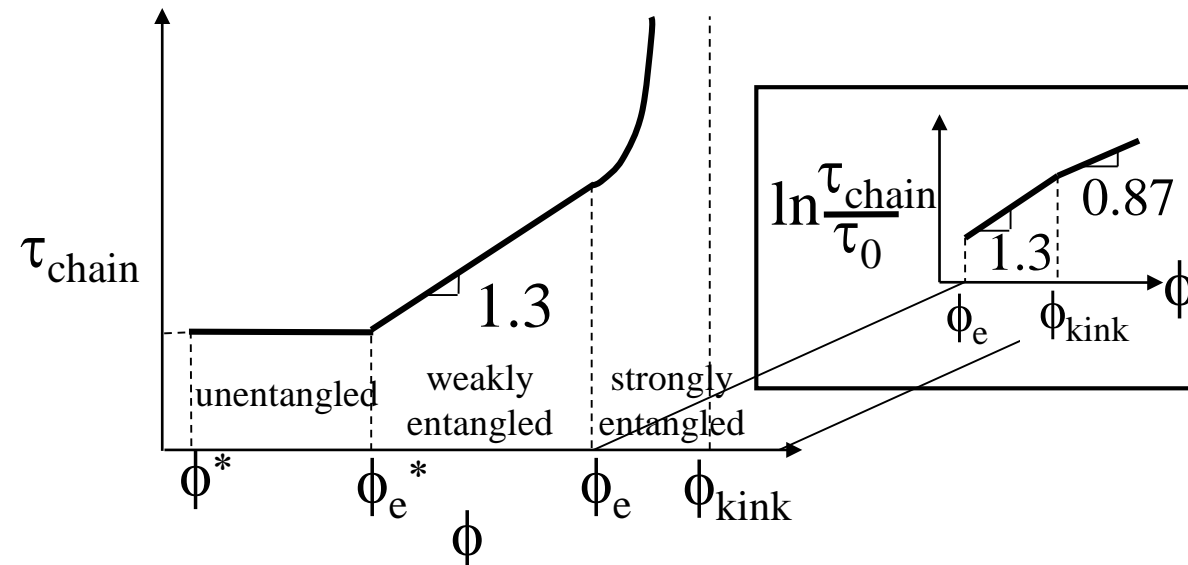
Chain relaxation time in the collective tube leakage mode

$$\tau_{rept} \approx \tau_b f^3 \exp\left(F^*/kT\right)$$

Dynamics of Micelles

Micelle hopping involves deformation free energy ΔF

To hop micelle has to remove its bridges with old neighbors and to create new bridges.

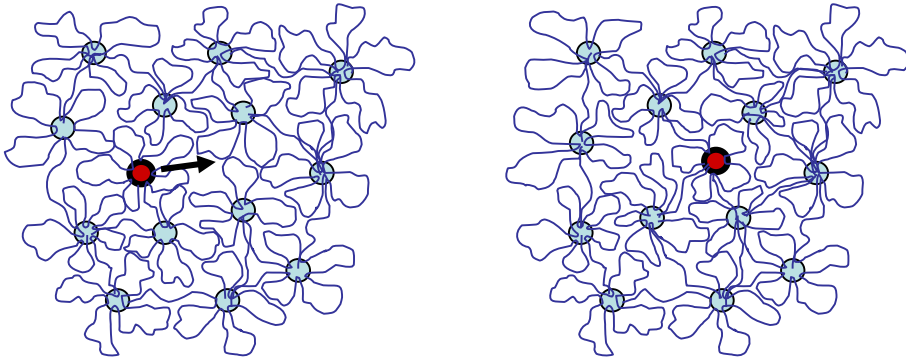All the entanglements with old neighbors must be relaxed.

Kinetic pathway 1 – all involved chains are relaxed at all stages of the micellar core displacement.

$$\tau_{h1} \approx \tau_{chain} \exp\left(\frac{\Delta F}{kT}\right)$$

Kinetic pathway 2

Debridging stage – all bridges are transformed into loops. $\quad F_b \approx kTN_b$

Hopping stage – micellar core hops into a new cell without dissociation of stickers paying additional deformation cost.
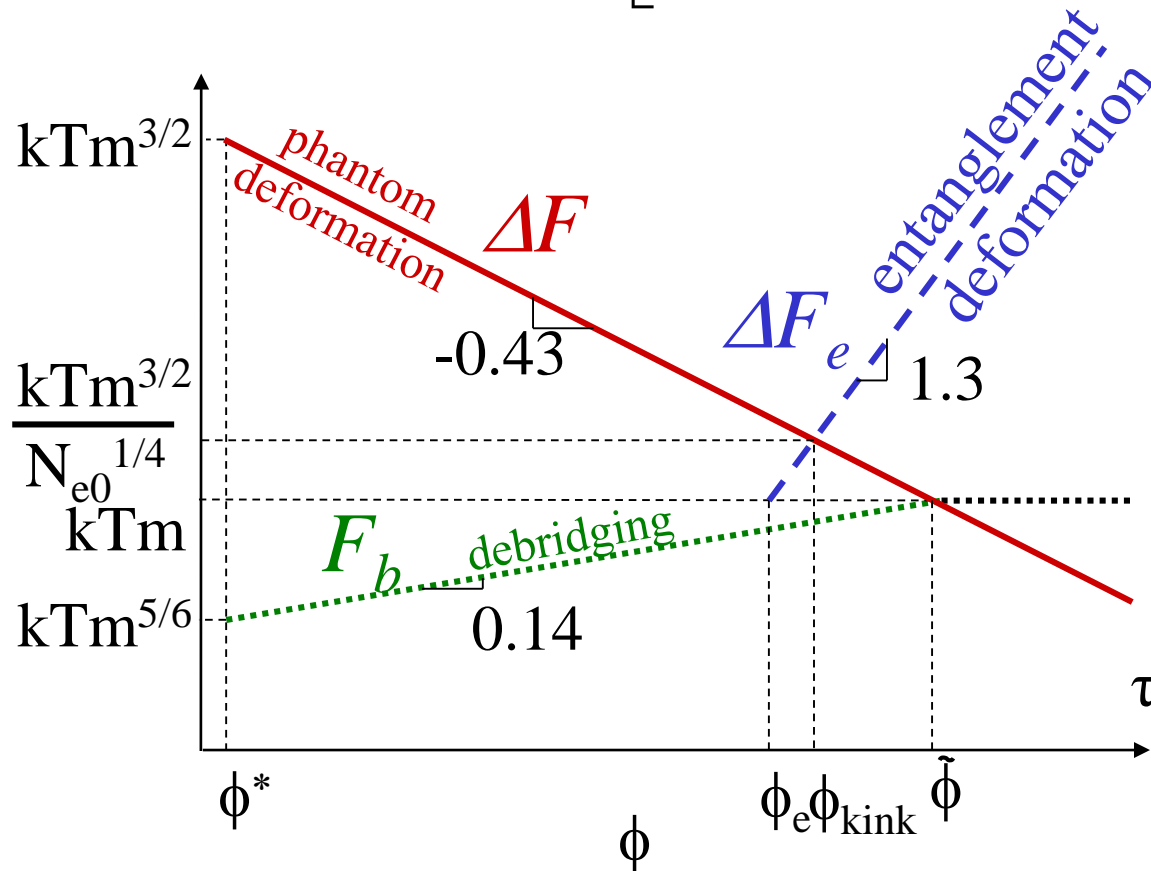
Deformation costs consists of phantom ΔF and entanglement ΔF_e part.

Entanglement cost per micelle
(kT per entanglement)

$$\Delta F_e \approx mF_e \approx kTm(\phi / \phi_e)^{1/(3\nu-1)}$$

Activation Energy of the Kinetic Pathway 2

$$F_a \approx F_b + \Delta F + \Delta F_e \approx kTm \left[\left(\frac{\phi}{\tilde{\phi}} \right)^{1/[9(3\nu-1)]} + \left(\frac{\tilde{\phi}}{\phi} \right)^{1/[3(3\nu-1)]} + \left(\frac{\phi}{\phi_e} \right)^{1/(3\nu-1)} \right]$$

Hopping time

$$\tau_{h2} \approx \tau_{db} + \tau_m \exp\left(\frac{F_a}{kT} \right)$$

Debridging time

$$\tau_{db} \approx \tau_{chain} \exp\left(\frac{F_b}{kT} \right)$$
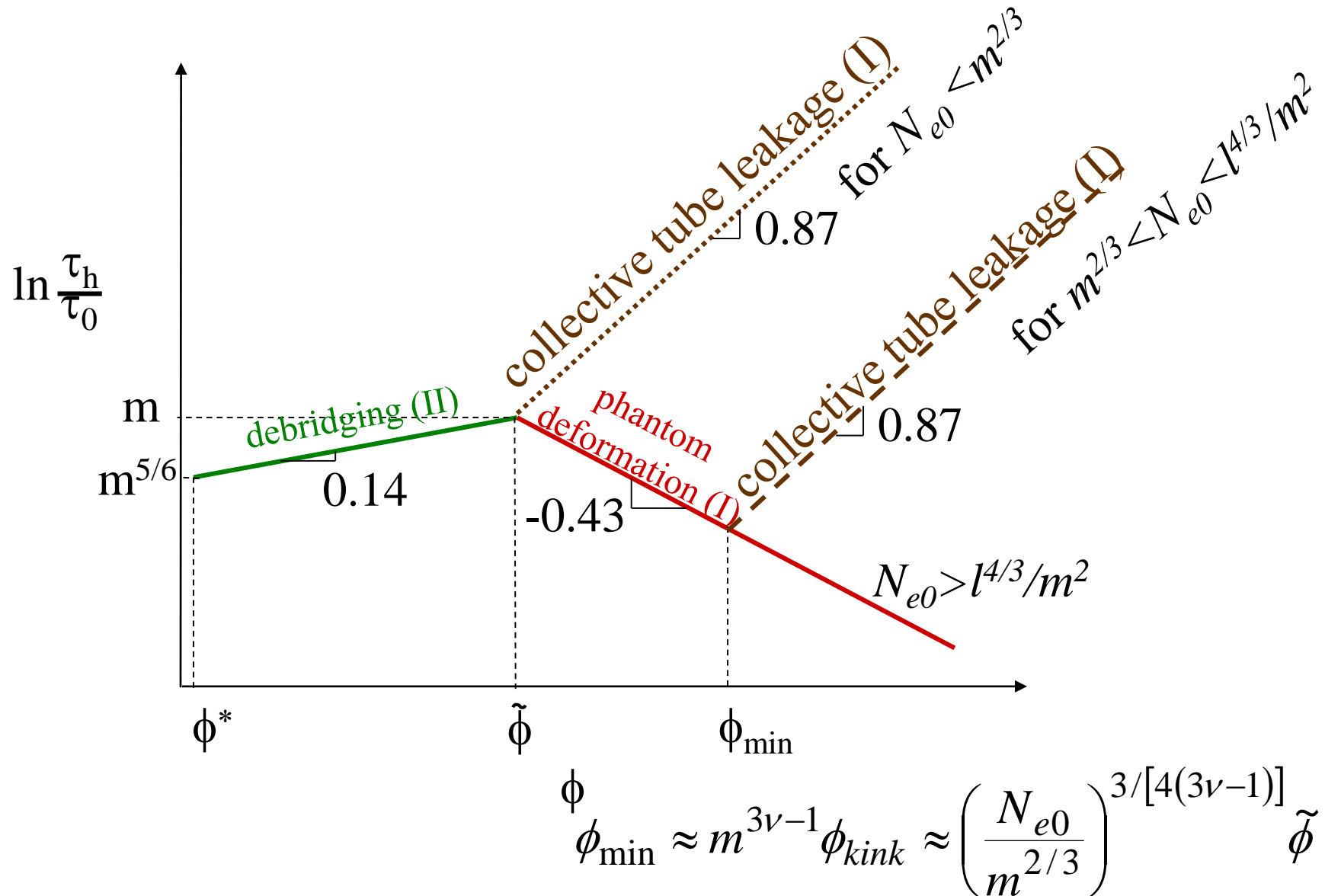
$$\approx \tau_{chain} \exp(N_b)$$

τ_m – Rouse-Zimm micellar diffusion time (ignoring entanglements)

Both kinetic pathways contribute to hopping frequency

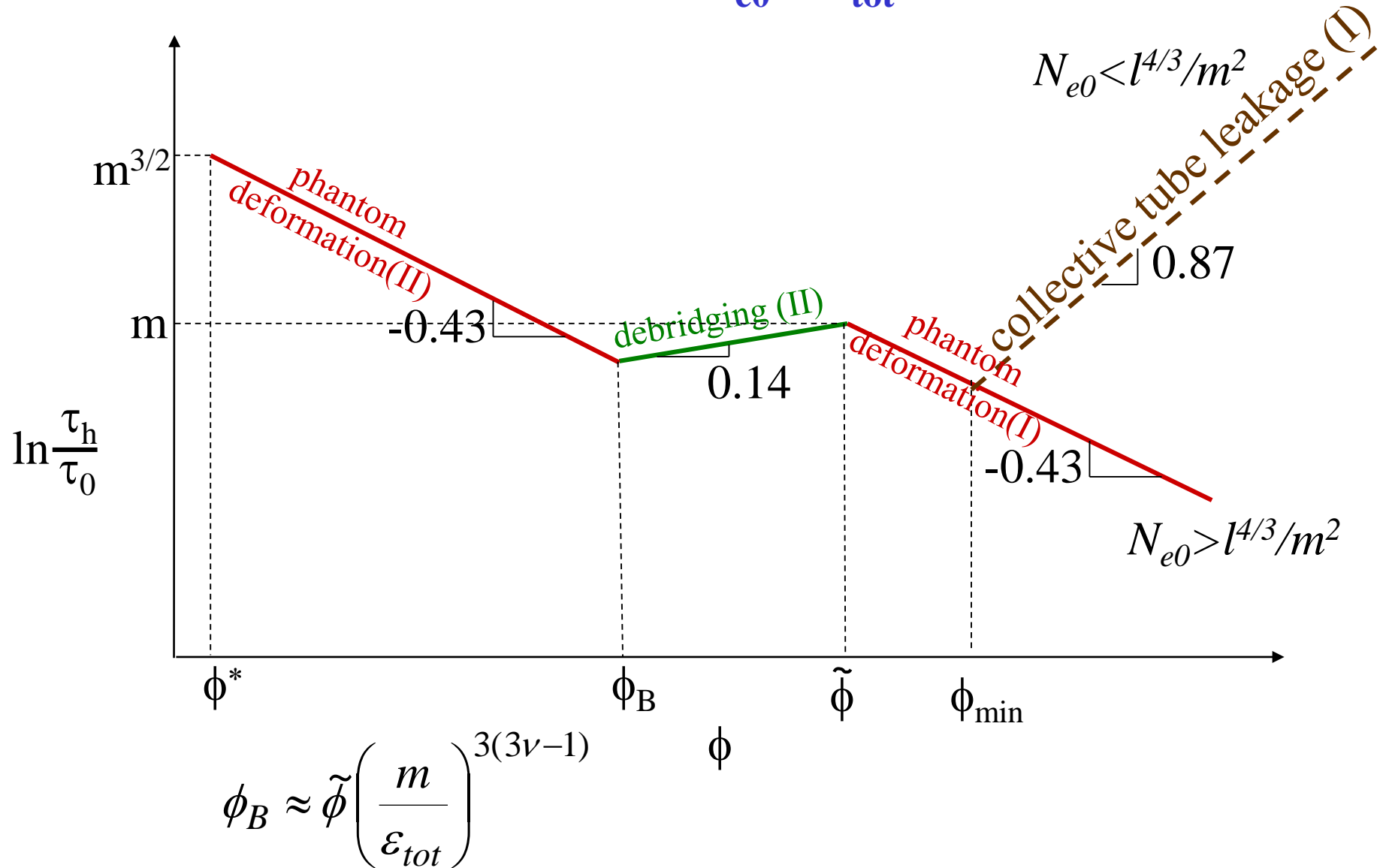$$1/\tau_h = 1/\tau_{h1} + 1/\tau_{h2}$$

Non-Monotonic Relaxation Time

Case A: $\varepsilon_{tot} > \max(m^{3/2}, m^3/N_{e0})$

Non-Monotonic Relaxation Time

Case B``: $m^3/N_{e0} < \varepsilon_{tot} < m^{3/2}$

$N_{e0} < l^{4/3}/m^2$

collective tube leakage (I)

0.87

phantom deformation(II)

-0.43

debridging (II)

0.14

phantom deformation(I)

-0.43

$N_{e0} > l^{4/3}/m^2$

$m^{3/2}$

m

$\ln \dfrac{\tau_h}{\tau_0}$

ϕ^* ϕ_B $\tilde{\phi}$ ϕ_{min}

ϕ

$$\phi_B \approx \tilde{\phi} \left(\frac{m}{\varepsilon_{tot}} \right)^{3(3\nu - 1)}$$

Non-Monotonic Relaxation Time

Case D: $m(N_{e0}/m^2)^{1/8} < \varepsilon_{tot} < m^{3/2}/N_{e0}^{1/4}$
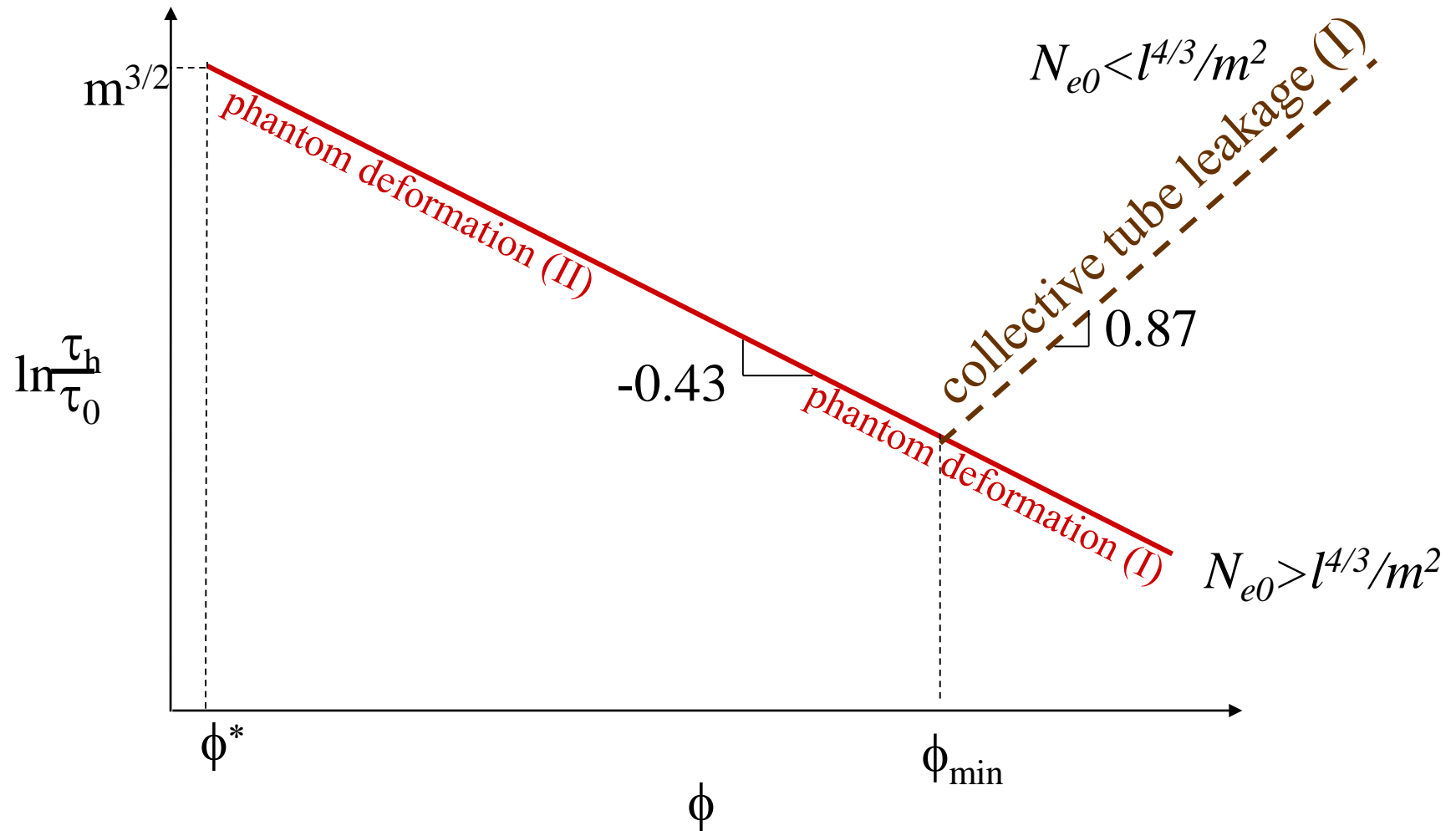
Summary

1. Conformational relaxation time of chains in strongly entangled regime increases exponentially with concentration.

2. Stress relaxation time of the reversible network is much longer than conformational relaxation time of individual chains.

3. Stress relaxation is determined by positional rearrangement of micelles which is very slow because of high barriers.

4. Non-monotonic dependence of relaxation time and viscosity on concentration with anomalous exponential decrease due to decrease in deformation energy controlling the activation barrier for micellar hops.